Cosmic Ray Anisotropy

Paolo Desiati

UNIVERSITY OF WISCONSIN–MADISON

desiati@wipac.wisc.edu

icecube.wisc.edu/~desiati

WISCONSIN ICECUBE PARTICLE ASTROPHYSICS CENTER

cosmic-ray energy spectrum

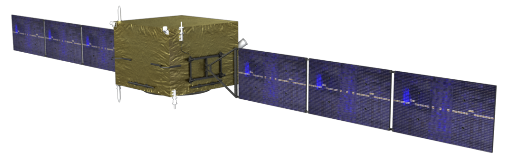

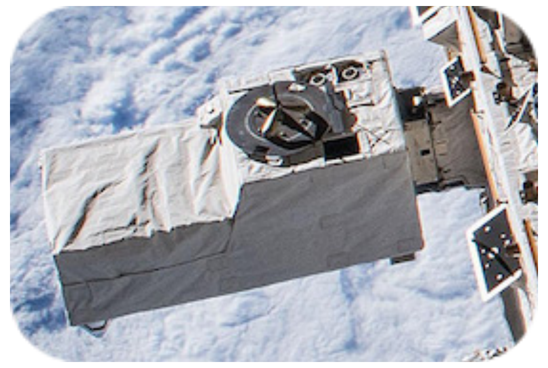

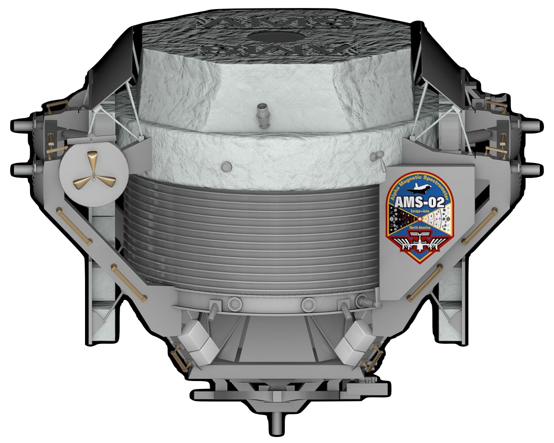

Results GSF 2024 model (Data set 1)

$\chi^2 / \mathrm{ndf} = 1034 / 1072 = 0.96$

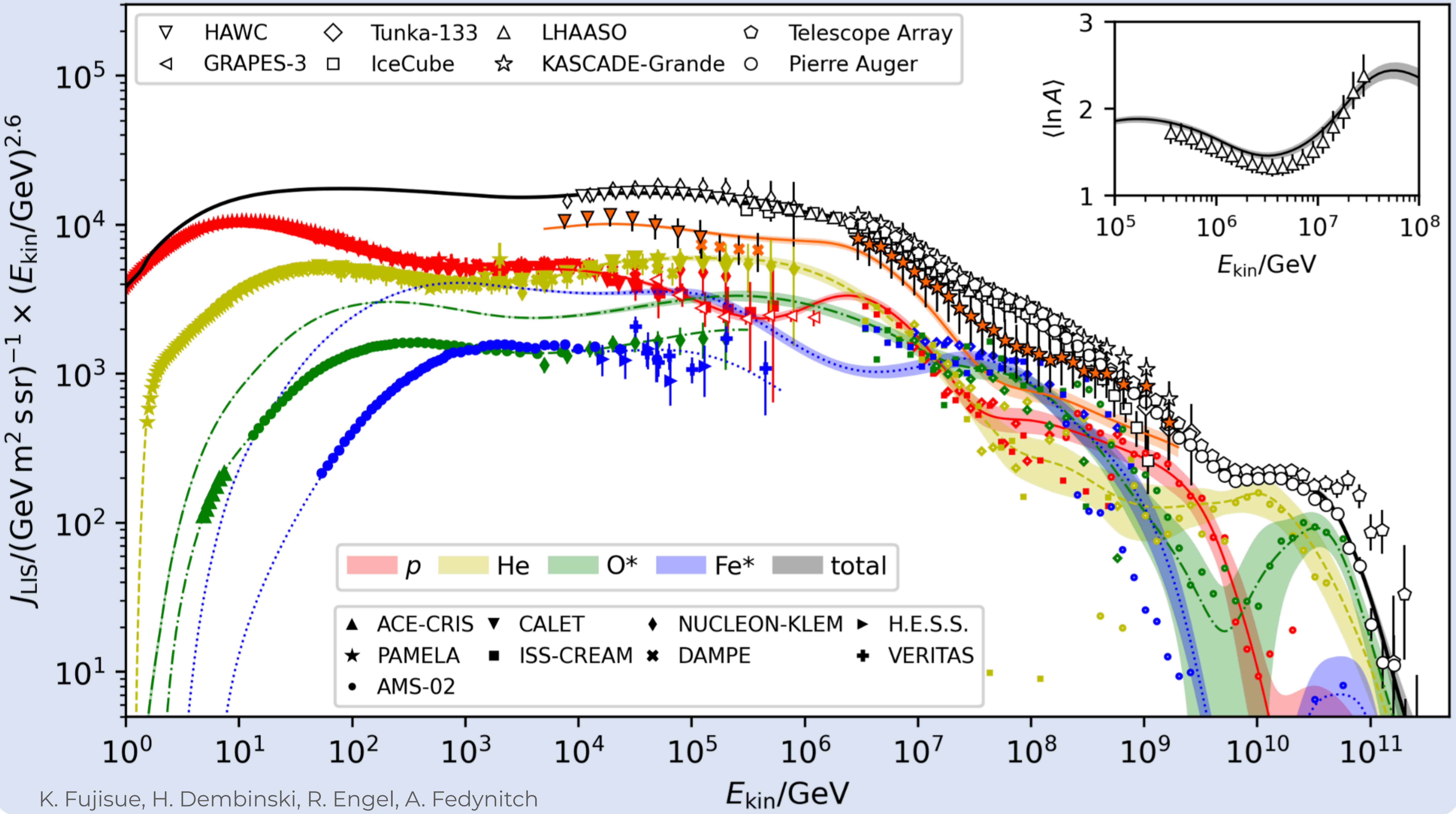

K. Fujisue, H. Dembinski, R. Engel, A. Fedynitch

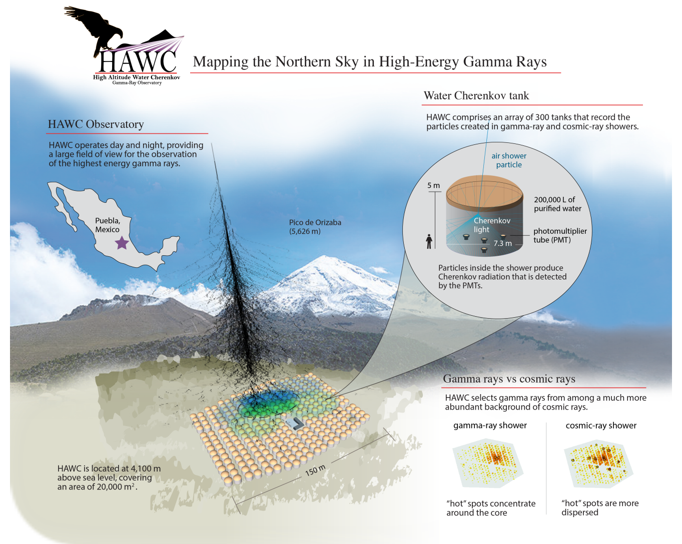

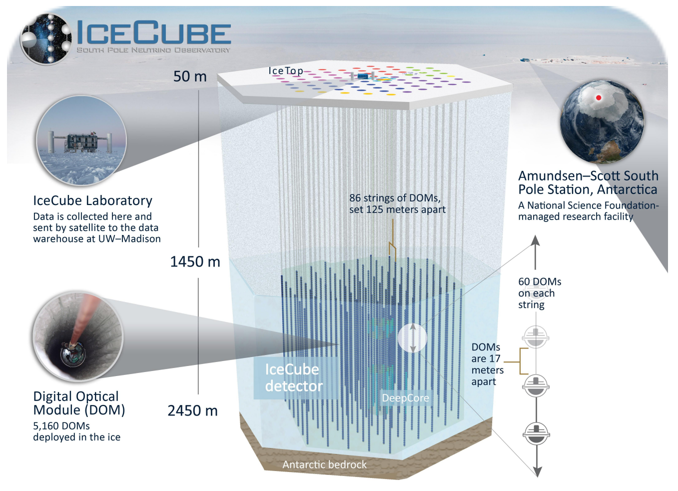

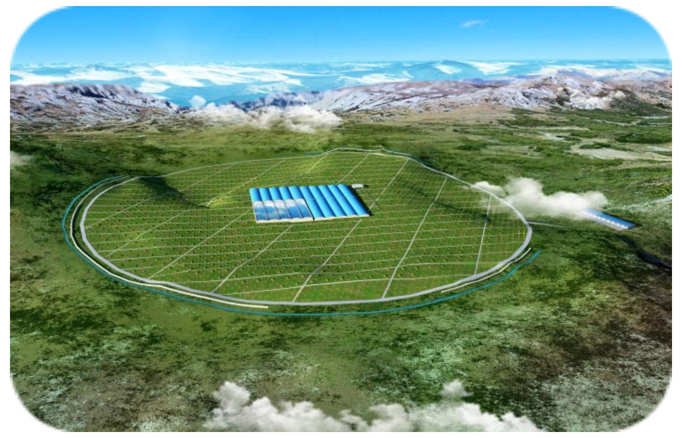

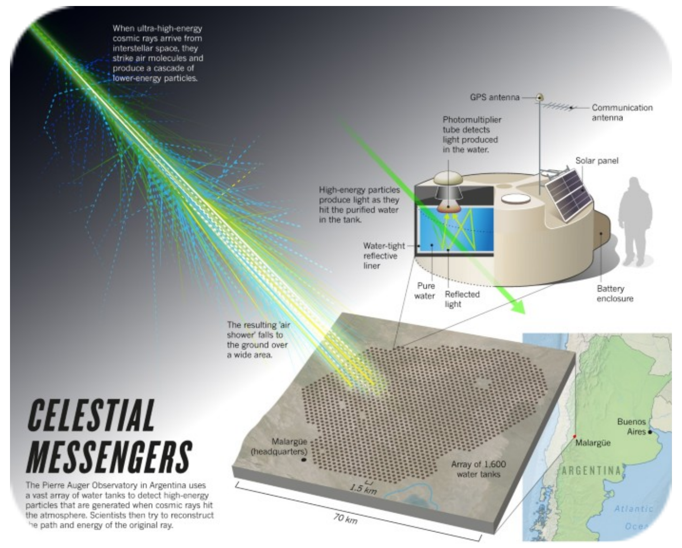

cosmic-ray's journey

accelerator

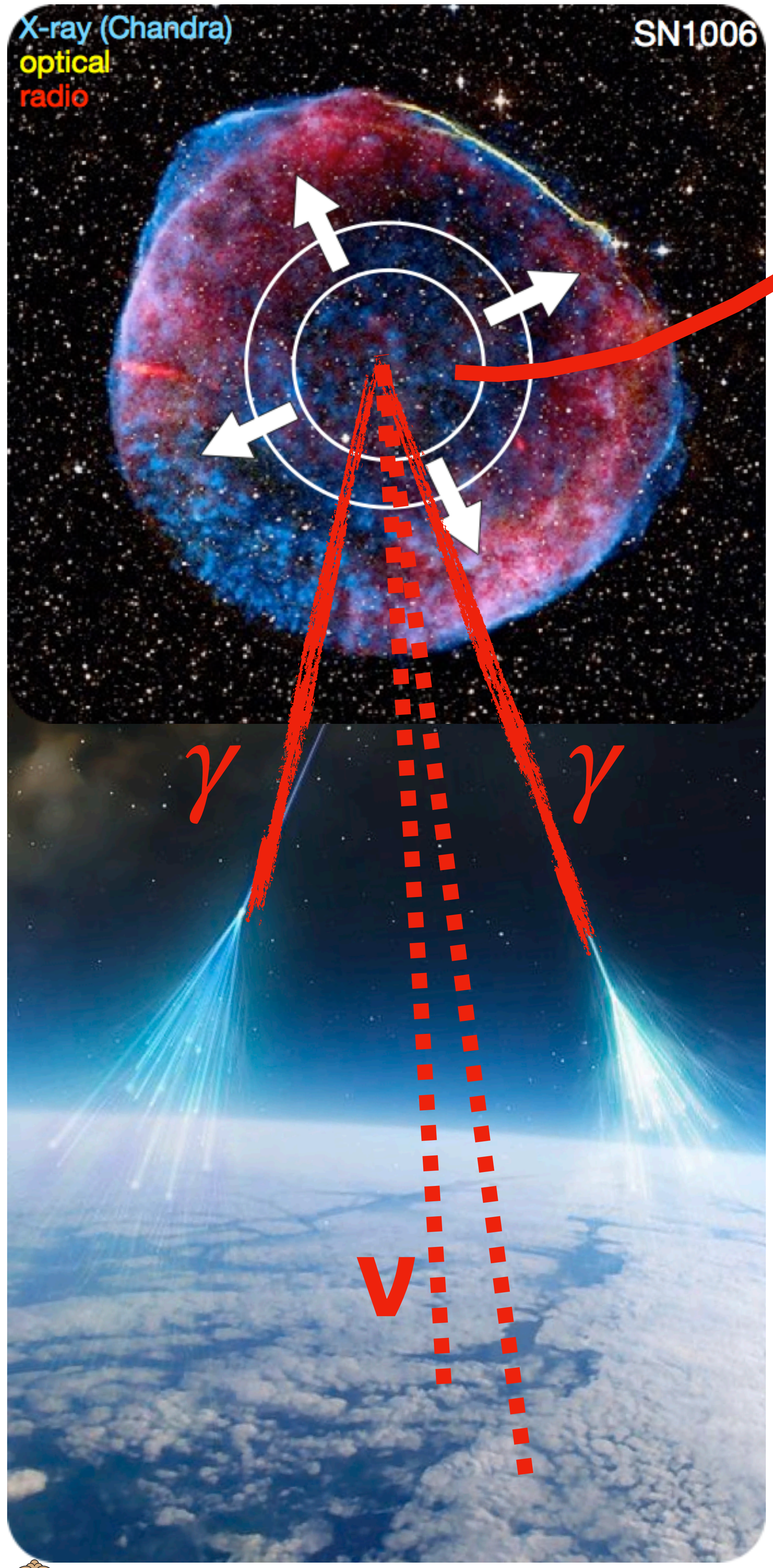

interstellar medium magnetic fields

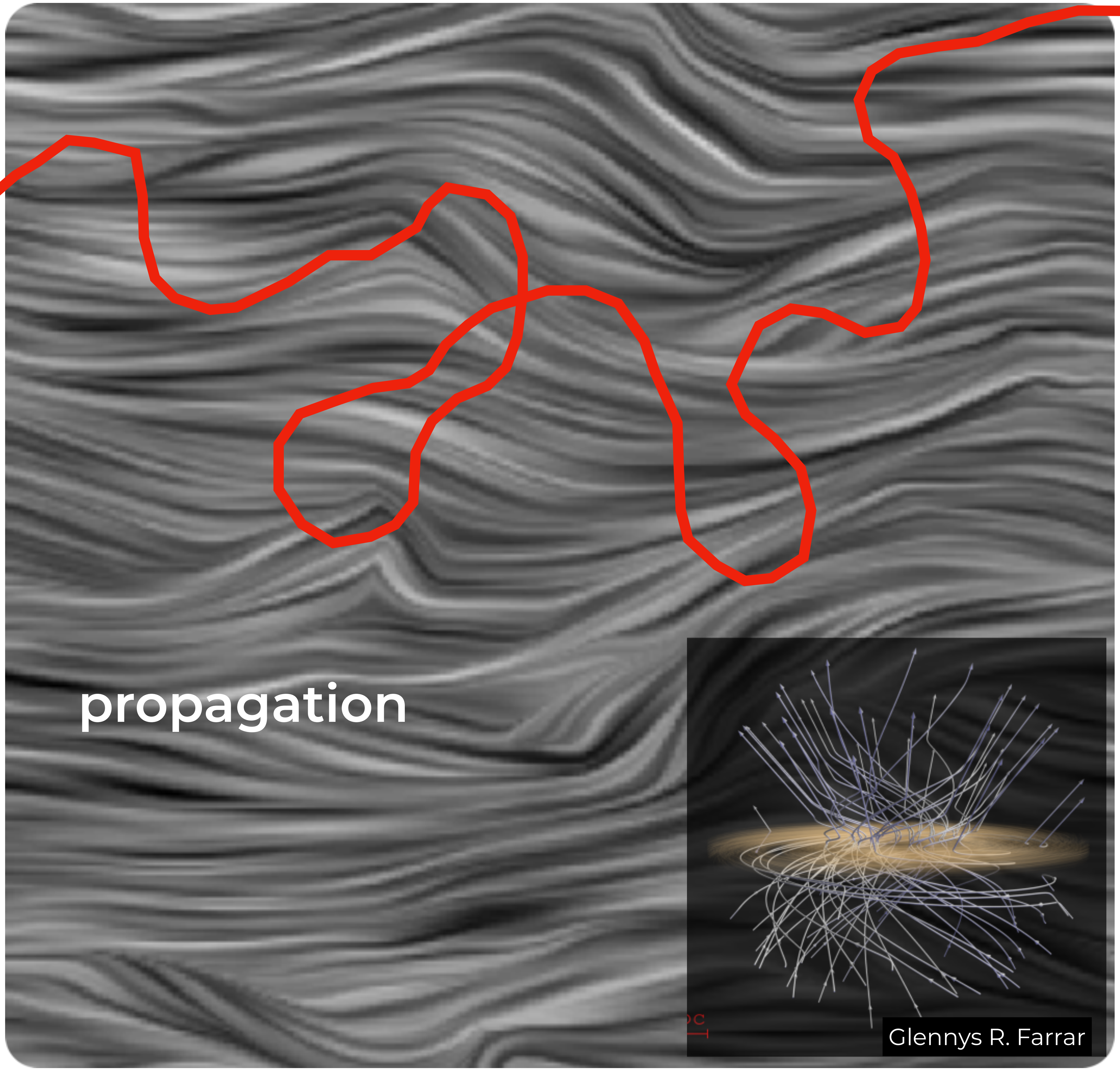

Earth's atmosphere dynamic target

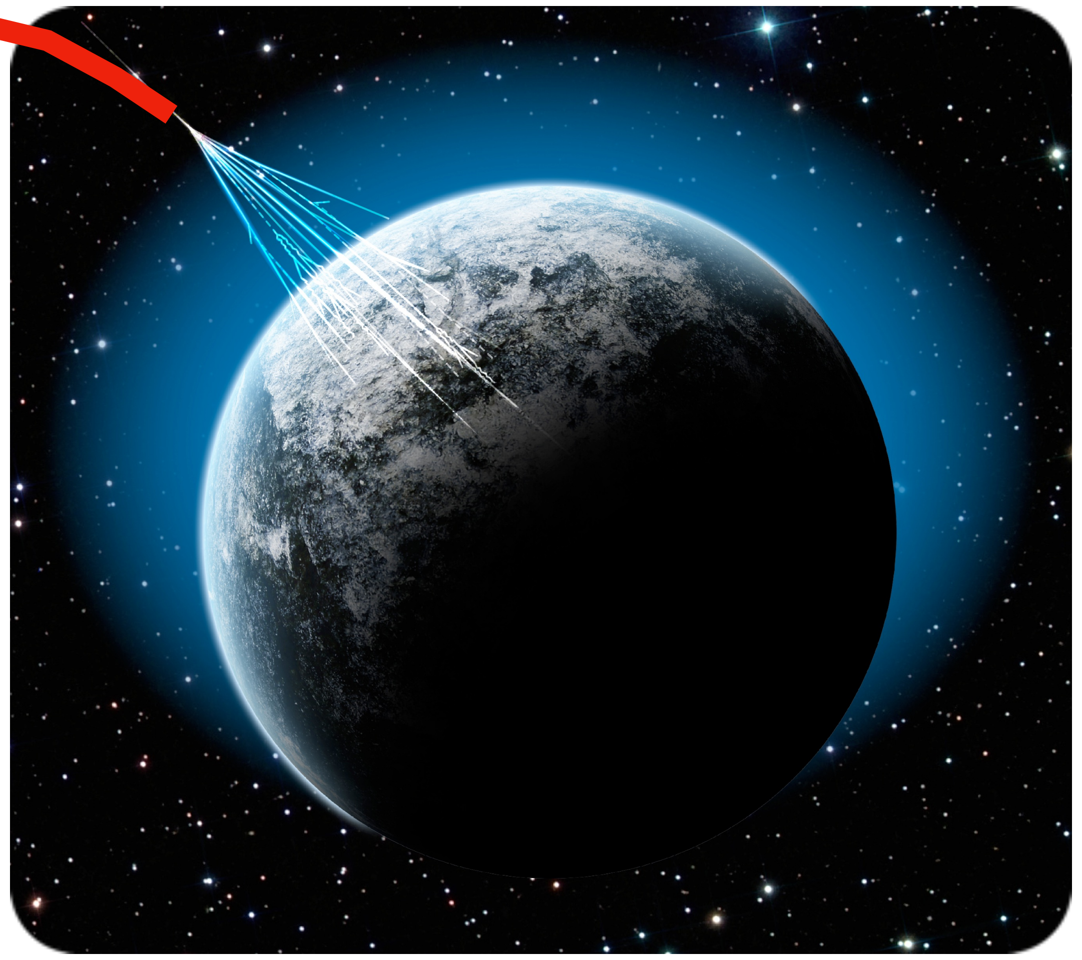

ground-based detection

nuclear & hadronic processes

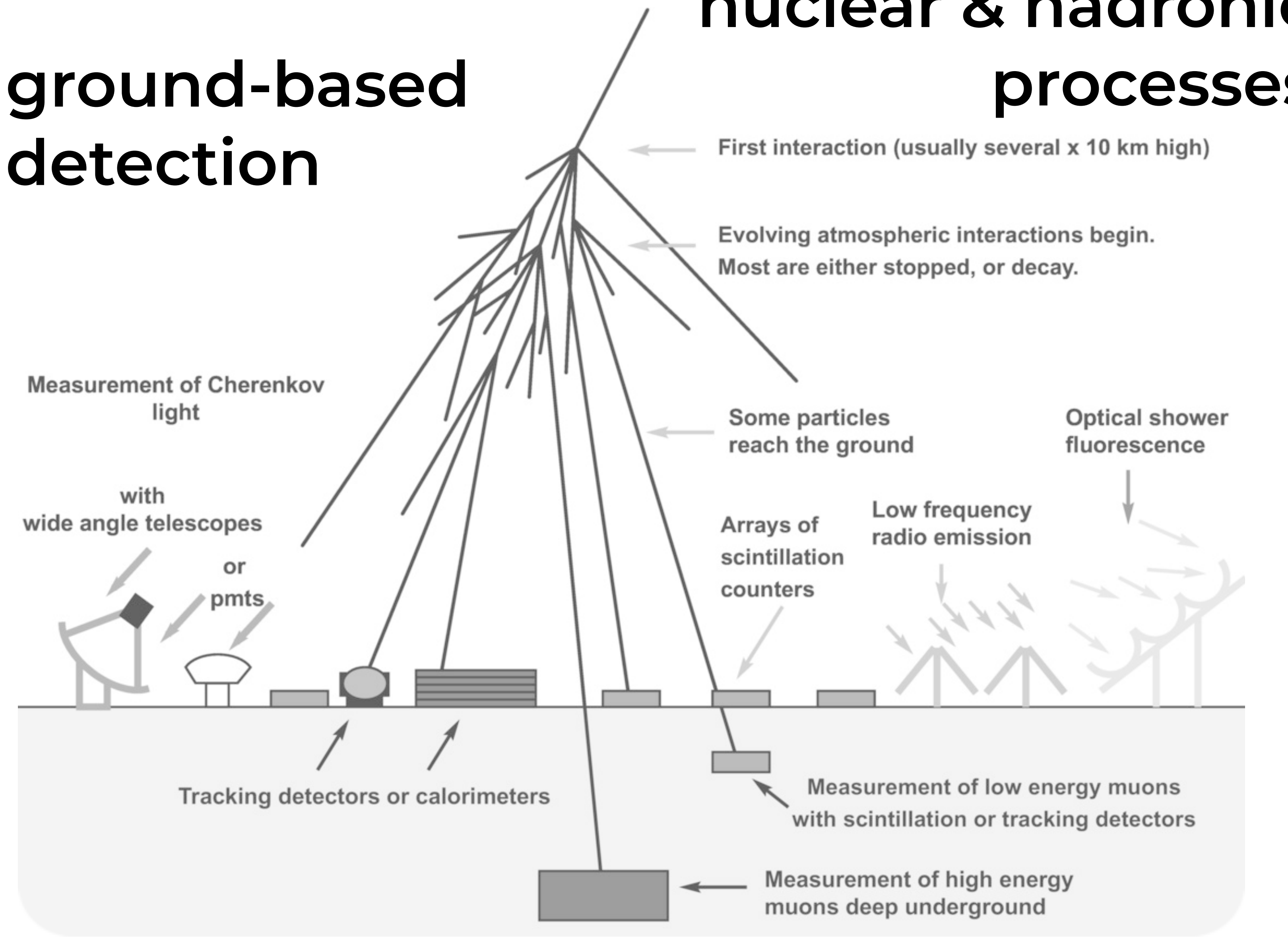

summary

energy range

1 TeV - 10 PeV

anisotropy ~10^{-3}

- Anisotropy observations
- Dipole and medium-scale anisotropy
- How do we make observations useful?
- Need for multi-experiment observations

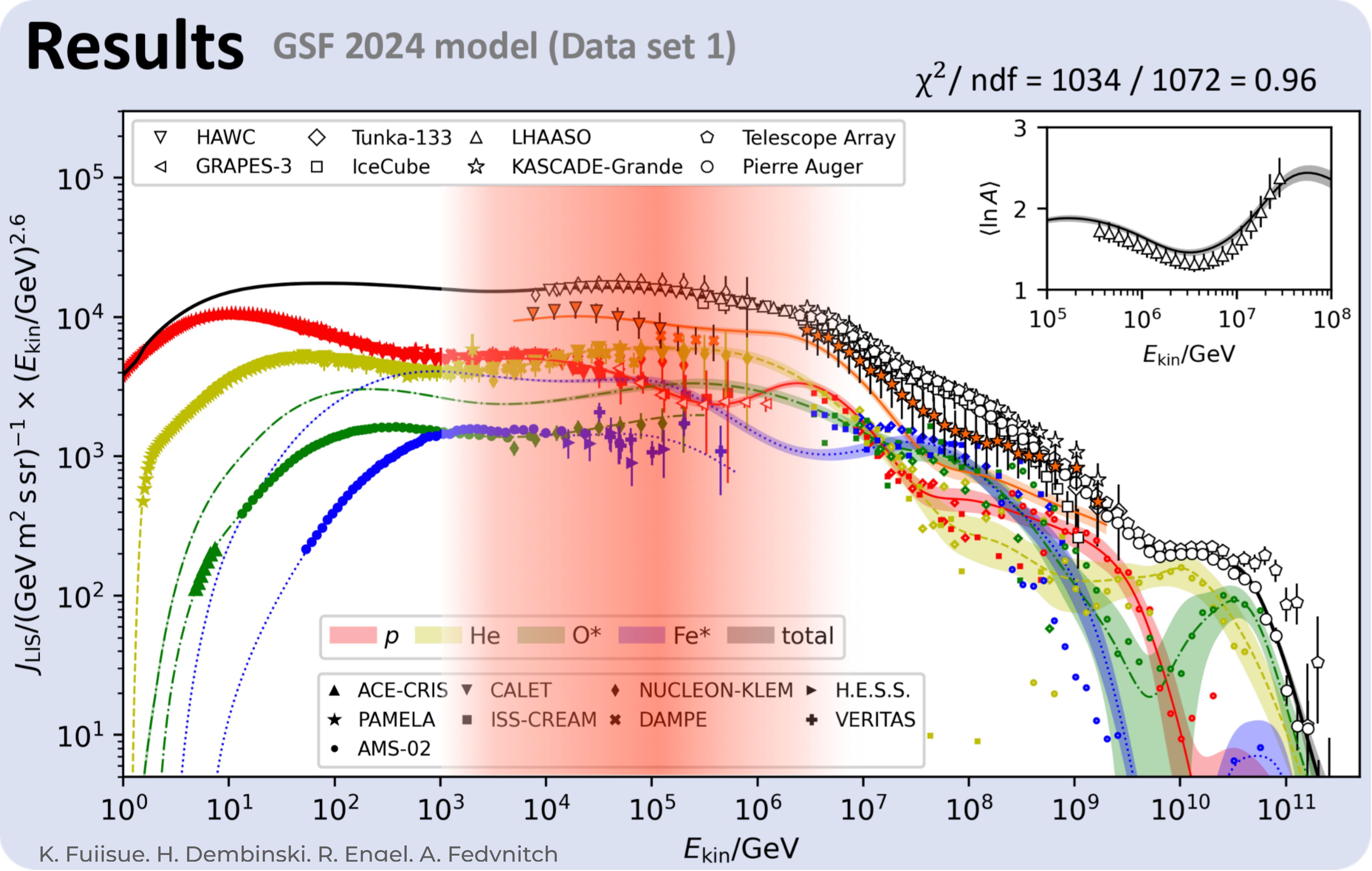

cosmic-ray experiments

twenty years

of high statistics anisotropy data

TA P-ONE KASCADE EAS-TOP Km3NET Tibet-ASγ

Baikal-GVD

Milagro ARGO-YBJ

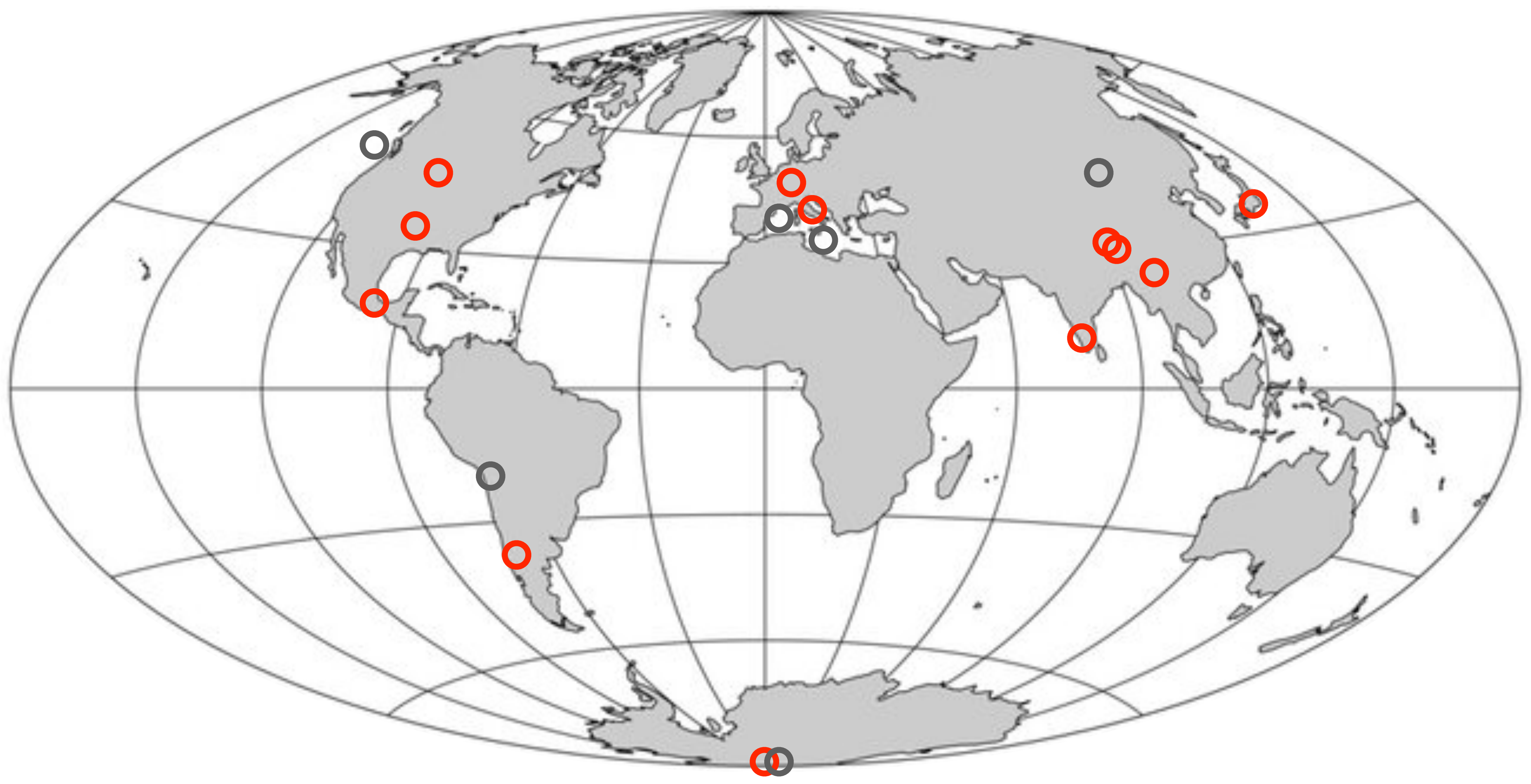

HAWC LHAASO

SWGO Super-K

Auger IceCube GRAPES-3

IceCube-Gen2

"Due to the small size of the anisotropies, quantitative studies require careful separation of detector effects from the observations."

how to measure anisotropy

N_i

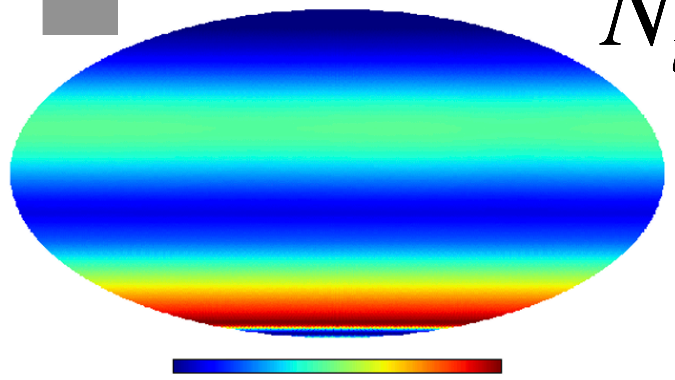

data count/pixel

Build a binned **data map** using the equatorial coordinates of the events

$\langle N_i \rangle$

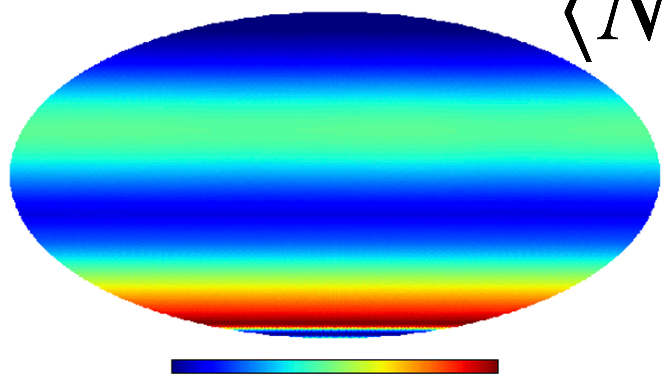

isotropy count/pixel

Construct a **reference map** by integrating acceptance over 24 hours

Time-scrambling $(\theta, \phi, t) \rightarrow (\alpha, \delta) \quad (\theta, \phi, t') \rightarrow (\alpha', \delta')$

Likelihood (Ahlers+, 2016)

$$\lambda = \frac{\mathscr{L}(n \,|\, I, \mathscr{N}, \mathscr{A})}{\mathscr{L}(n \,|\, I^{(0)}, \mathscr{N}^{(0)}, \mathscr{A}^{(0)})}$$

Correlate pixels to increase sensitivity to different angular scales **(smoothing)**

$\delta I(\alpha, \delta)_i$

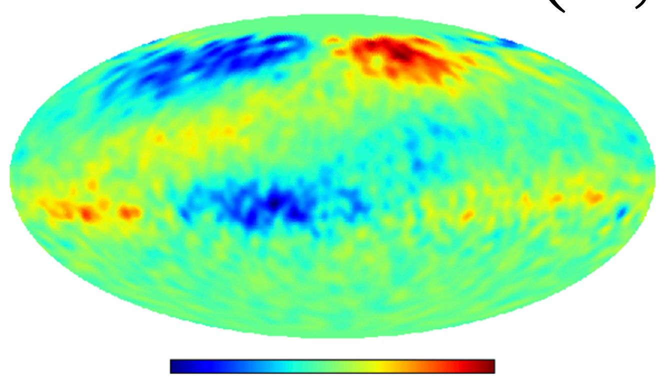

relative intensity

Calculate **relative differences** between data and reference with significance

$$\delta I(\alpha, \delta)_i = \frac{N(\alpha, \delta)_i - \langle N \rangle(\alpha, \delta)_i}{\langle N \rangle(\alpha, \delta)_i}$$

s_i

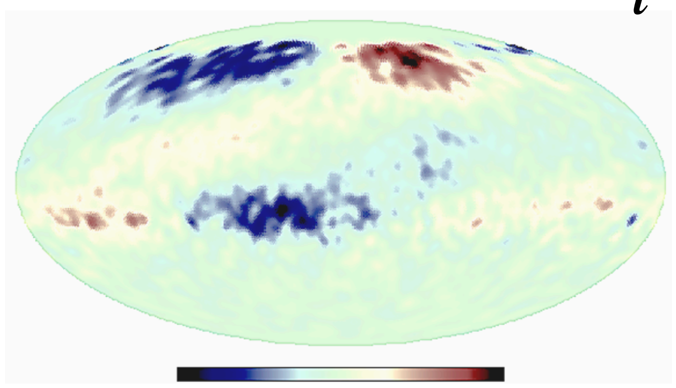

significance

Calculate **statistical significance** for each pixel

$$s_i = \sqrt{2} \left\{ N_i \log \left[\frac{1+\alpha}{\alpha} \left(\frac{N_i}{N_i + N_0} \right) \right] + N_0 \log \left[(1+\alpha) \left(\frac{N_0}{N_i + N_0} \right) \right] \right\}^{1/2}$$

Li and Ma (1993)

consequences of measuring anisotropy

2

N_i

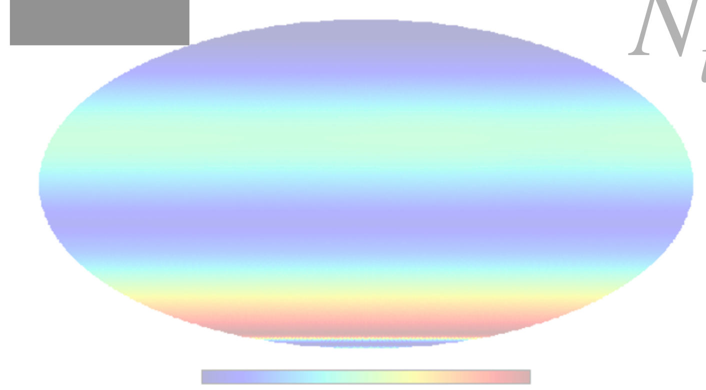

data count/pixel

$\langle N_i \rangle$

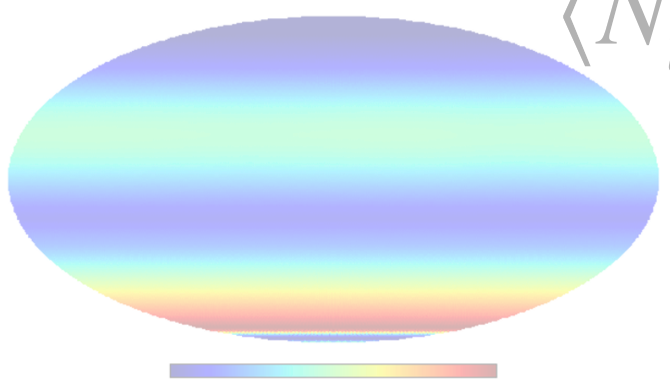

isotropy count/pixel

$\delta I(\alpha, \delta)_i$

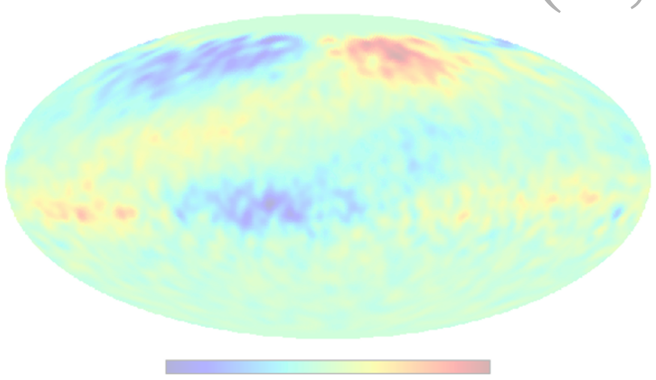

relative intensity

s_i

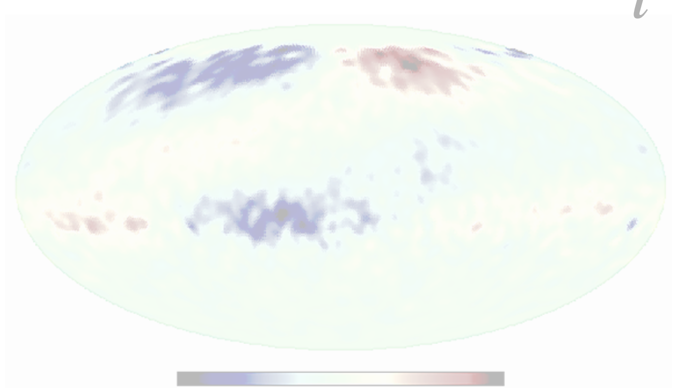

significance

The data-driven detection acceptance estimation *"scrambles the event's R.A. but not its declination, while keeping the events' local coordinates constant."*

This makes the **relative intensity average on R.A. equal to zero**

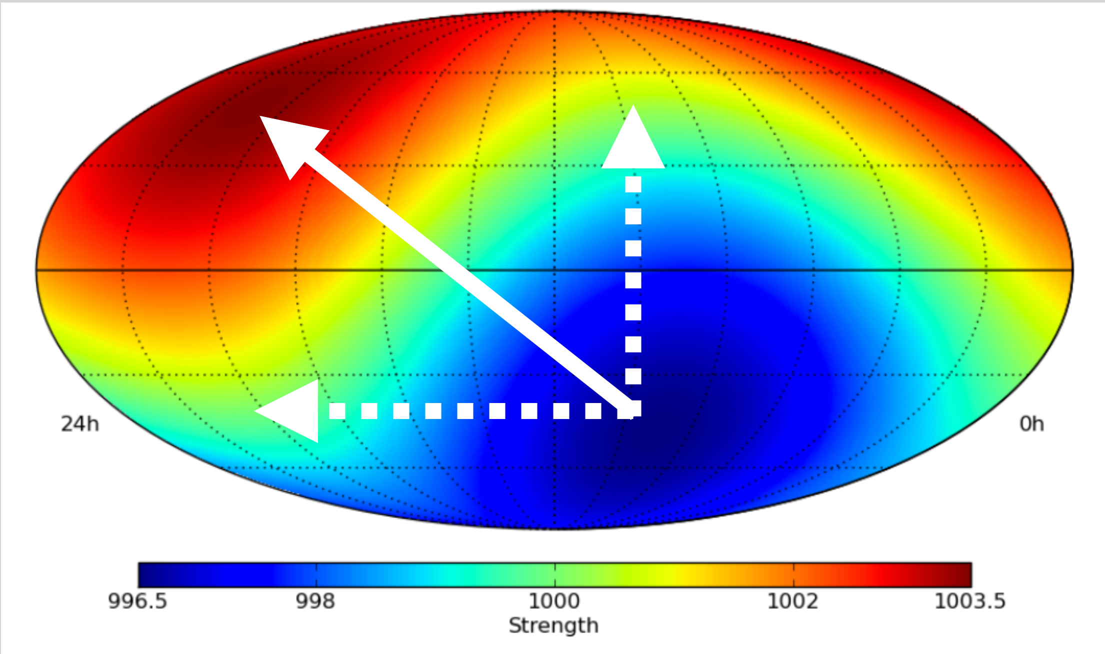

measurement methods ***eliminate*** the vertical component of the dipole

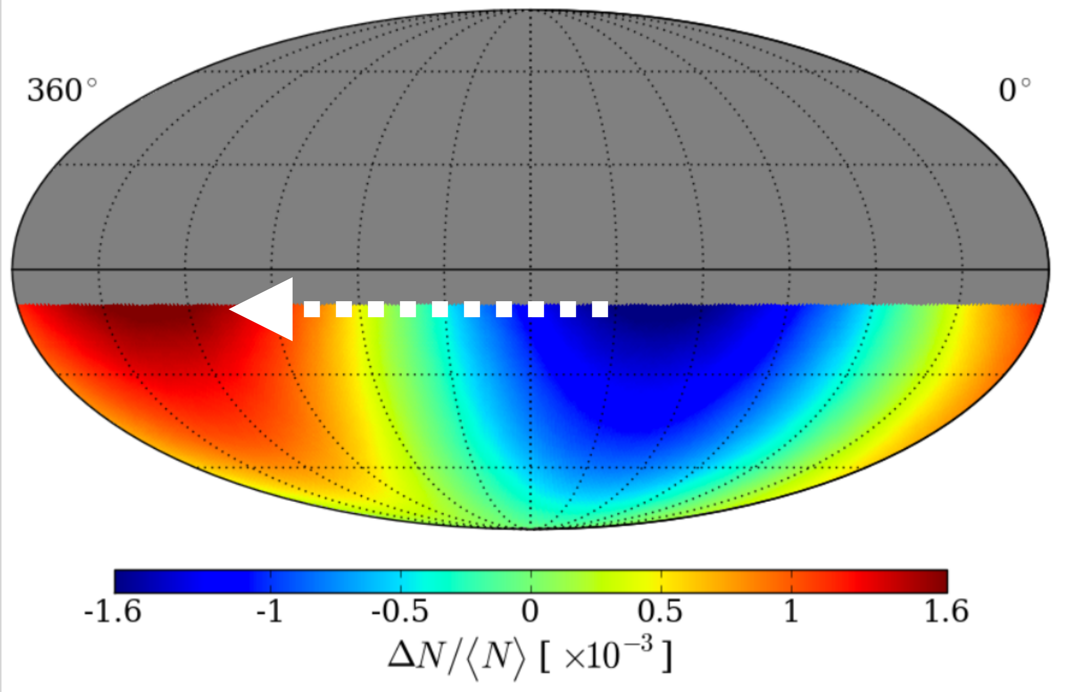

equatorial component of the dipole

3

observed anisotropy

Energy ~ 1-10 TeV

2 TeV

3 TeV

4.4 TeV

6.8 TeV

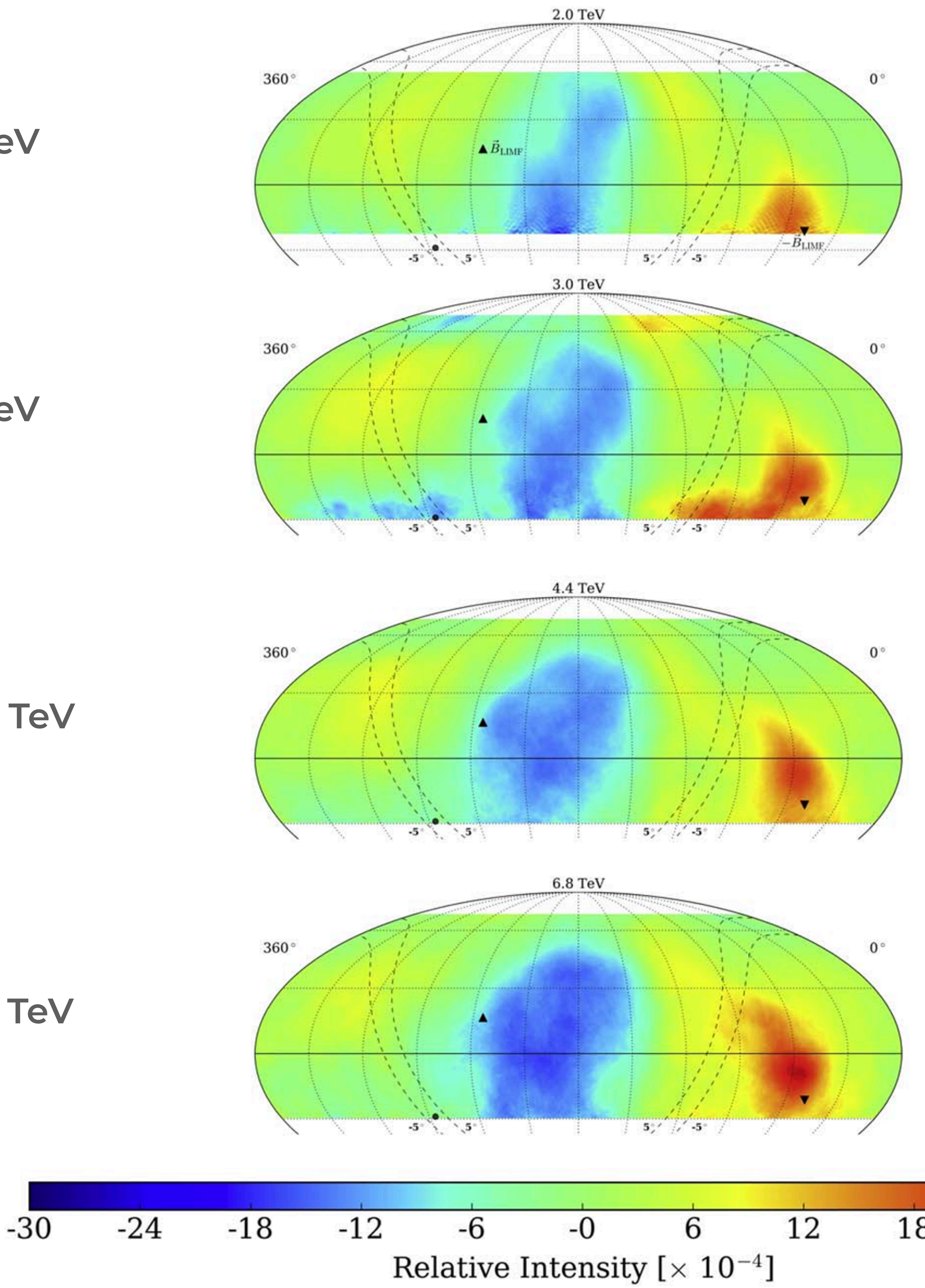

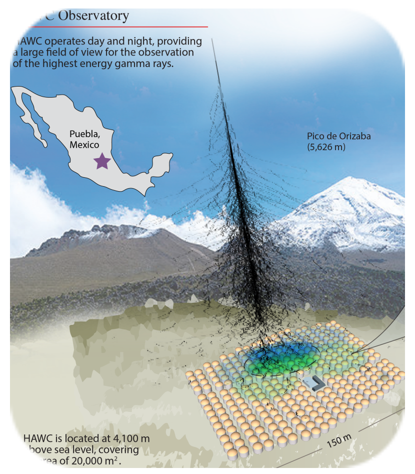

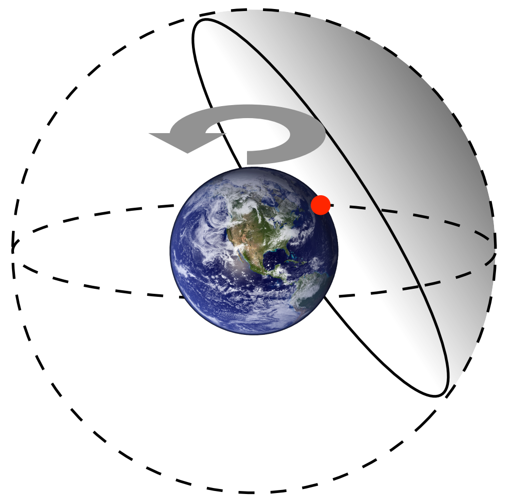

HAWC
ApJ 865 57 (2018)

2 observed anisotropy

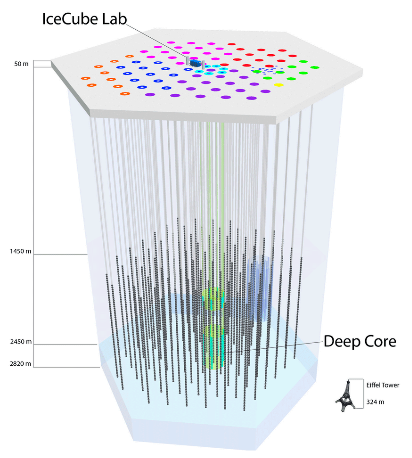

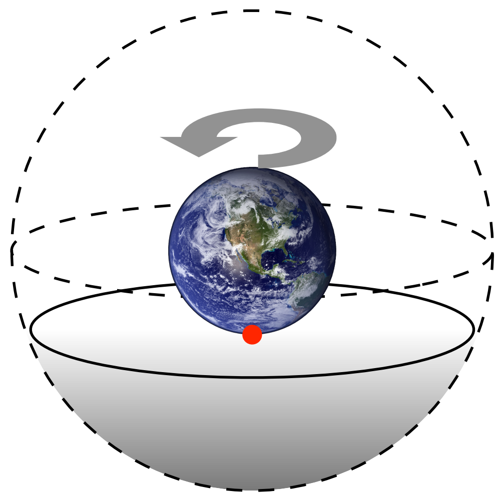

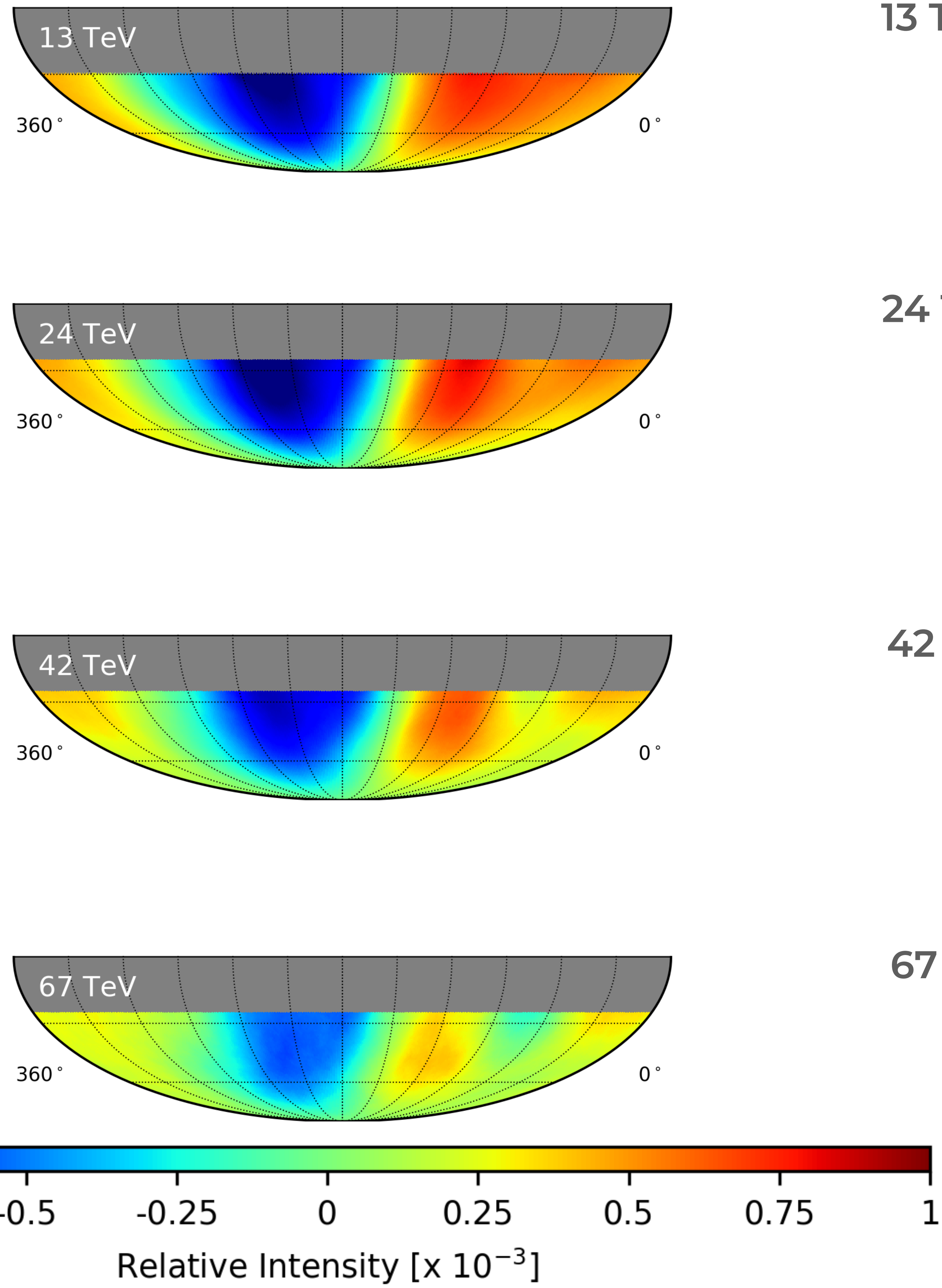

IceCube
[ApJ 981 182 (2025)]

Energy ~ 10-100 TeV

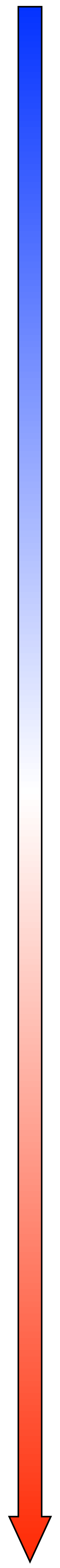

IceCube	HAWC
13 TeV	11.2 TeV
24 TeV	18.6 TeV
42 TeV	30.3 TeV
67 TeV	72.8 TeV

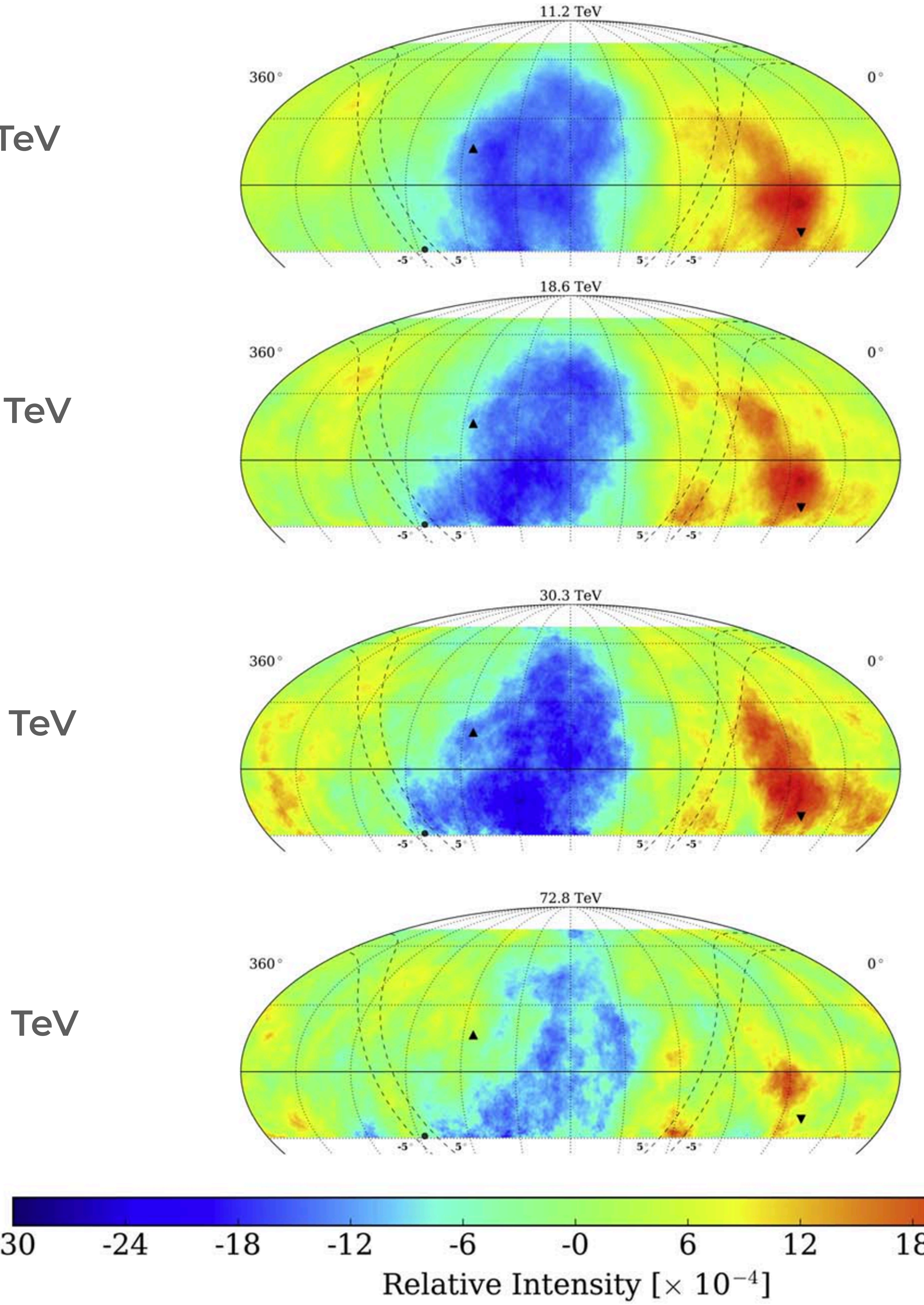

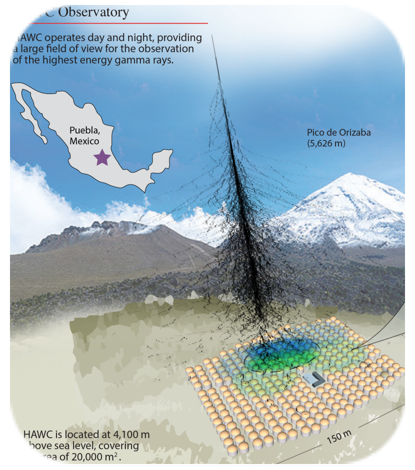

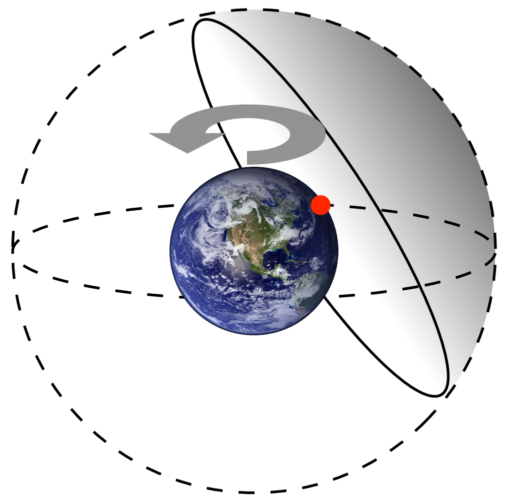

HAWC
[ApJ 865 57 (2018)]

3 observed anisotropy

Energy ~ 100-1000 TeV

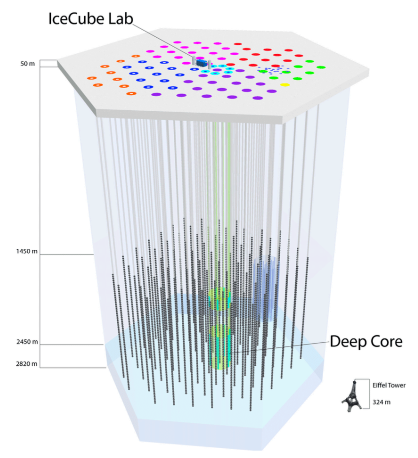

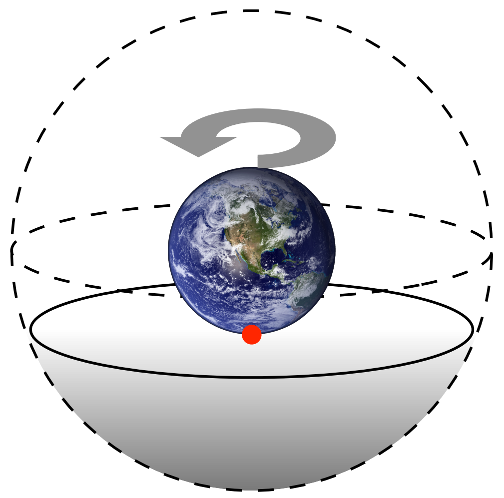

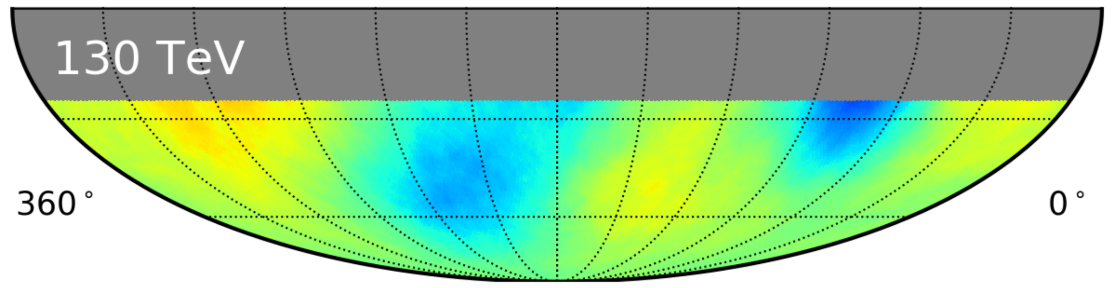

130 TeV

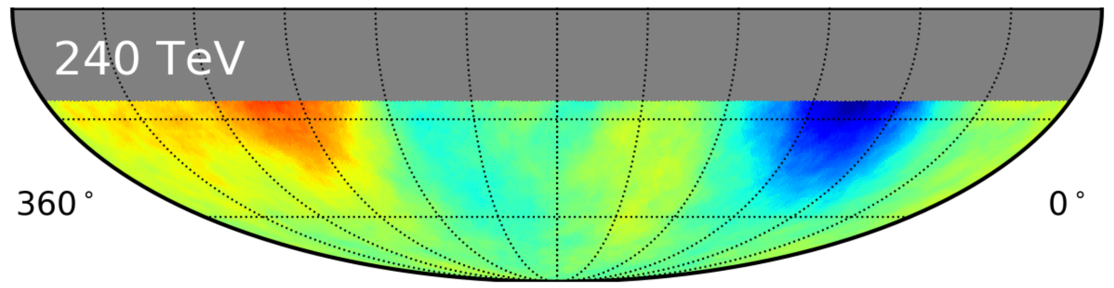

240 TeV

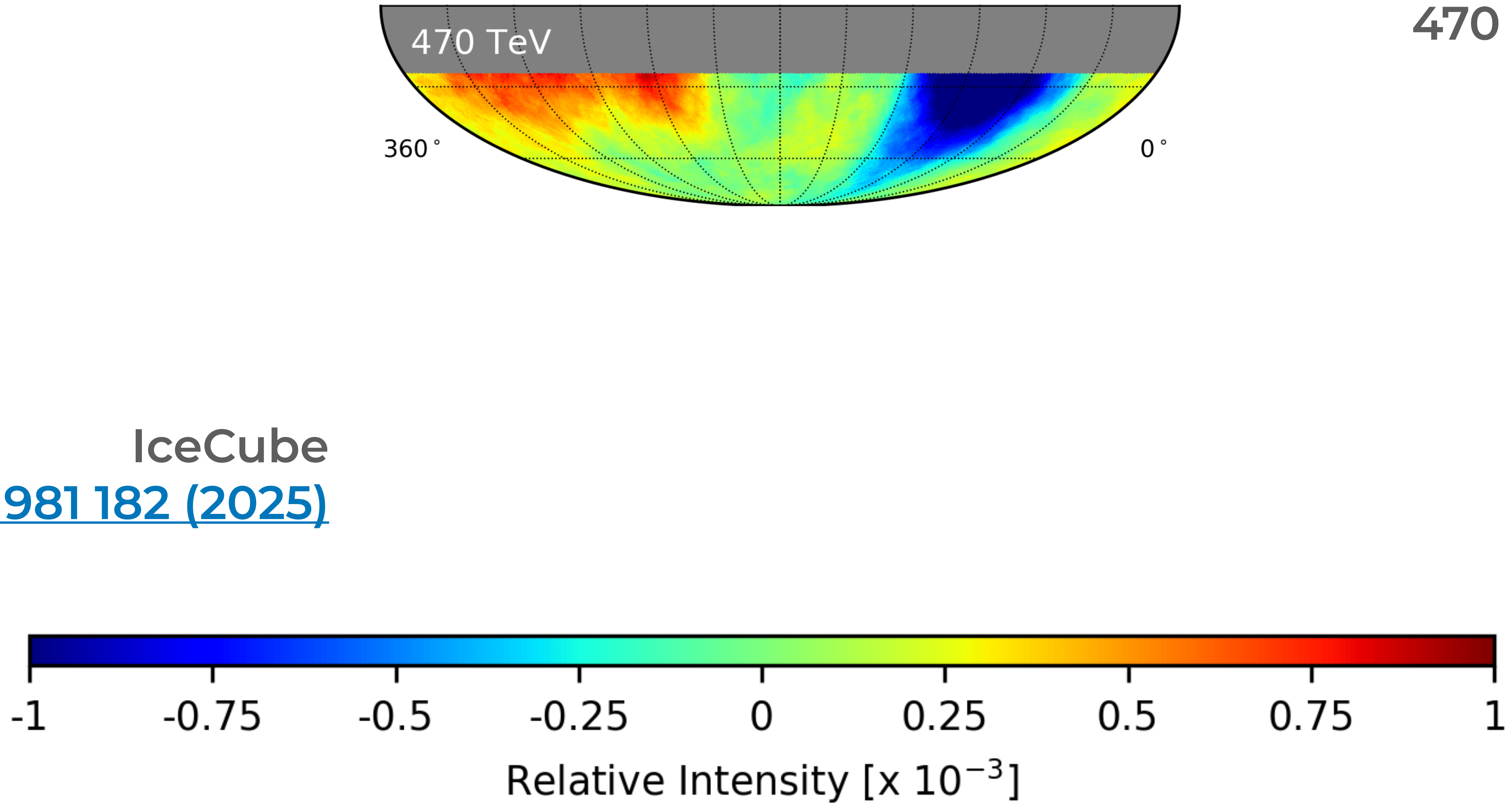

470 TeV

128 TeV

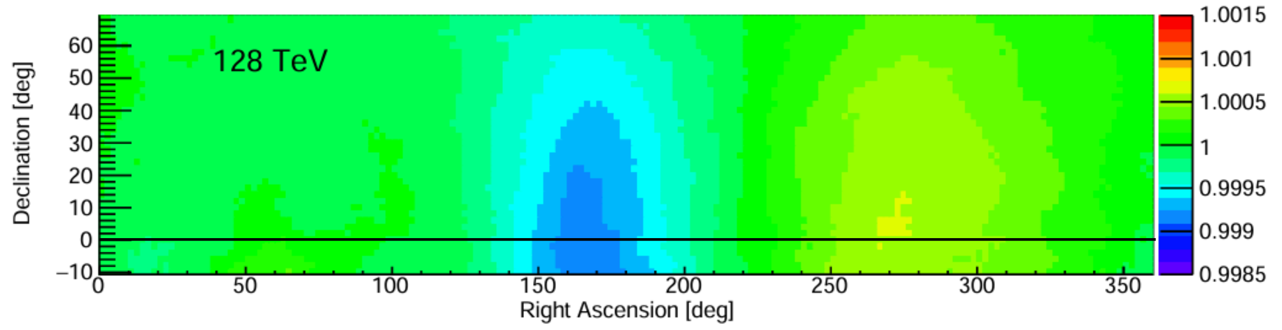

267 TeV

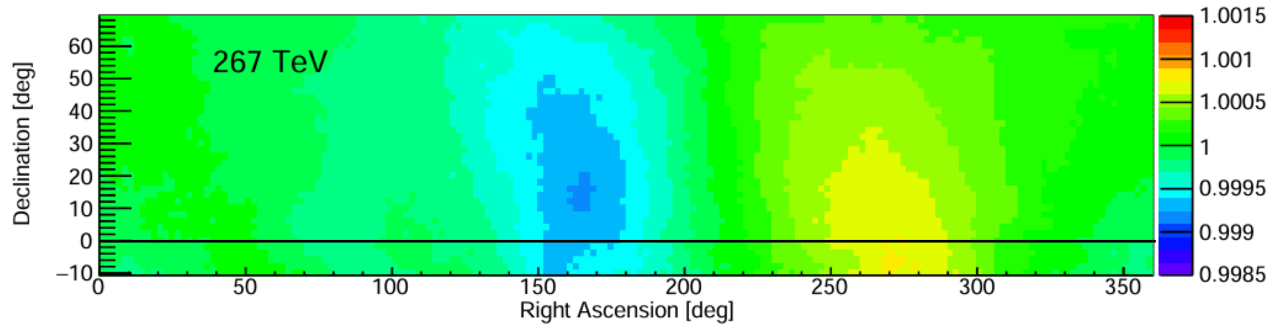

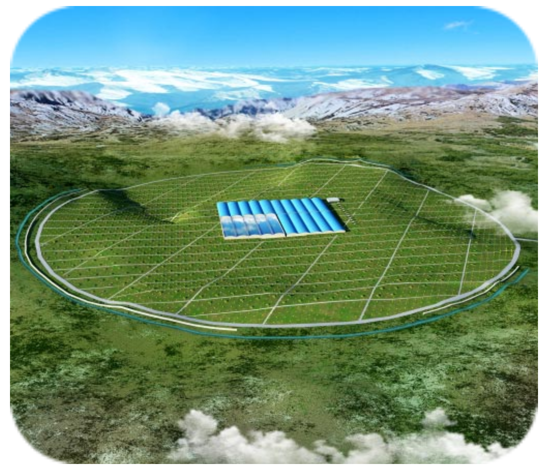

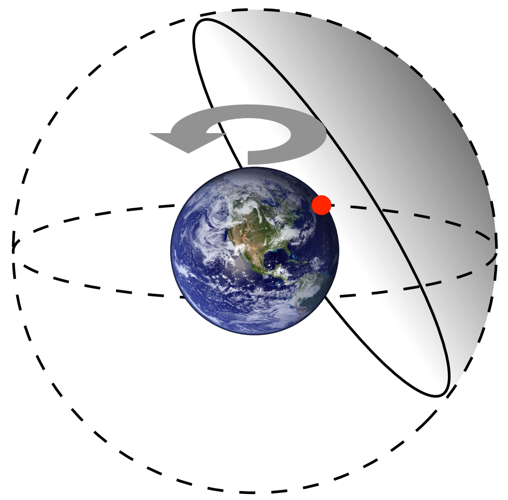

IceCube
[ApJ 981 182 (2025)]

LHAASO
[PoS(ICRC2023)478]

4 observed anisotropy

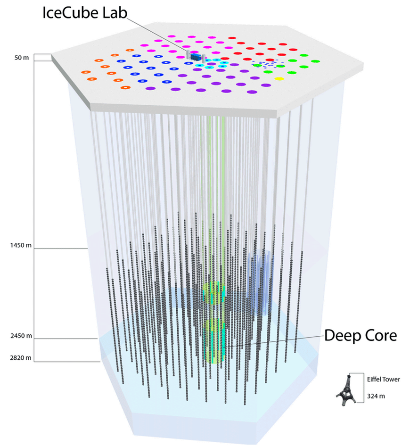

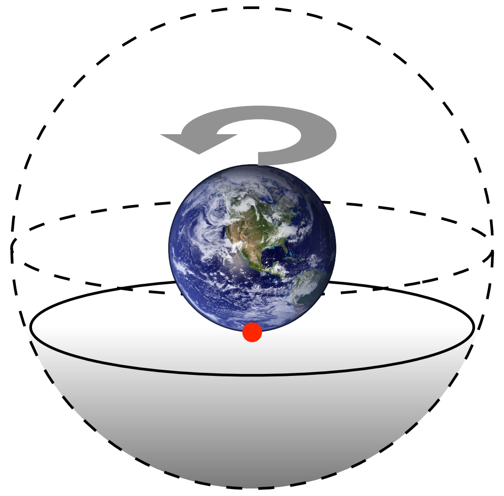

Energy ~ 1-10 PeV

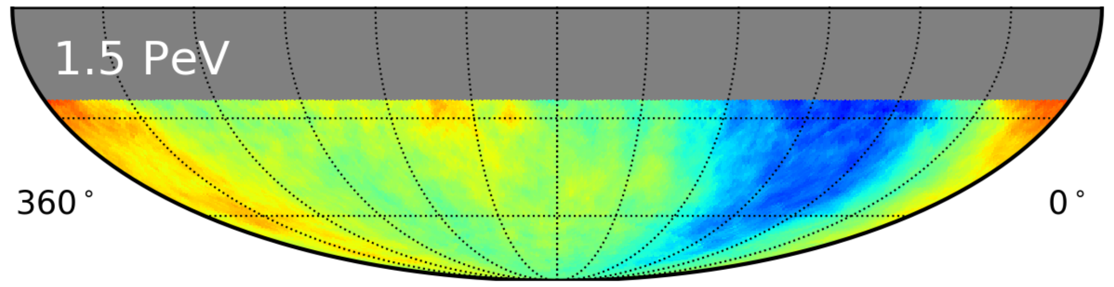

1.5 PeV

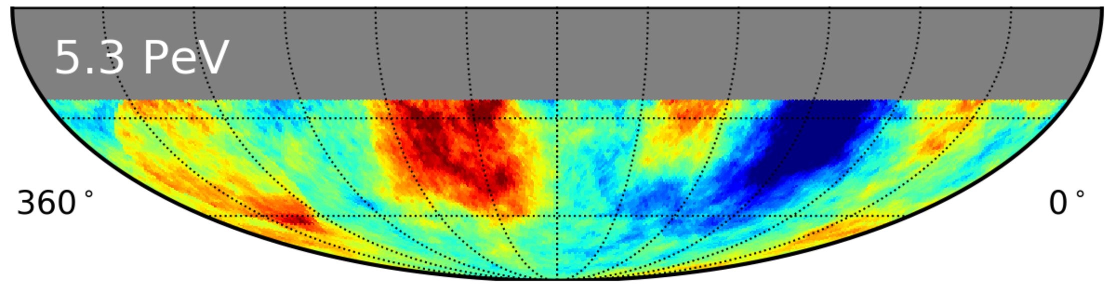

5.3 PeV

1 PeV

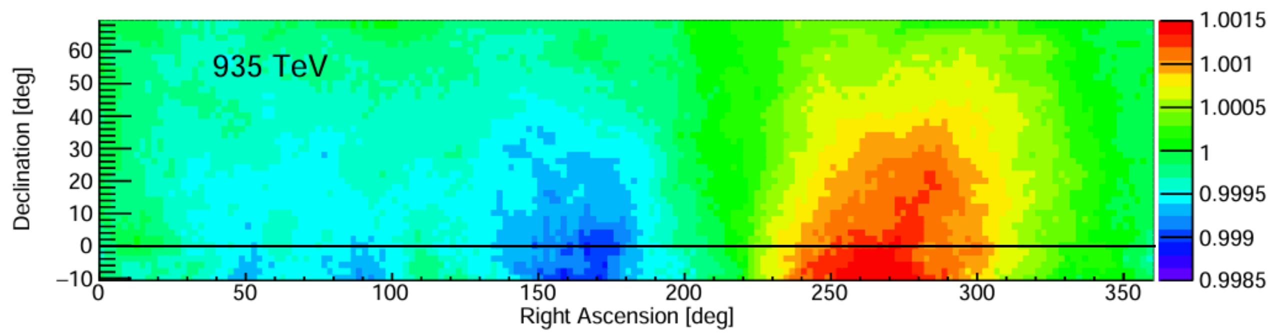

~10 PeV

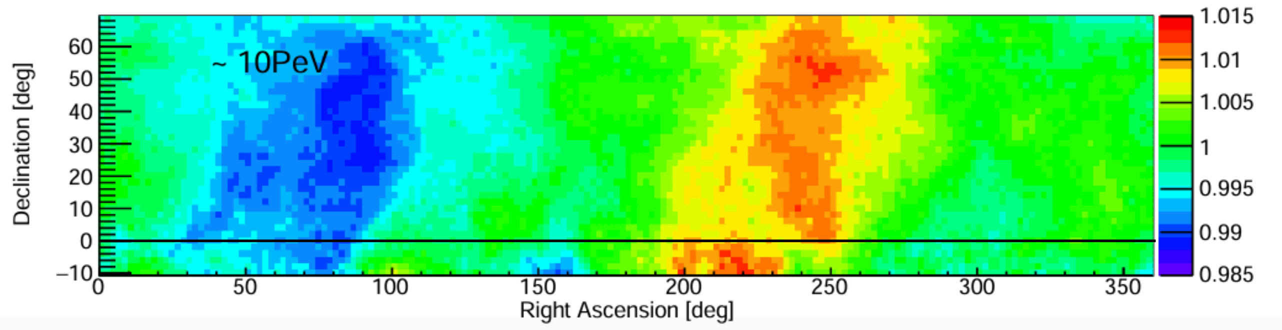

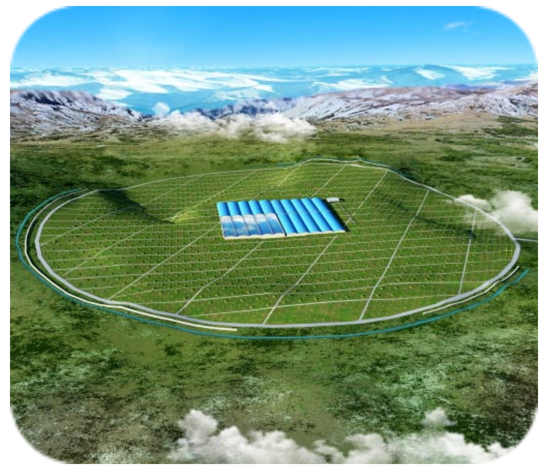

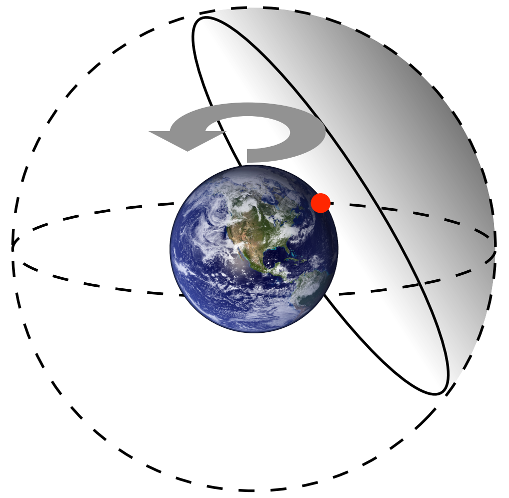

IceCube
[ApJ 981 182 (2025)]

LHAASO
[PoS(ICRC2023)478]

breaking down anisotropy
angular power spectrum

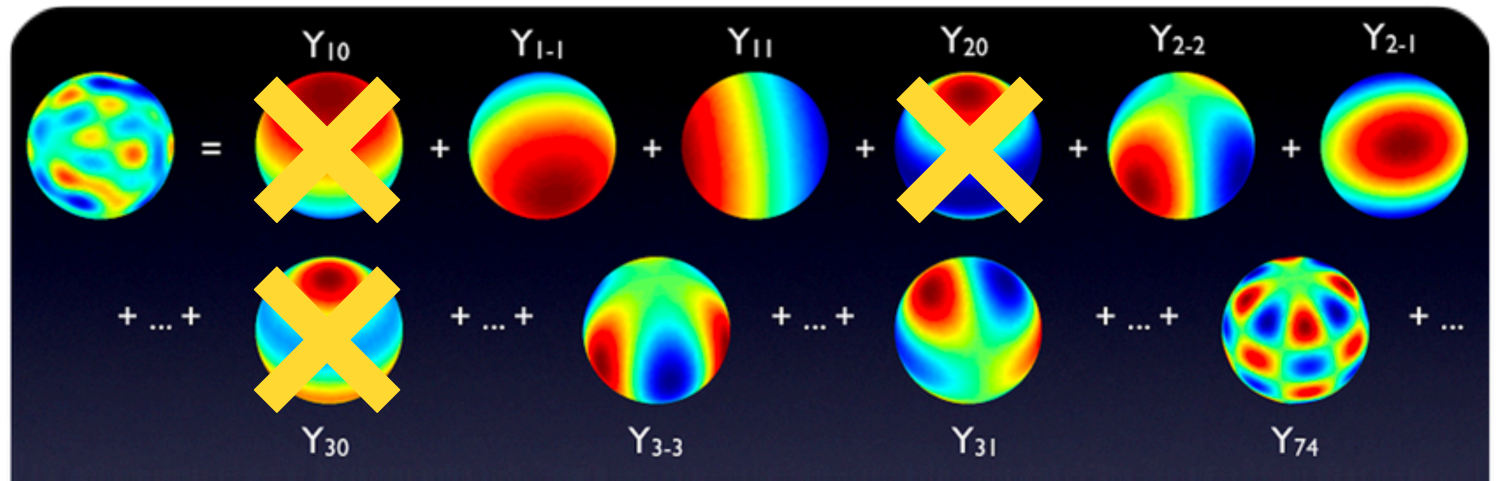

decomposing the relative intensity sky map in Spherical Harmonics functions

$$\delta I(\alpha,\delta)_i = \sum_{\ell=1}^{\infty} \sum_{m=-\ell}^{\ell} a_{\ell m} Y_{\ell m}(\alpha,\delta)_i$$

$$C_\ell = \frac{1}{2\ell+1} \sum_{m=-\ell}^{\ell} |a_{\ell m}|^2$$

$$\tilde{C}_\ell = \frac{1}{2\ell+1} \sum_{m=-\ell, m\neq 0}^{\ell} |\hat{a}_{\ell m}|^2$$

IceCube
ApJ 981 182 (2025)

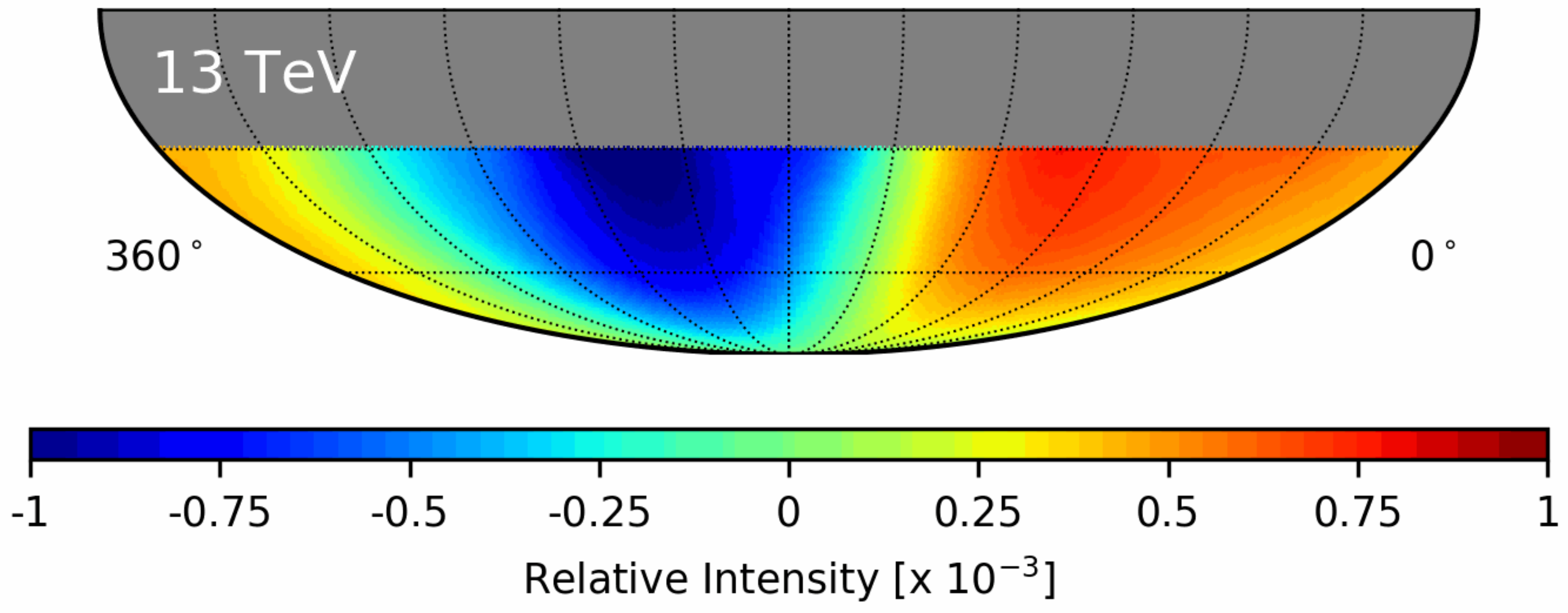

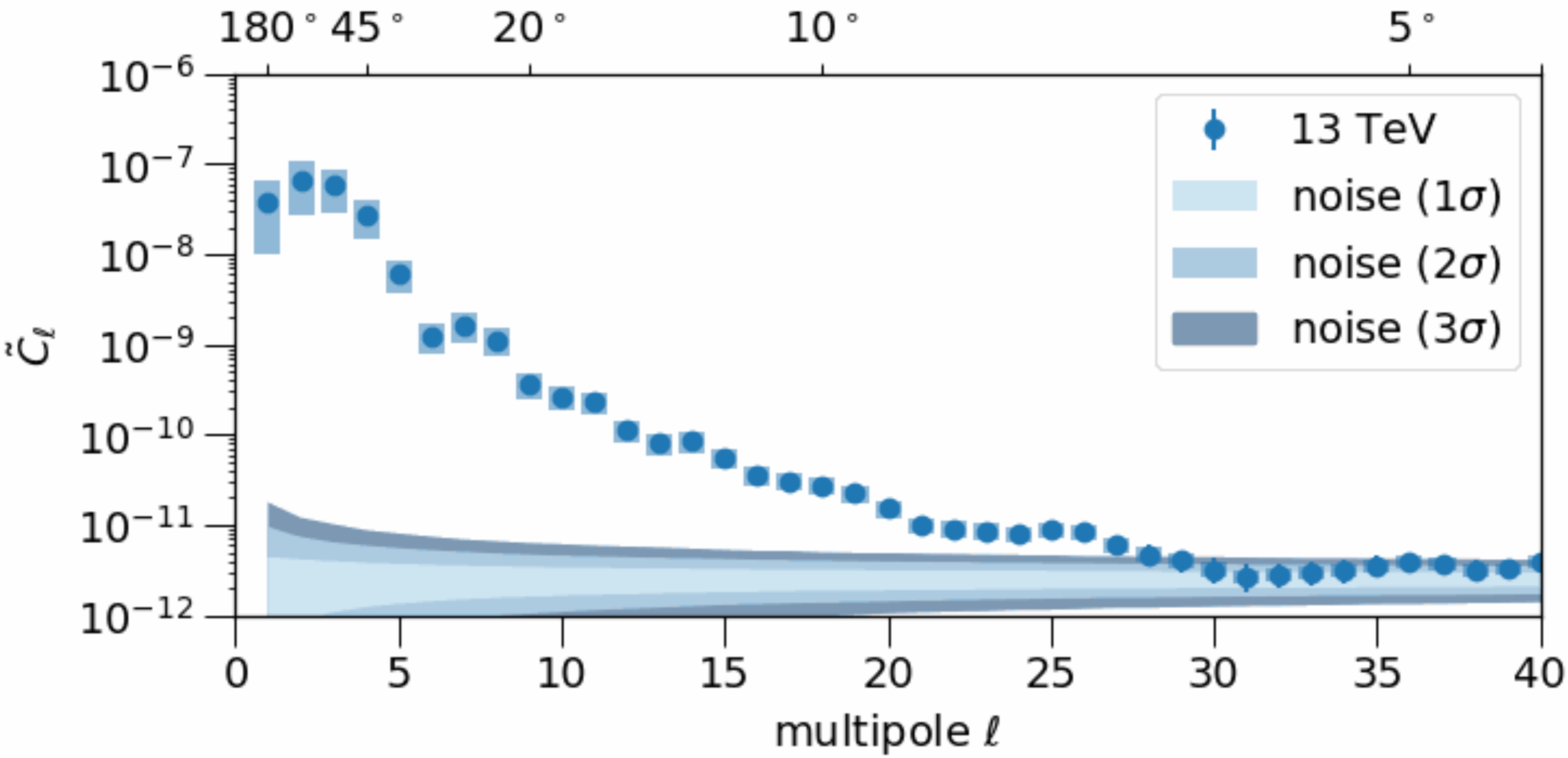

the dipole component

decomposing the relative intensity sky map in Spherical Harmonics functions

$$\delta I(\alpha,\delta)_i = \sum_{\ell=1}^{\infty}\sum_{m=-\ell}^{\ell} a_{\ell m} Y_{\ell m}(\alpha,\delta)_i$$

$$C_\ell = \frac{1}{2\ell+1}\sum_{m=-\ell}^{\ell} |a_{\ell m}|^2$$

$$\tilde{C}_\ell = \frac{1}{2\ell+1}\sum_{m=-\ell, m\neq 0}^{\ell} |\hat{a}_{\ell m}|^2$$

IceCube
ApJ 981 182 (2025)

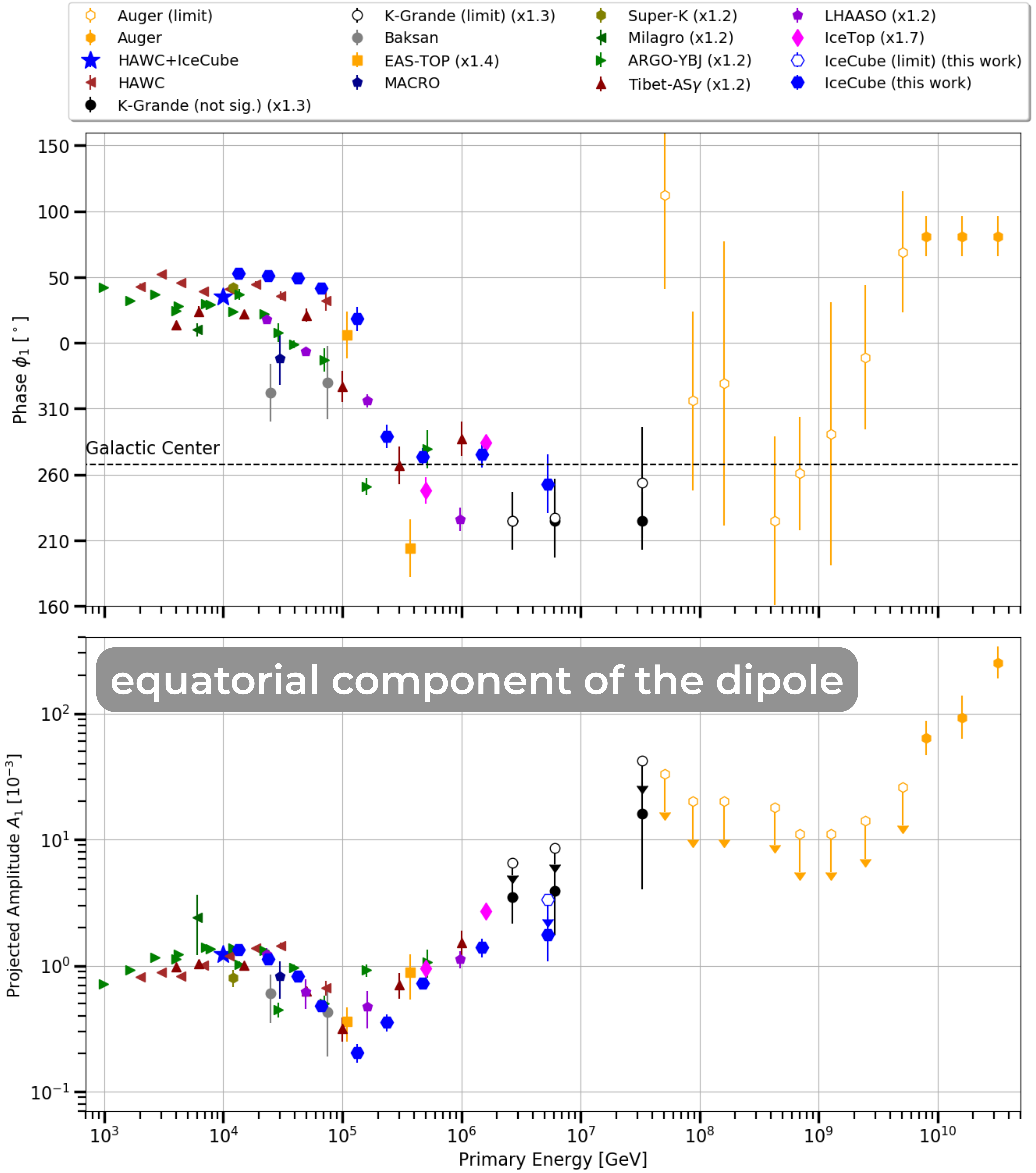

large & small scale anisotropy

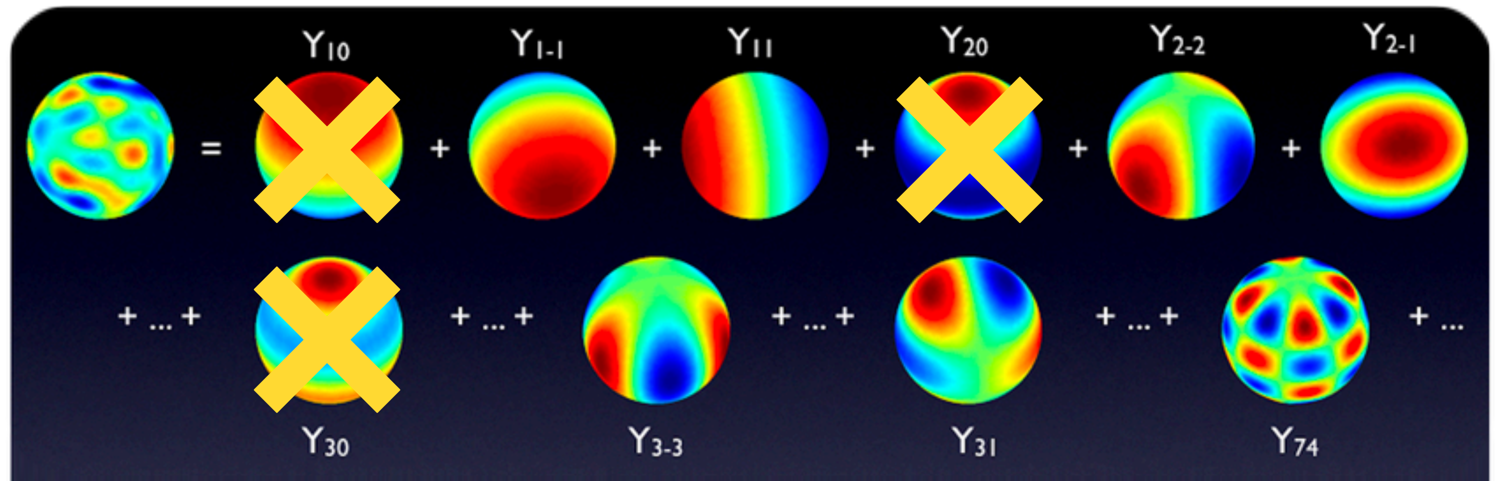

$$\delta I(\alpha,\delta)_i = \sum_{\ell=1}^{\infty}\sum_{m=-\ell}^{\ell} a_{\ell m} Y_{\ell m}(\alpha,\delta)_i$$

$$\mathcal{C}_\ell = \frac{1}{2\ell+1}\sum_{m=-\ell}^{\ell} |a_{\ell m}|^2$$

$$\tilde{\mathcal{C}}_\ell = \frac{1}{2\ell+1}\sum_{m=-\ell, m\neq 0}^{\ell} |\hat{a}_{\ell m}|^2$$

IceCube
ApJ 981 182 (2025)

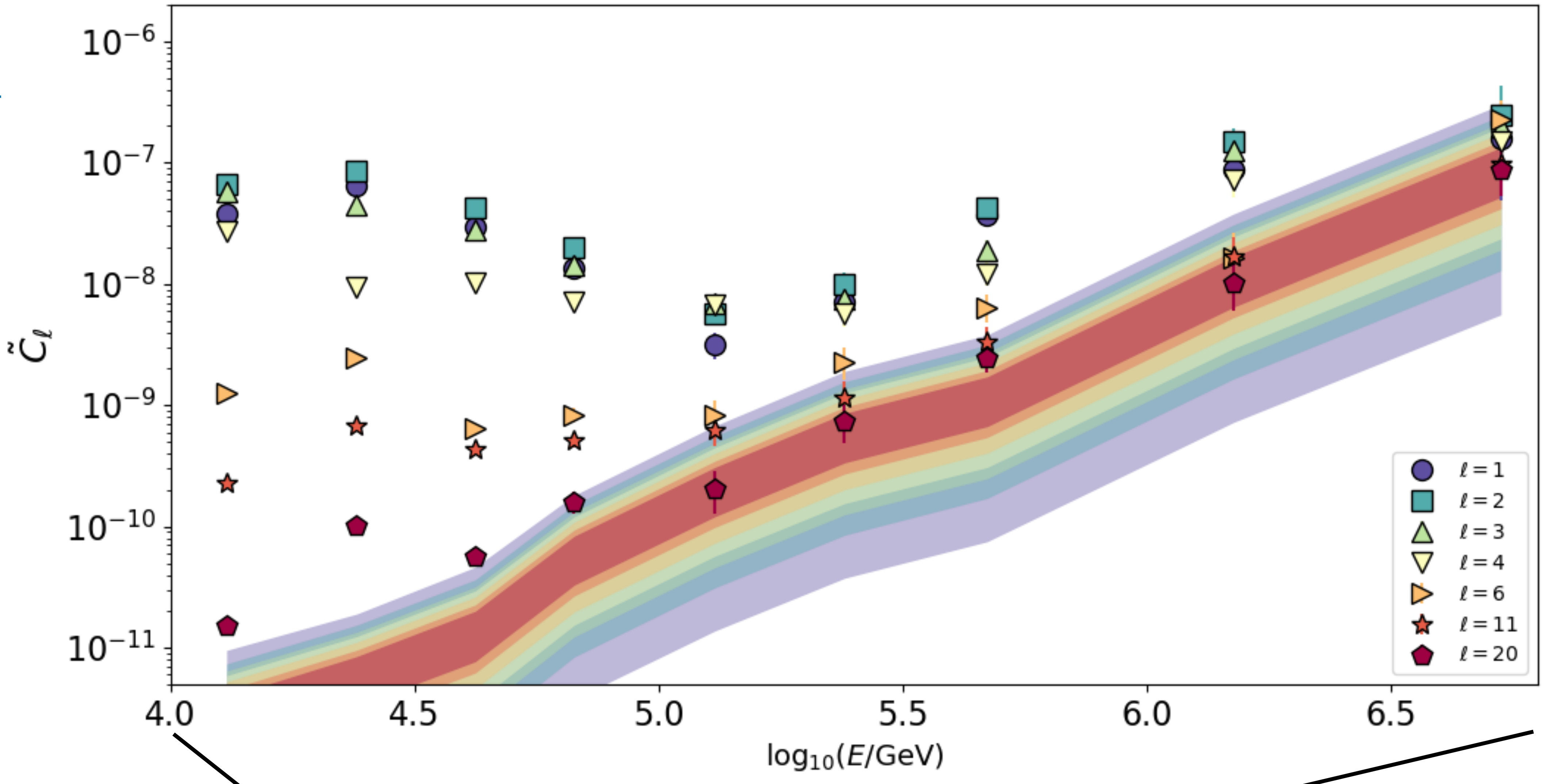

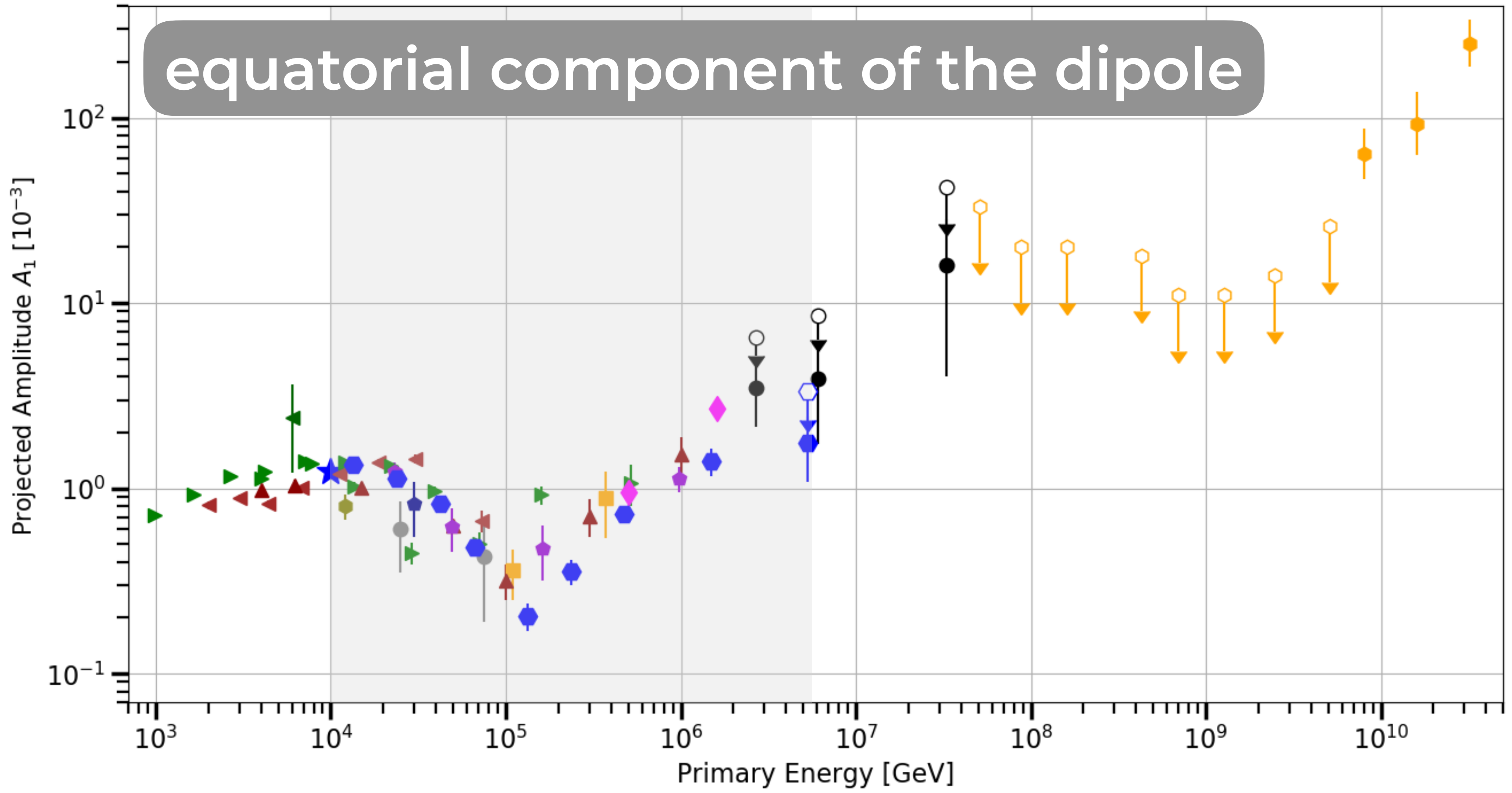

large & small scale anisotropy

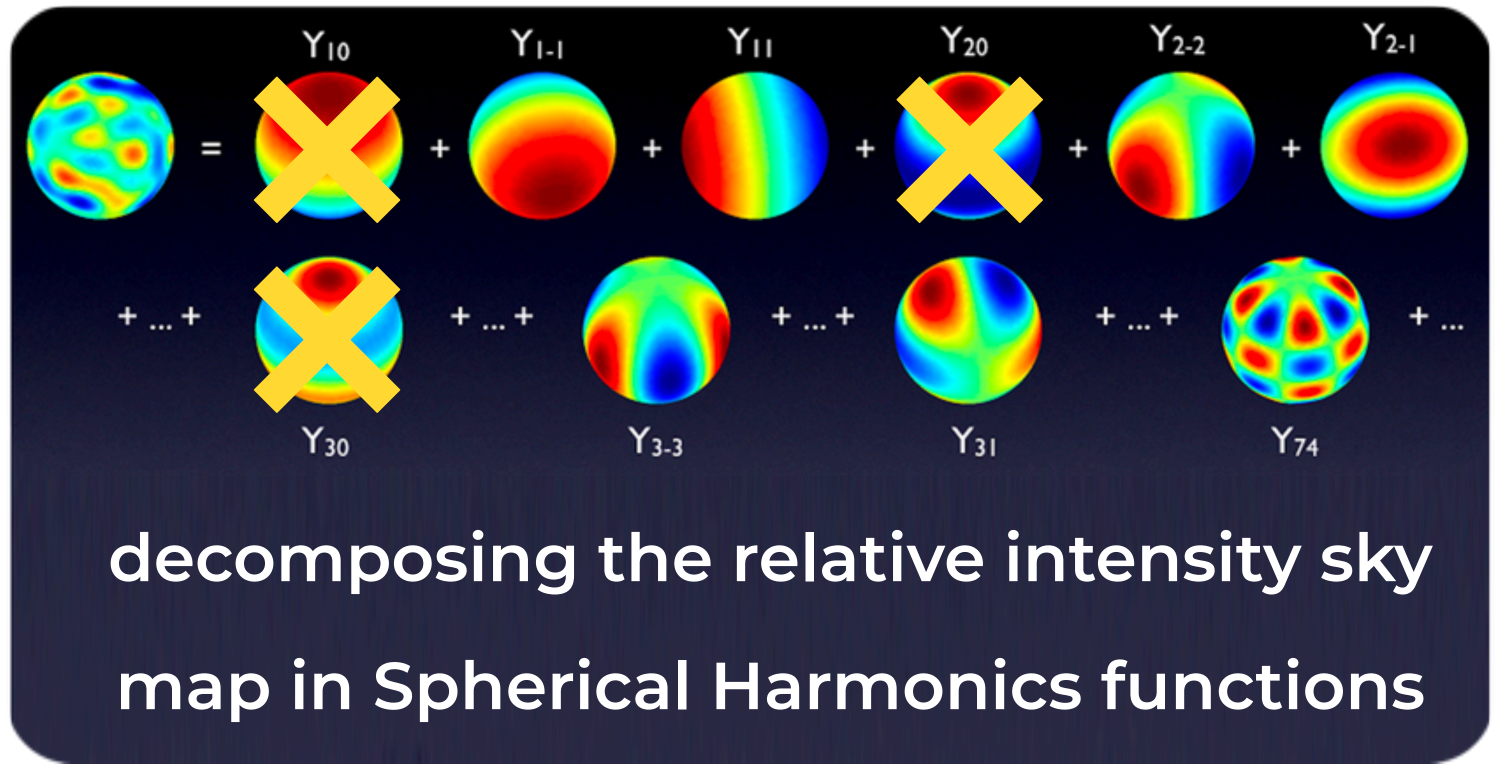

IceCube
ApJ 981 182 (2025)

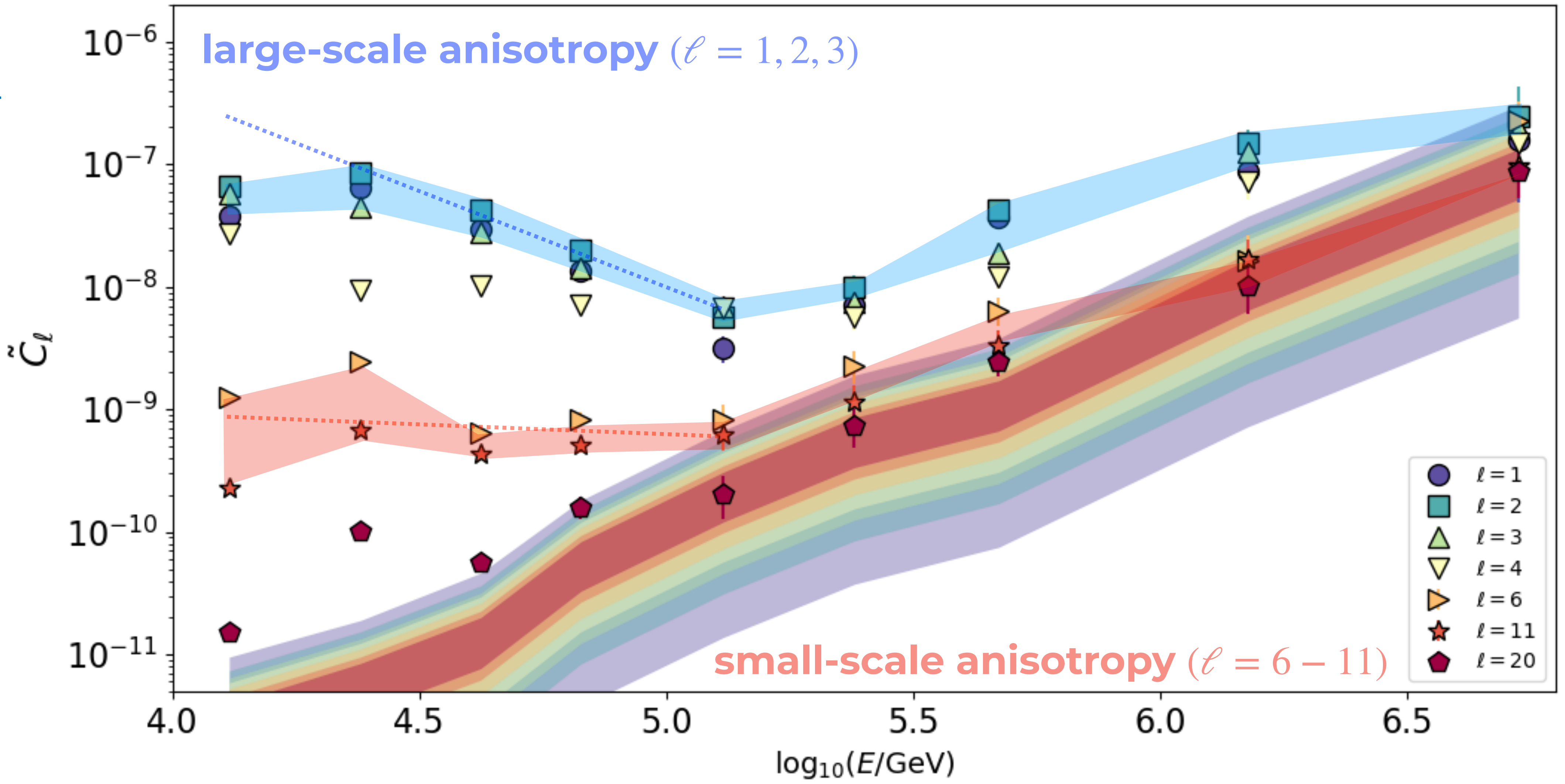

$$\delta I(\alpha,\delta)_i = \sum_{\ell=1}^{\infty} \sum_{m=-\ell}^{\ell} a_{\ell m} Y_{\ell m}(\alpha,\delta)_i$$

$$\mathcal{C}_\ell = \frac{1}{2\ell+1} \sum_{m=-\ell}^{\ell} |a_{\ell m}|^2$$

$$\tilde{\mathcal{C}}_\ell = \frac{1}{2\ell+1} \sum_{m=-\ell, m\neq 0}^{\ell} |\hat{a}_{\ell m}|^2$$

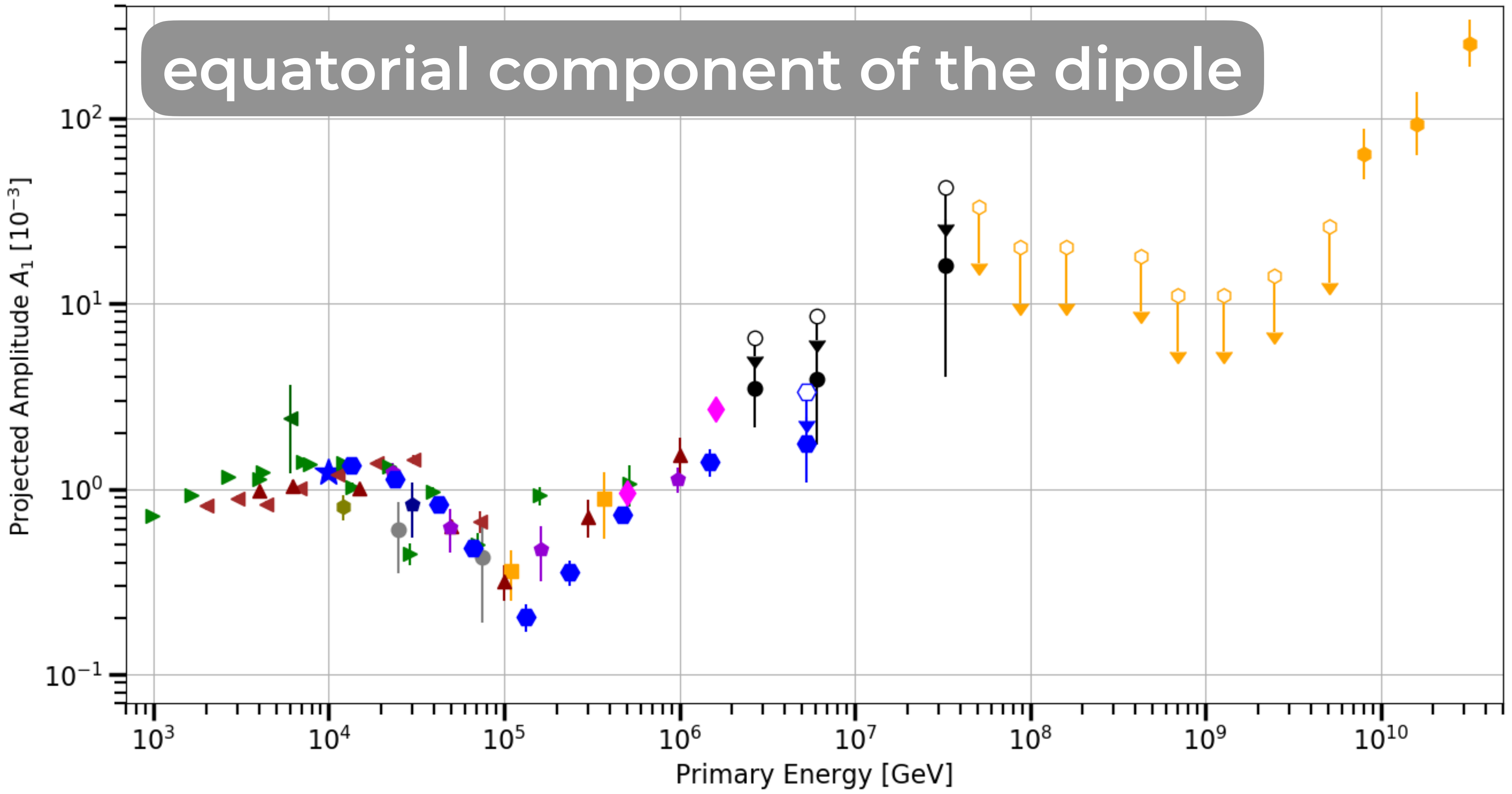

interstellar magnetic fields

Unger & Farrar (2024)

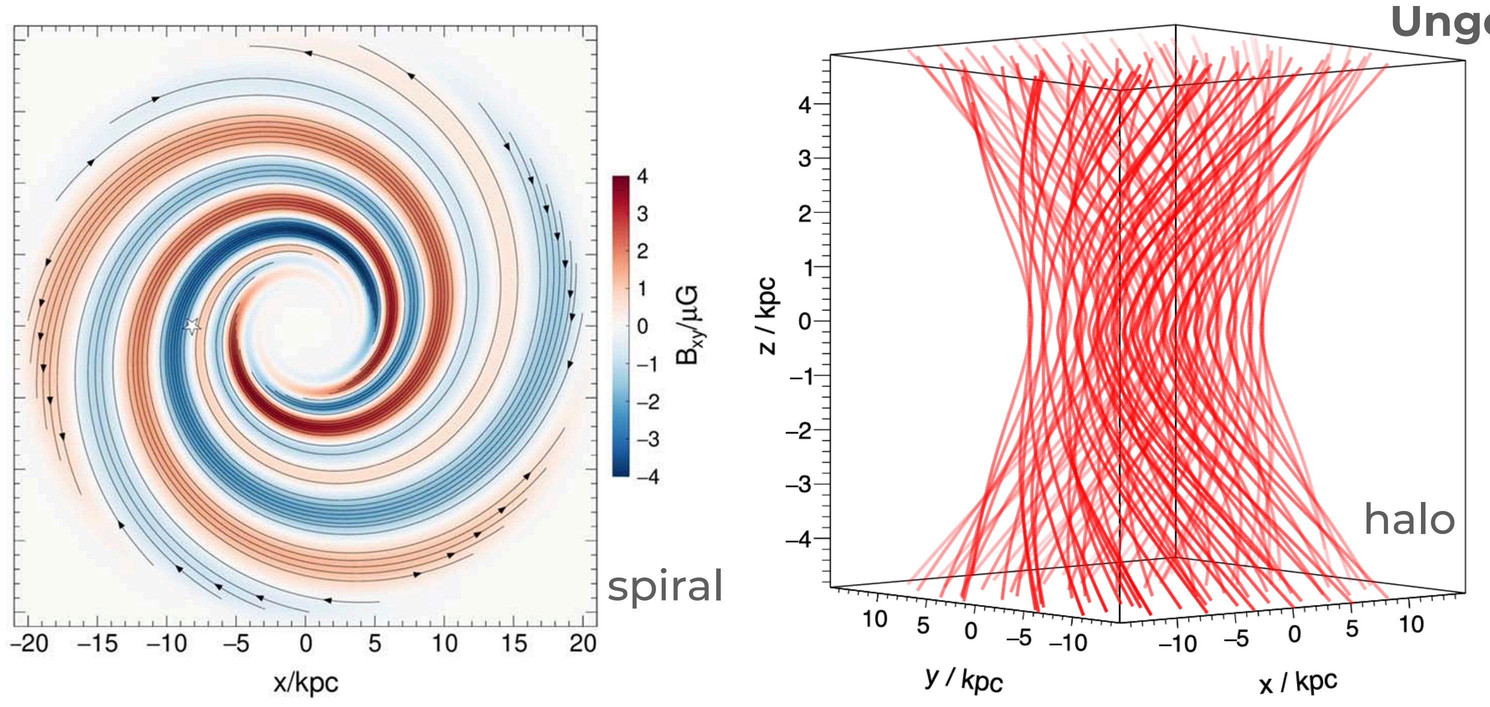

regular

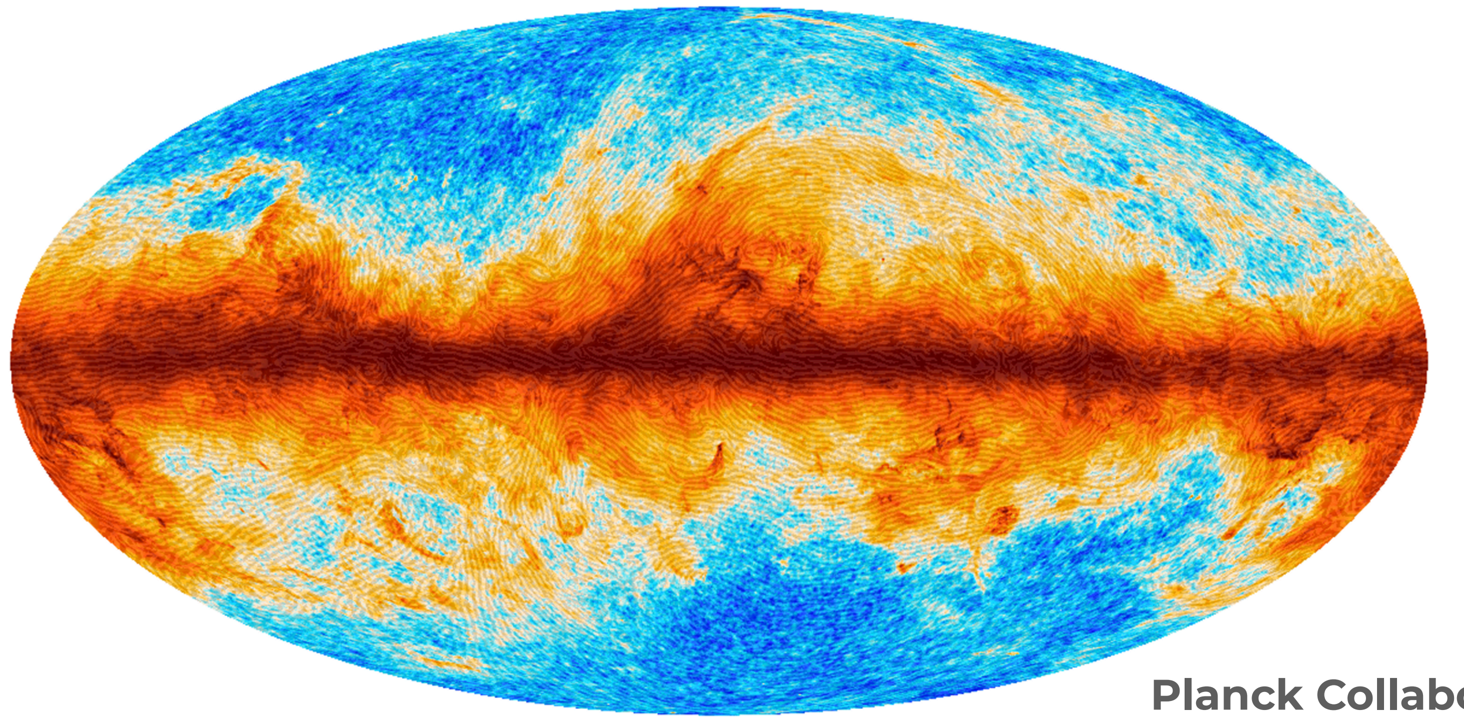

coherent structures

Planck Collaboration (2014)

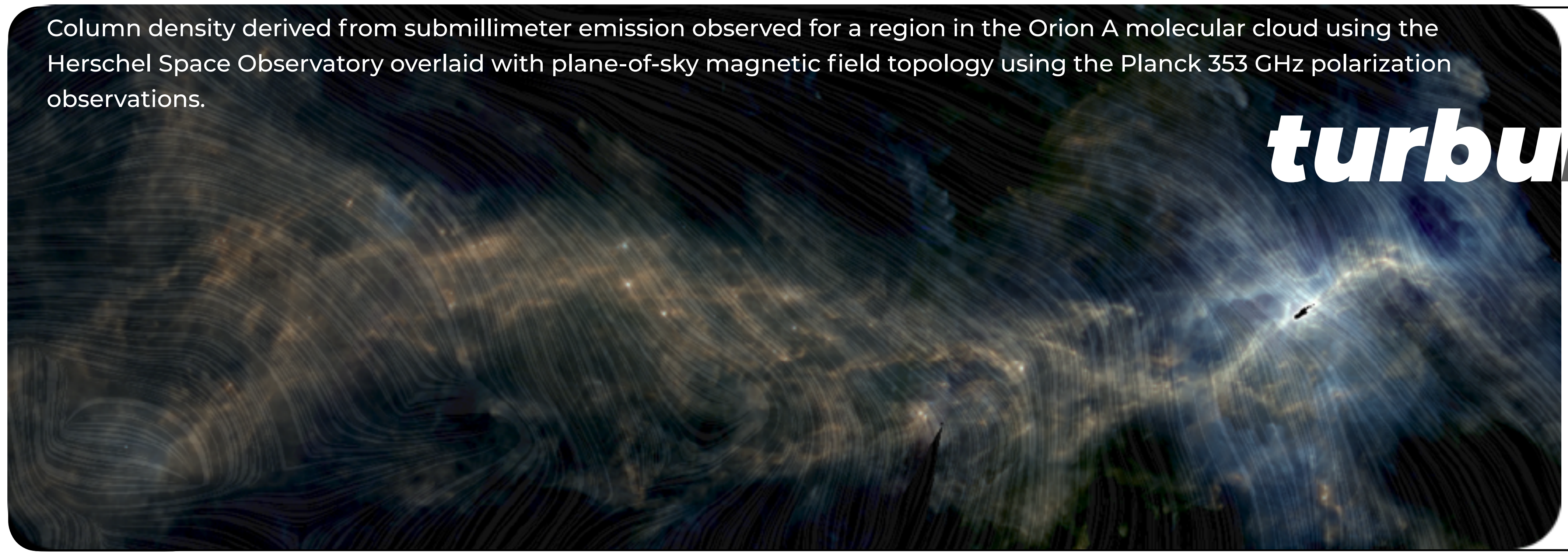

turbulence

Soler (2019)

cosmic-ray propagation

Farrar (2024)

regular

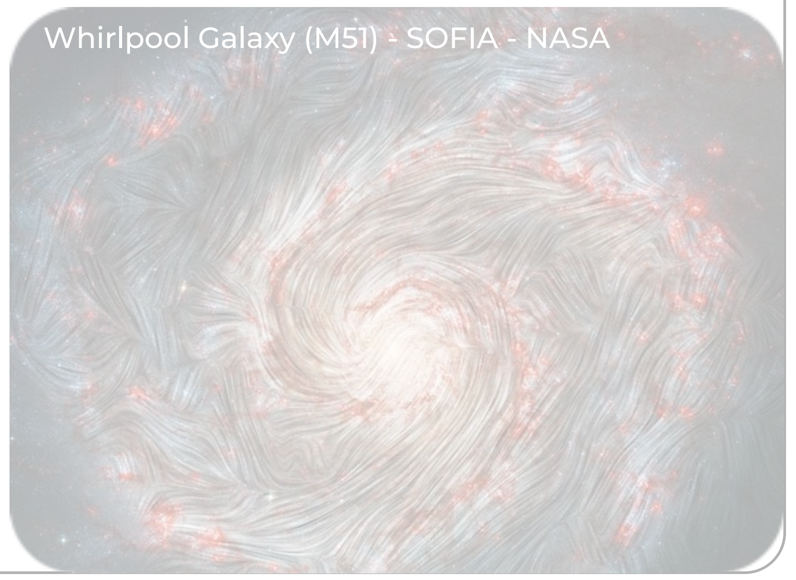

coherent structures

on (2014)

turbulence

Soler (2019)

regular
magnetic field

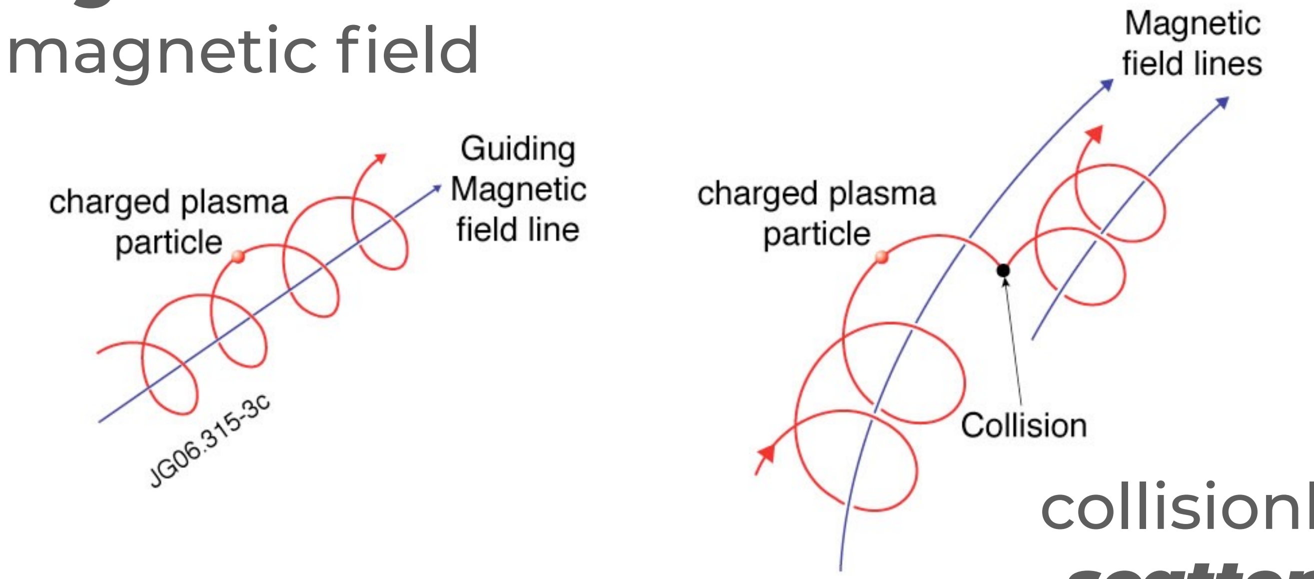

collisionless ***scattering***

pitch angle ***scattering***

coherent structures

time variations

intermittent fields

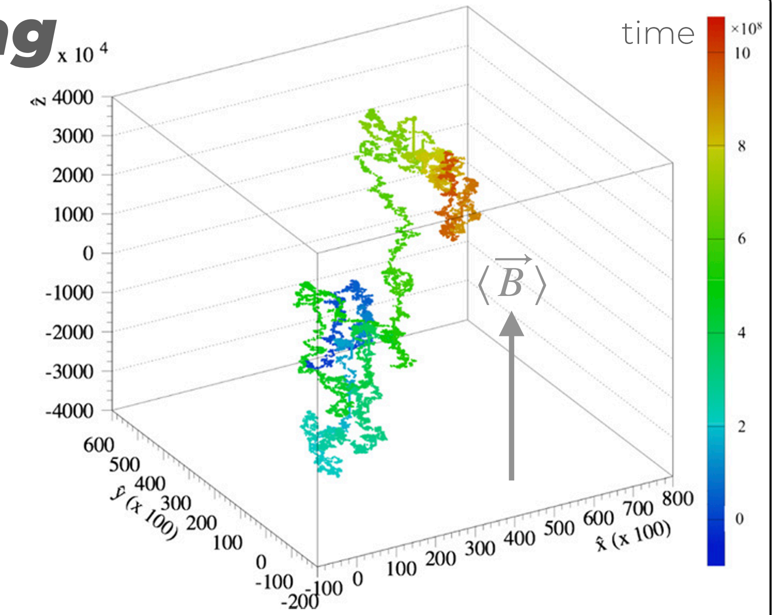

anomalous diffusion

PD & Zweibel (2014)

magnetic superdiffusion

causes ***bouncing CRs*** to

parallel diffusion

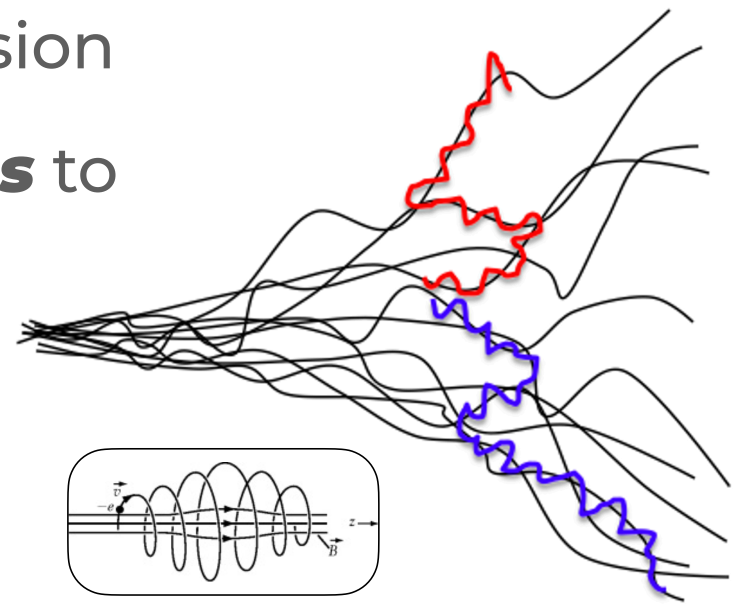

mirror diffusion

Lazarian & Xu (2021)

field line ***random walk***

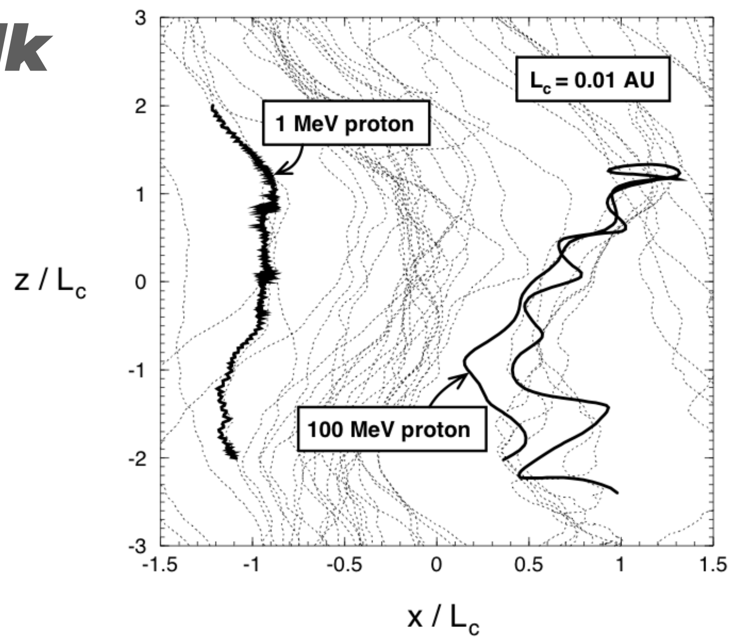

superdiffusion

Lazarian & Vishniac (1999)

Giacalone & Jokipii (1999)

Xu & Yan (2013)

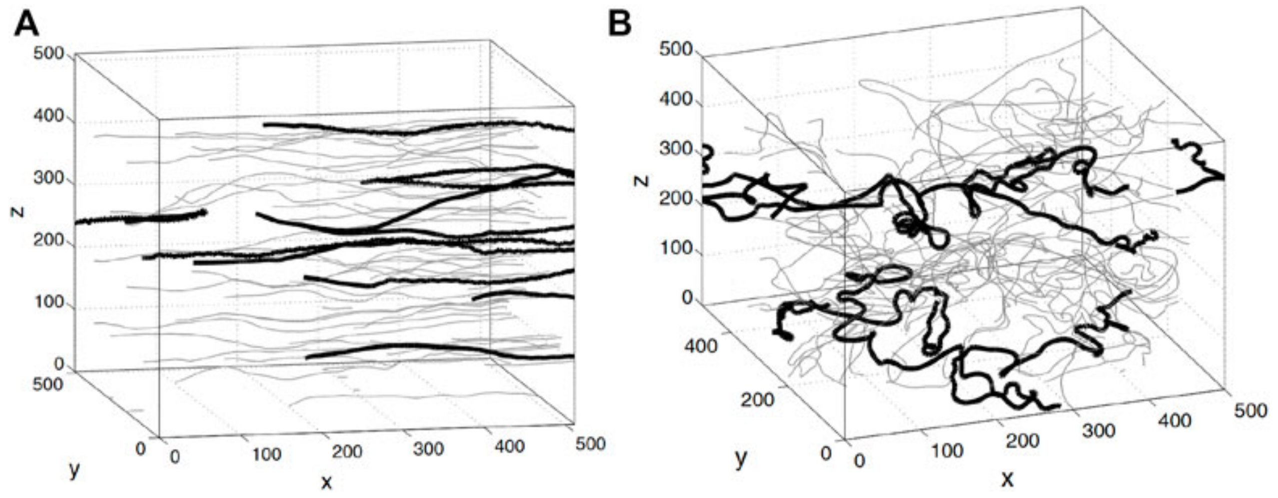

particles in ***Alfvénic turbulence***

1 dipole anisotropy component

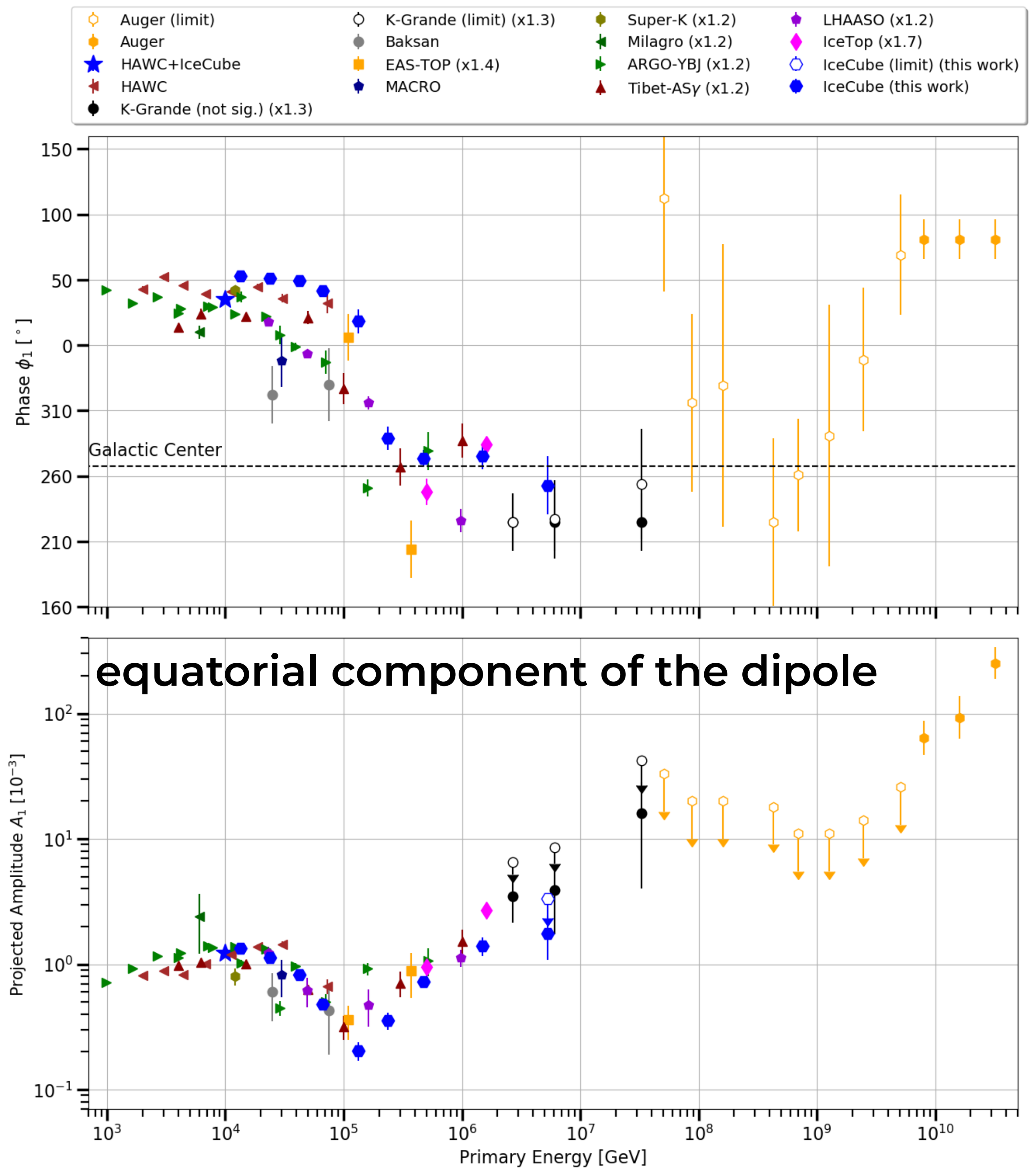

Blasi & Amato (2012)

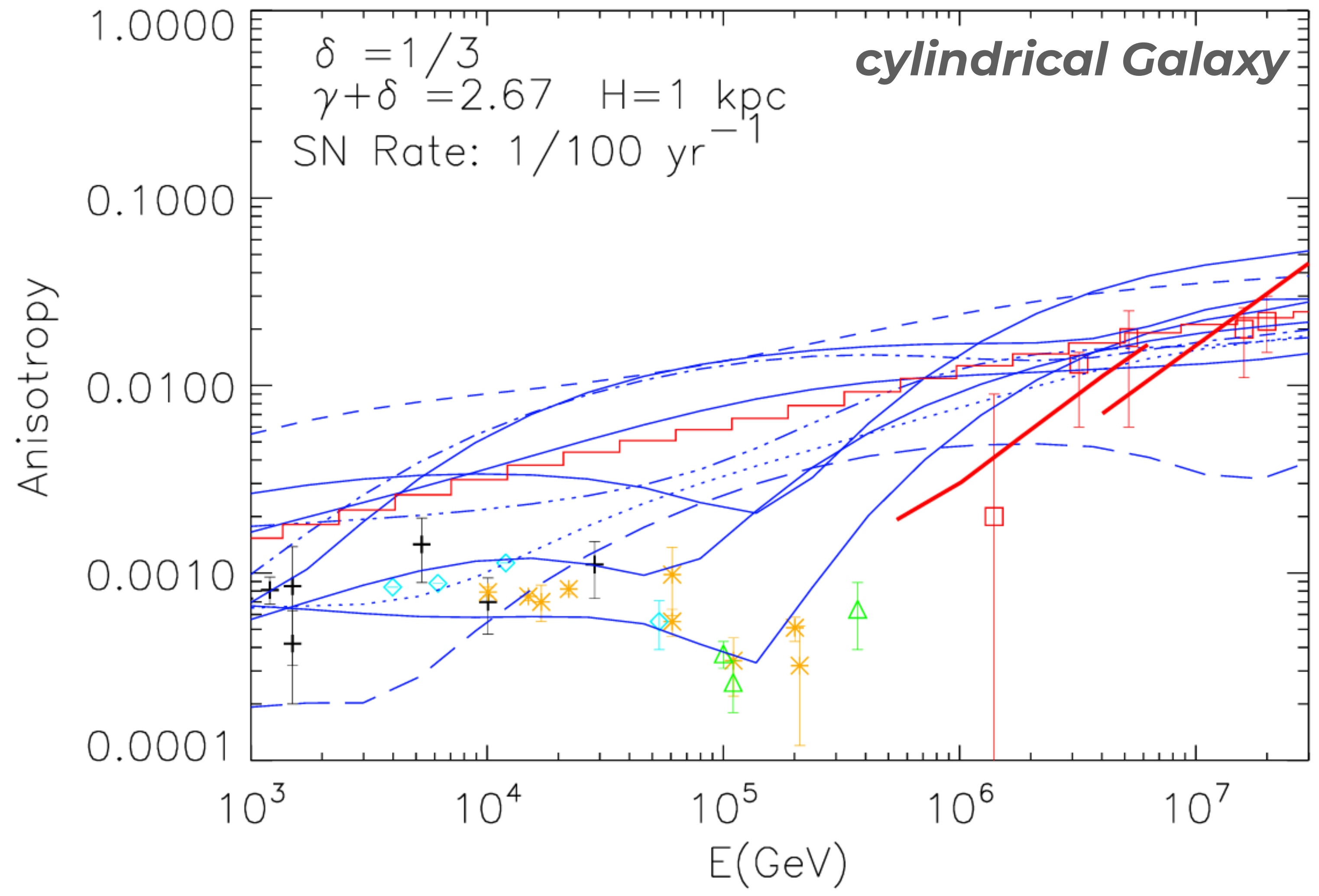

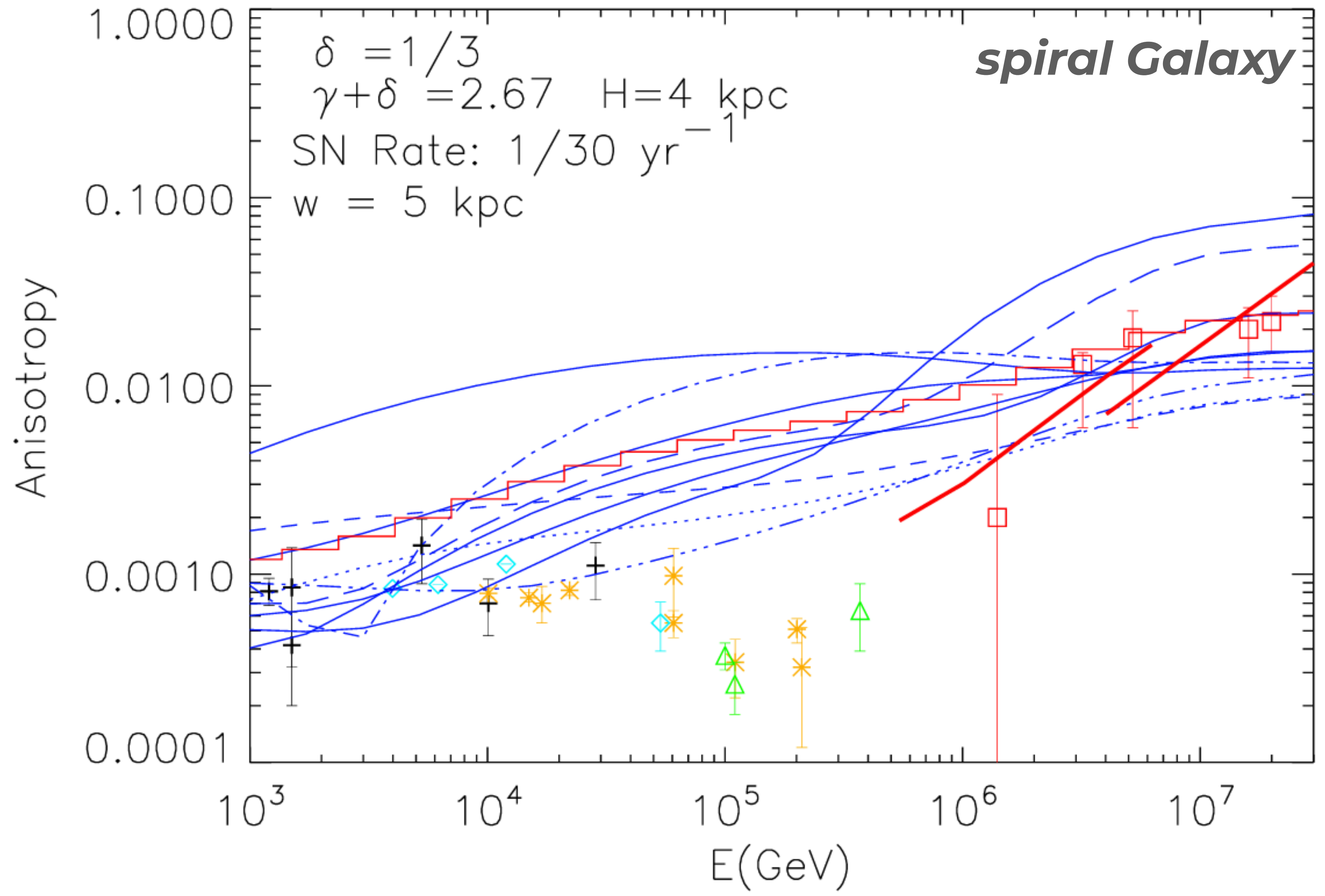

Impossible to infer information on the global distribution of cosmic-ray sources in the Milky Way.

We may observe just a random instantiation of galactic contribution.

Local sources scenario may explain observations as a manifestation of our position in the Milky Way.

Cosmic ray propagation in magnetic turbulence is described as spatial diffusion, leading to a small **dipole anisotropy**.

dipole anisotropy component

a local source

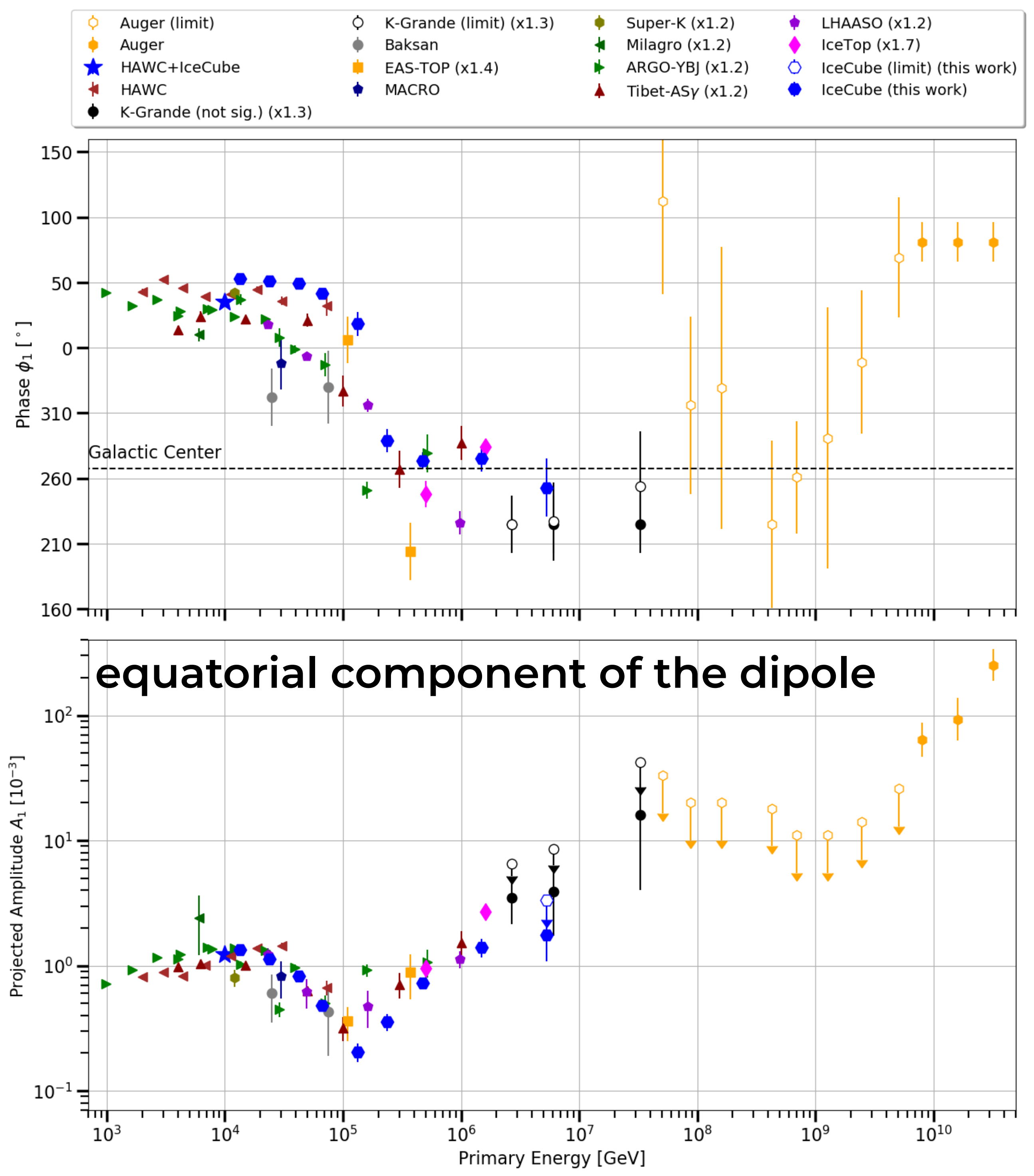

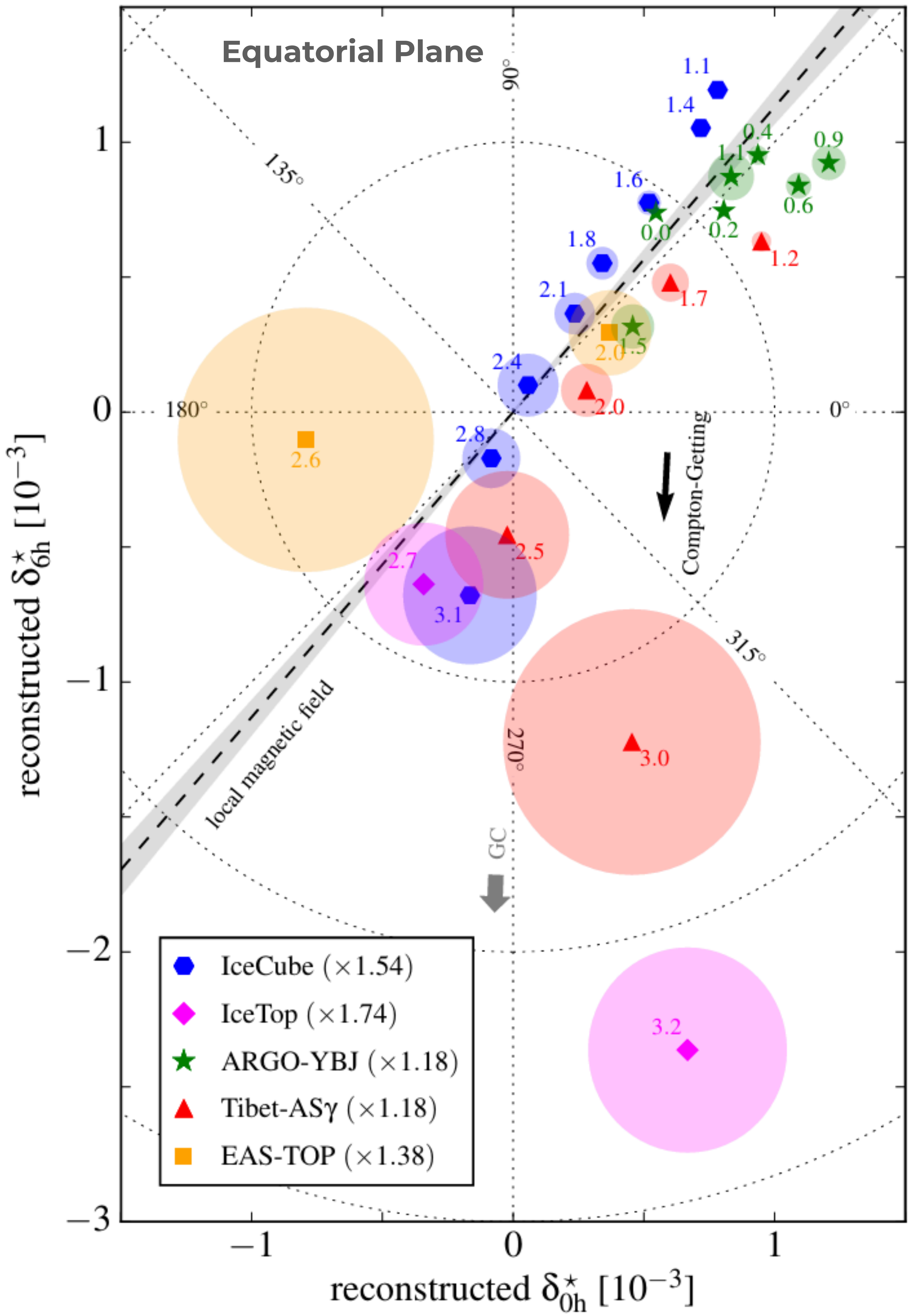

Vela SNR as candidate of the local CR source responsible for the dipole anisotropy at 1–100 TeV.

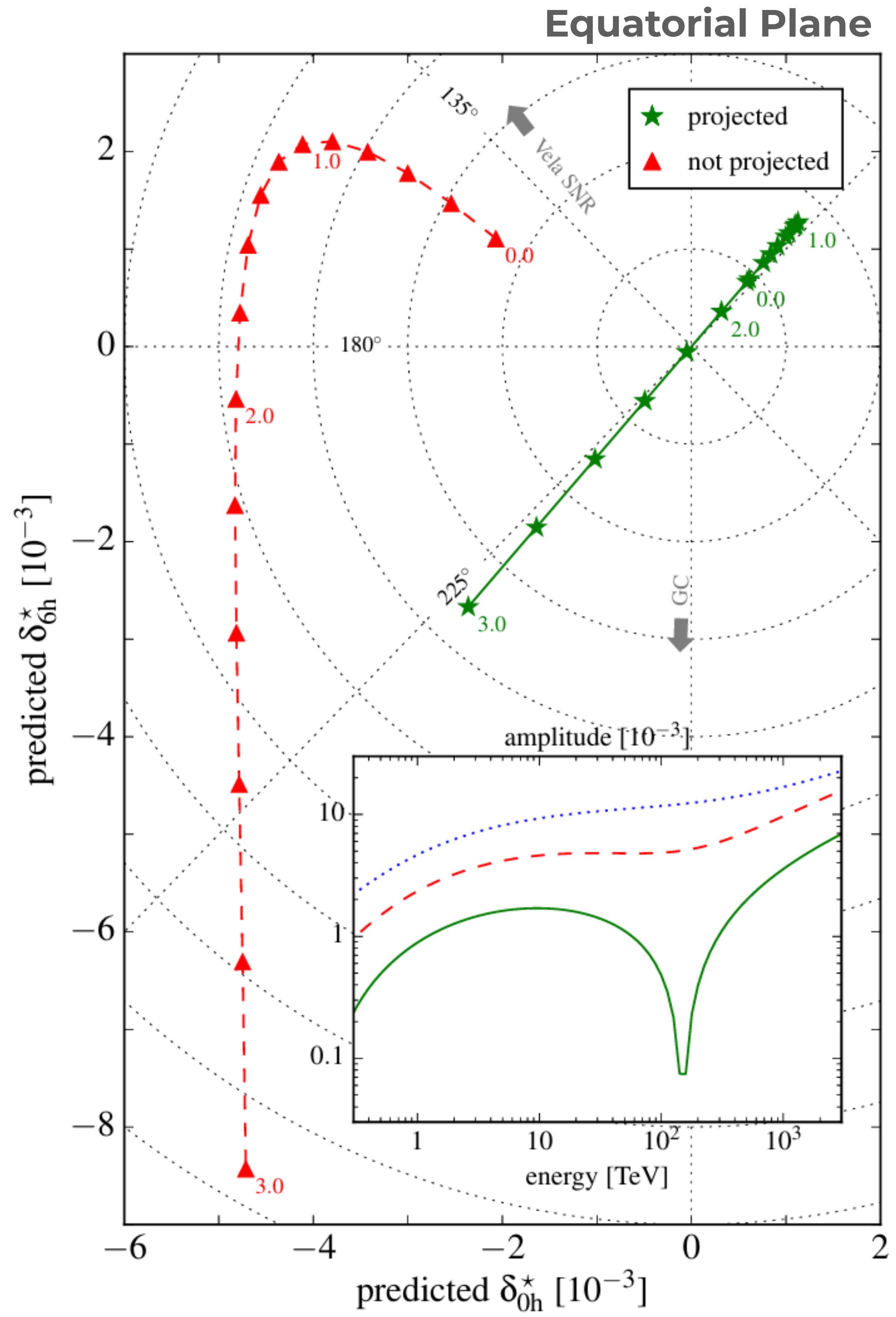

Ahlers (2016)

1

medium/small-scale anisotropy

fingerprint of local turbulence

Ahlers (2013) - Ahlers & Mertsch (2015)

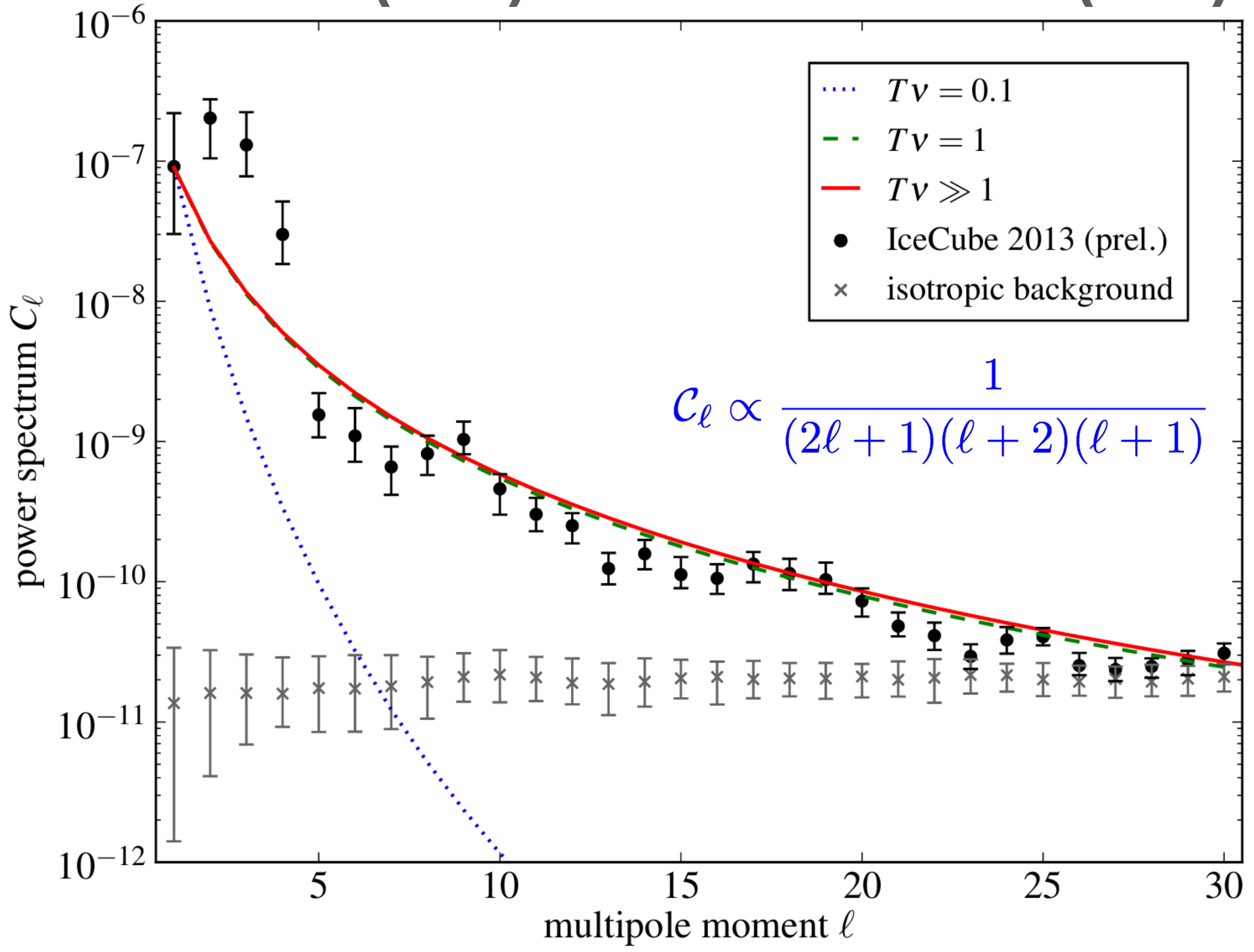

magnetic turbulence and transition from diffusive to ballistic

*"the existence of a global CR dipole moment necessarily generates a **spectrum of higher multipole moments** in the local CR distribution."*

dipole energy dissipated to small angular scales

López Barquero, PD+ (2016)

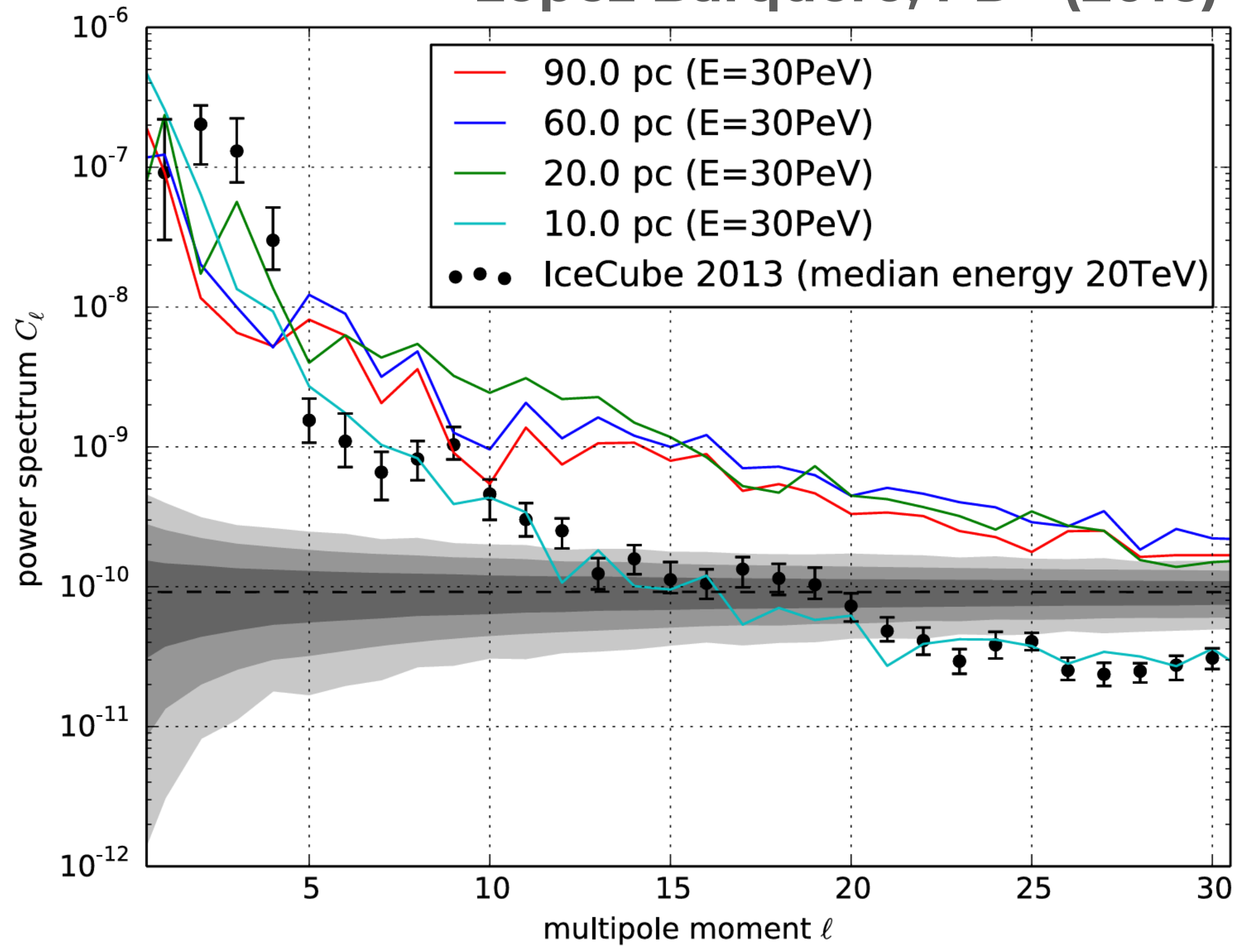

Long-baseline numerical calculation in *compressible MHD turbulence*

(Cho & Lazarian, 2002)

injected dipole breaks down to small-scale anisotropy

saturation at the mean free path distance scale

Bian, Giacinti, Reville (2025)

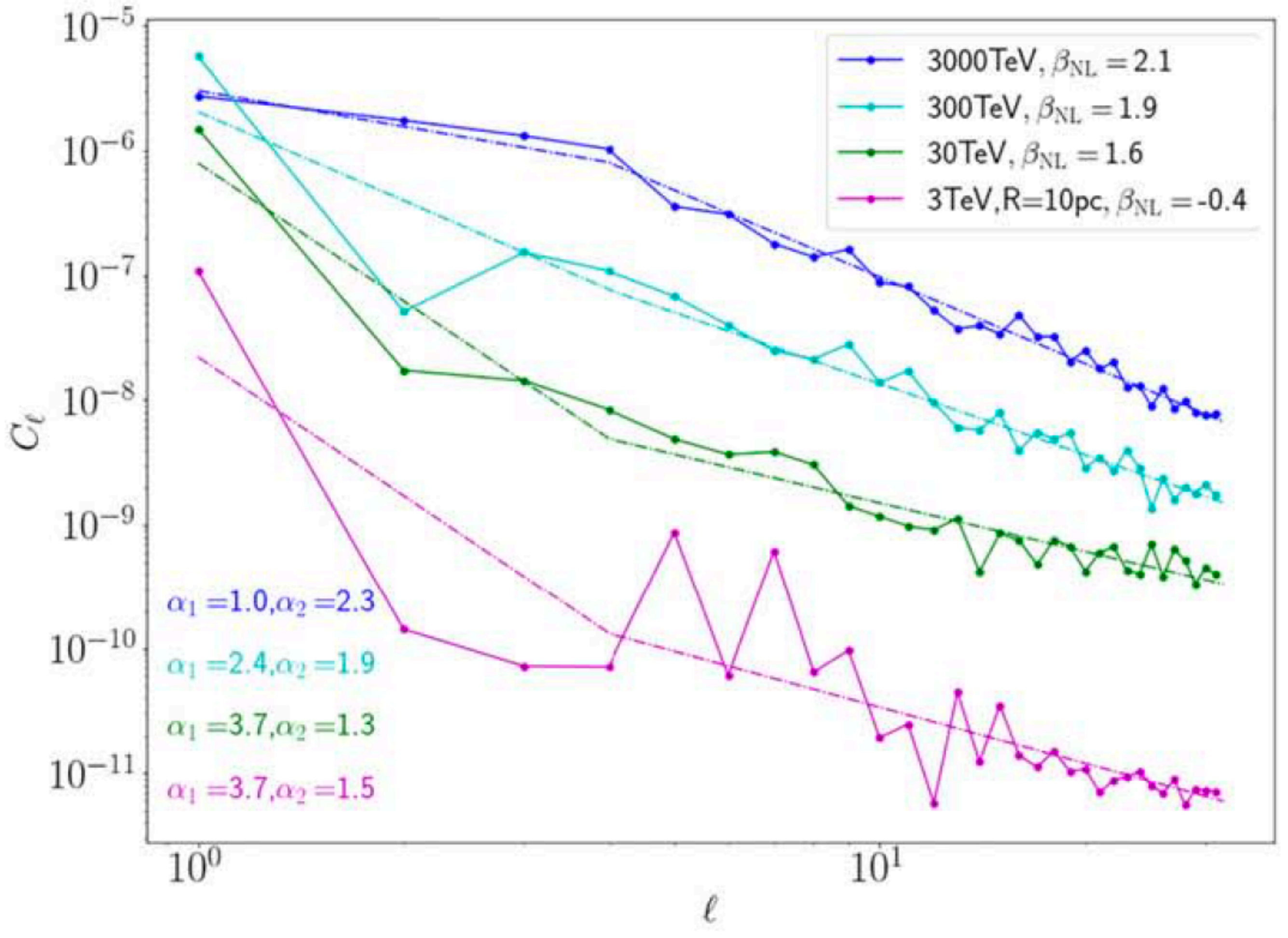

long-baseline numerical calculation in *synthetic turbulence*

small-scale anisotropy as turbulence fingerprint

*"The formation of the **large-scale** anisotropy is closely related to the surrounding magnetic field environment, in particular to the shape of the local magnetic flux tube containing the observer"*

1 our magnetic backyard
influence of the heliosphere

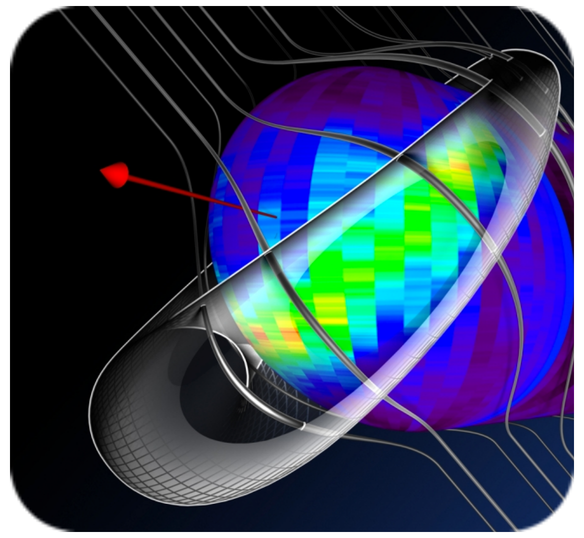

Schwadron, PD+ (2014)

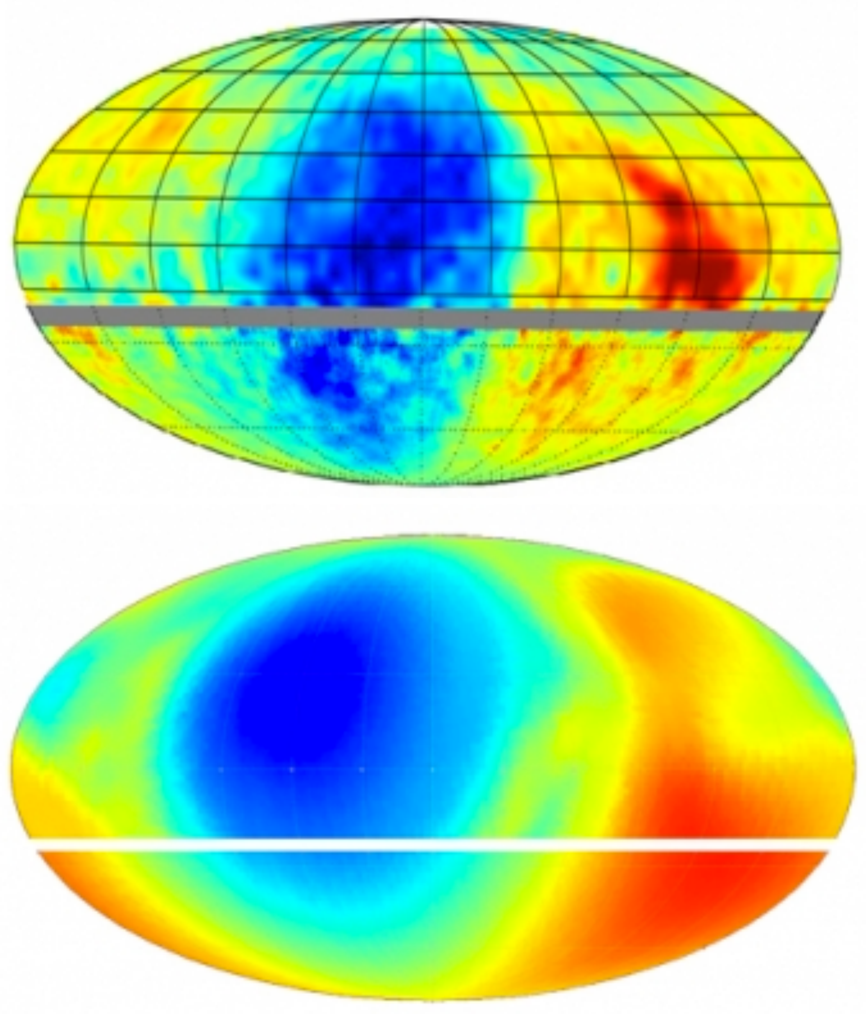

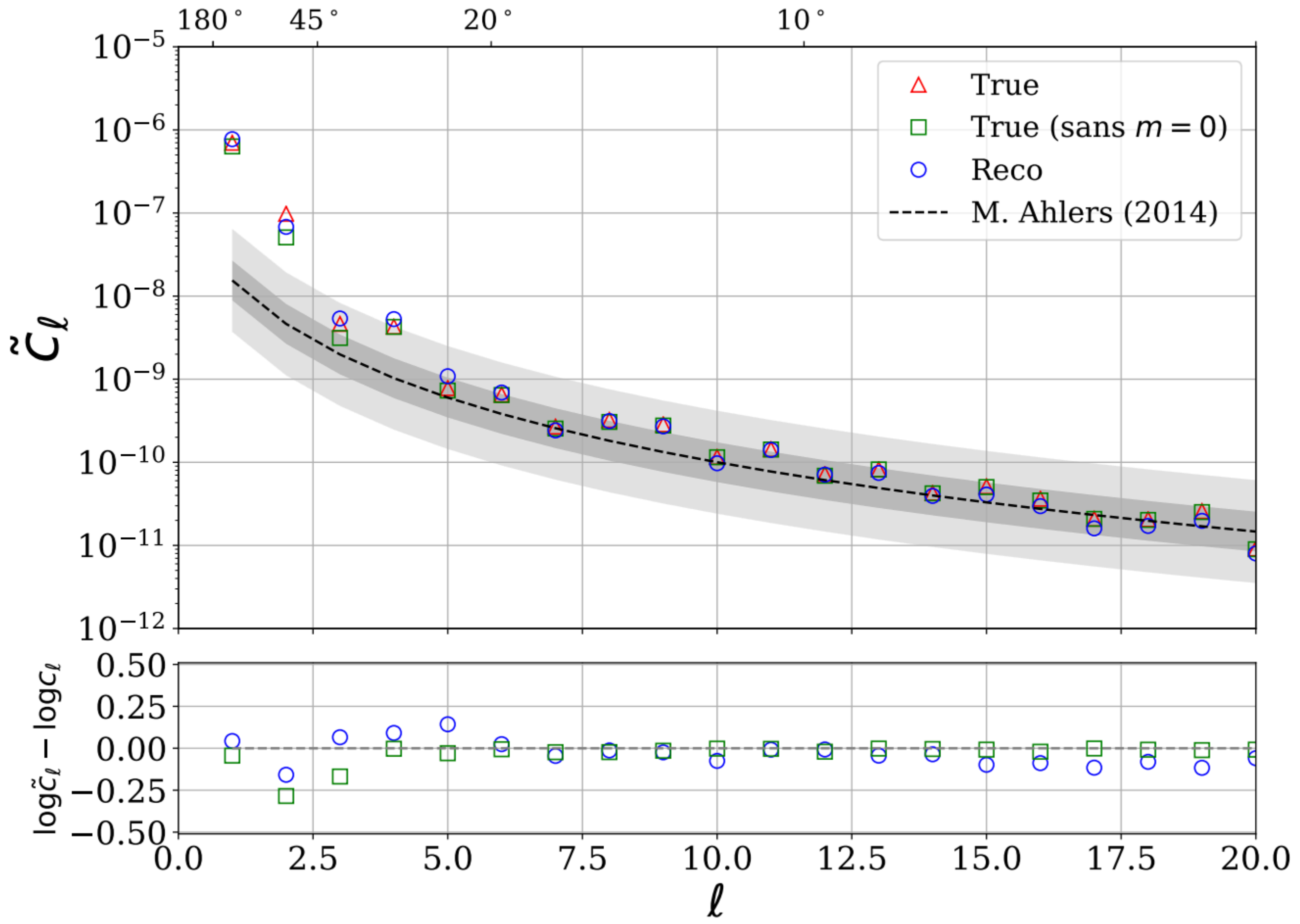

10 TeV cosmic rays

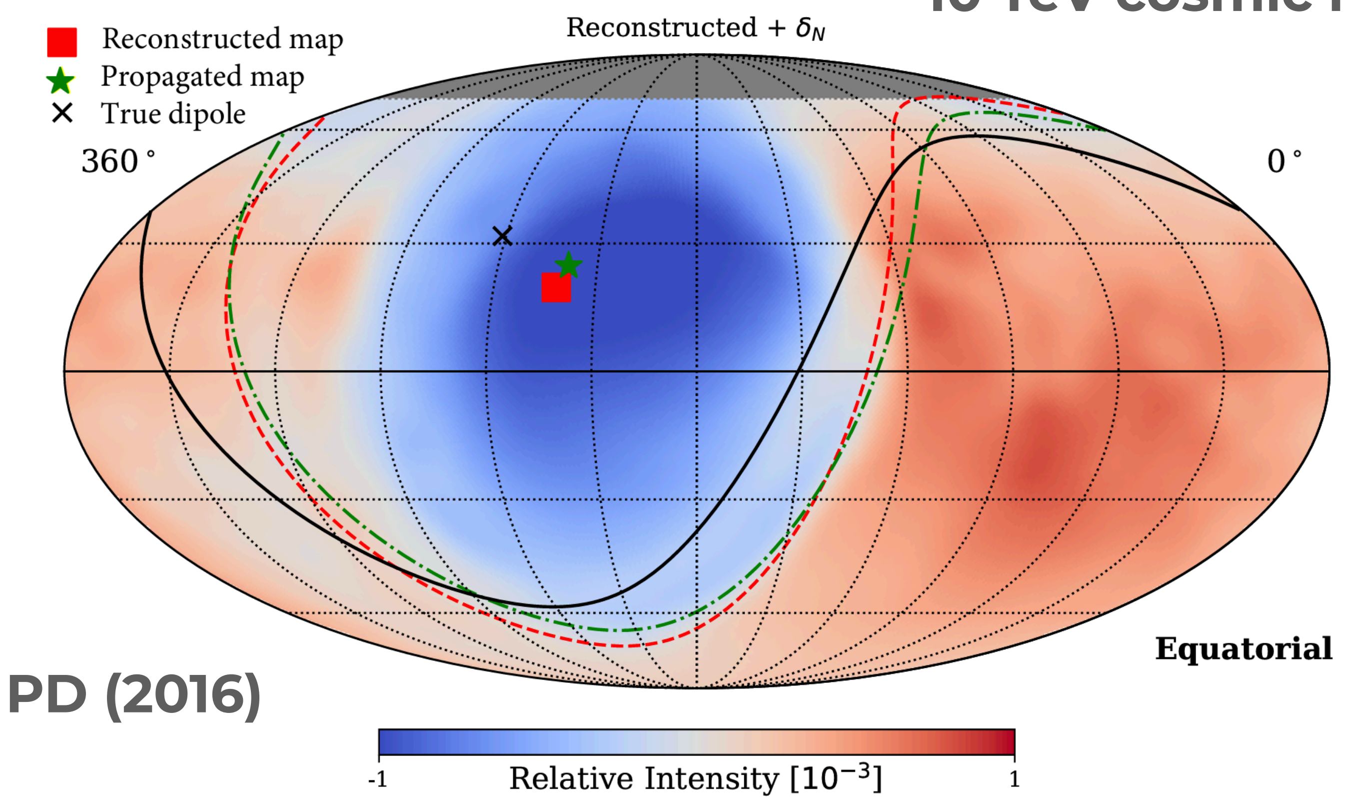

Díaz Vélez & PD (2016)

HAWC-IceCube
ApJ 871 96 (2019)

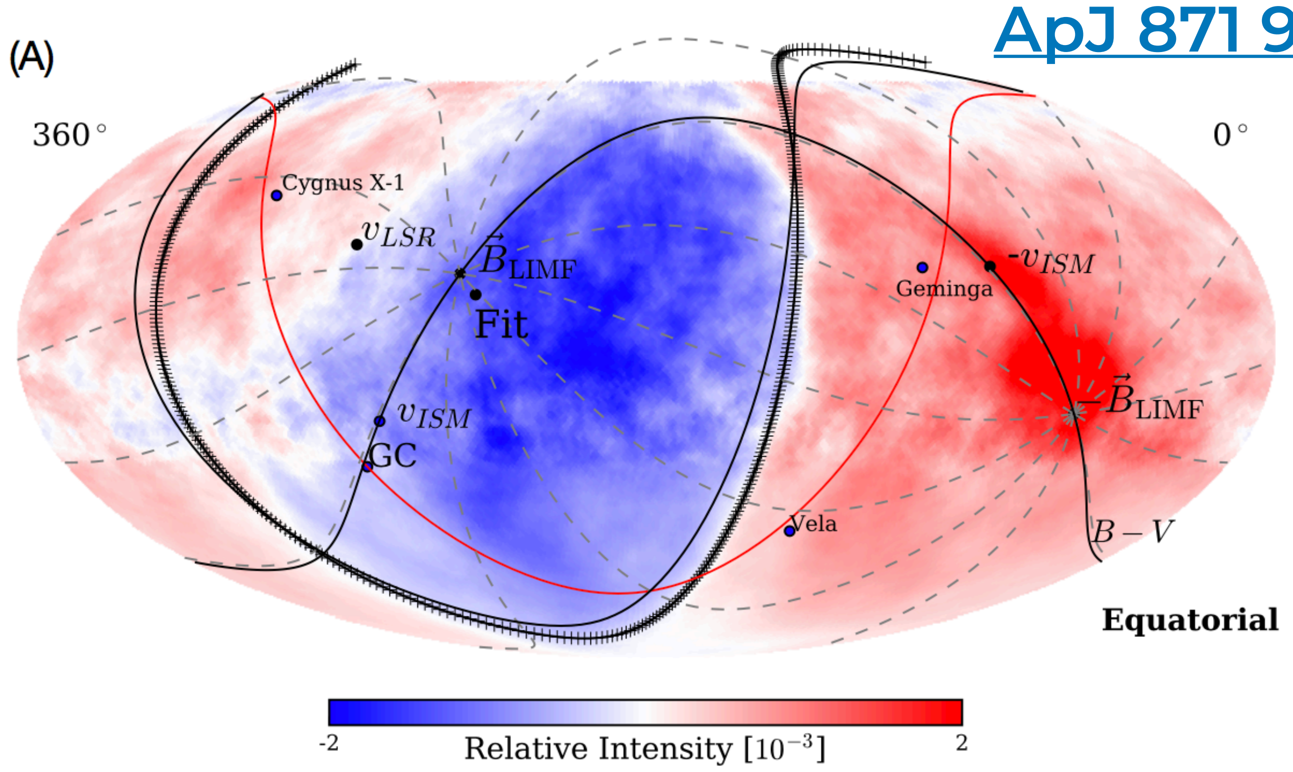

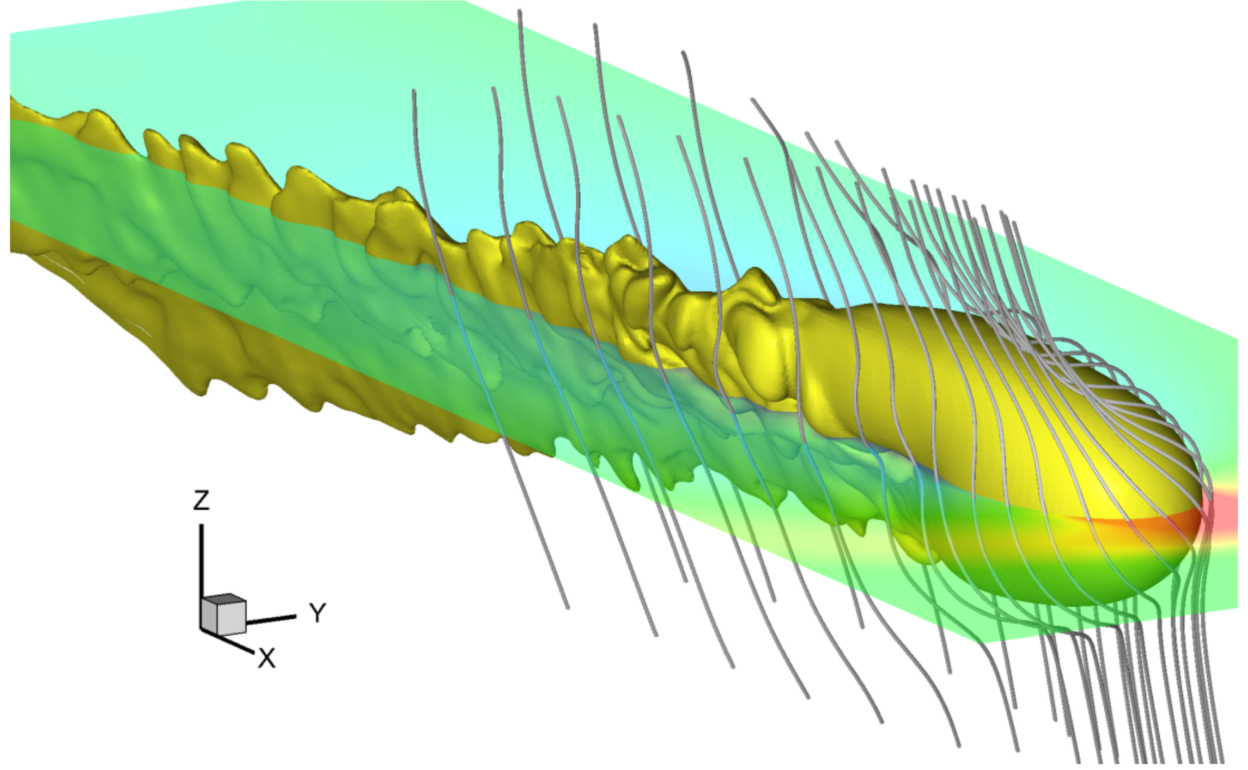

Borovikov, Heerikhuisen, Pogorelov (2015)

laminar model of heliosphere
global properties of TeV CR propagation

TeV cosmic rays are affected by the *heliospheric magnetic bubble*

numerical model of solar wind interacting with ISM
solving plasma MHD equations coupled with kinetic transport of neutral atoms

Lazarian & PD (2010)
PD & Lazarian (2012)

A dipole distribution injected in the ISM produces a complex anisotropy on Earth

our magnetic backyard
influence of the heliosphere

(A) Tibet-ASγ relative intensity sky map from the at 4 TeV energy **Amenomori+ (2006)**

(B) numerically computed trajectory distribution at Erth after fit to Tibet-ASγ data

(C) inferred large-scale anisotropy in the ISM without heliospheric influence

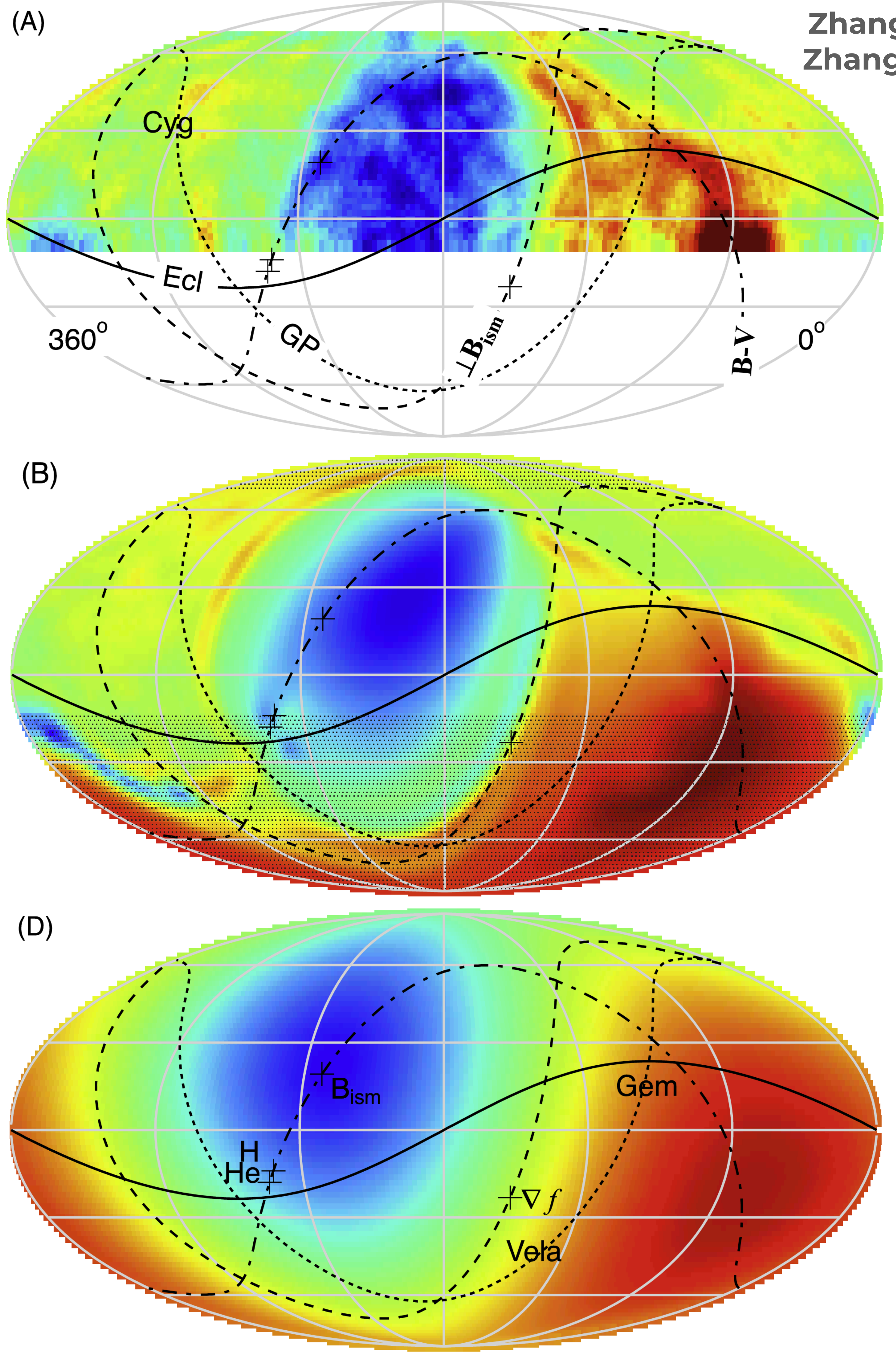

Zhang+ (2014)
Zhang+ (2020)

how to make observations useful?

are anisotropy measurements good enough?

what about

experimental biases

instrumental resolutions

we need

multi-experiment observations

theorists - experimentalists collaboration

1

limited field of view
iterative maximum likelihood method

(Ahlers+, 2016)

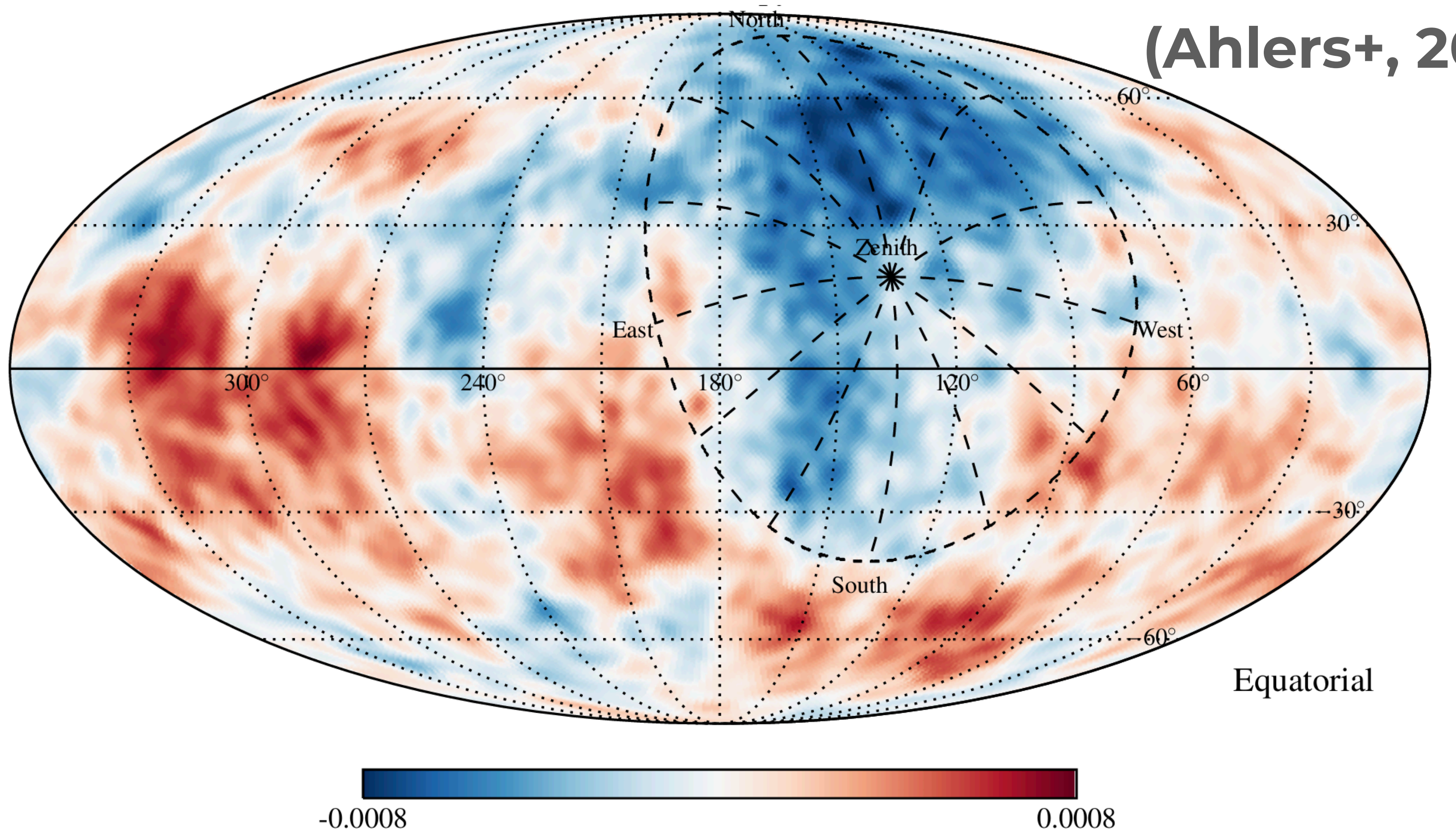

attenuation of large-scale structures exceeding

the size of the **instantaneous field of view**

when smaller than 24hr **integrated field of view**

relative intensity

$$\mu_{\tau i} \simeq I_{\tau i} \mathcal{N}_\tau \mathcal{A}_i$$

relative acceptance

total #events

$$\mathcal{L}(n|I,\mathcal{N},\mathcal{A}) = \prod_{\tau i} \frac{(\mu_{\tau i})^{n_{\tau i}} e^{-\mu_{\tau i}}}{n_{\tau i}!}$$

iterative likelihood maximization

$$\lambda = \frac{\mathcal{L}(n|I,\mathcal{N},\mathcal{A})}{\mathcal{L}(n|I^{(0)},\mathcal{N}^{(0)},\mathcal{A}^{(0)})}$$

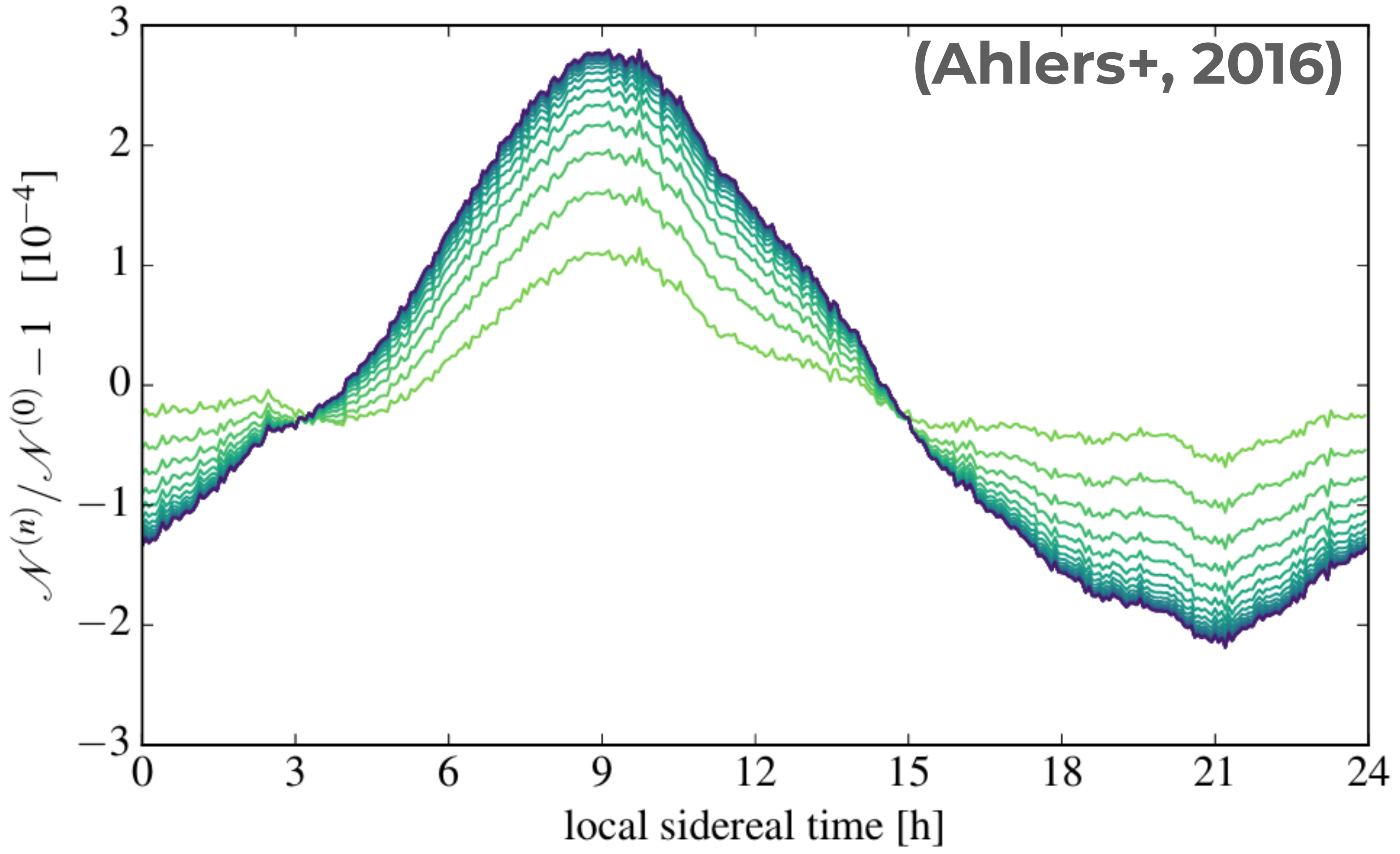

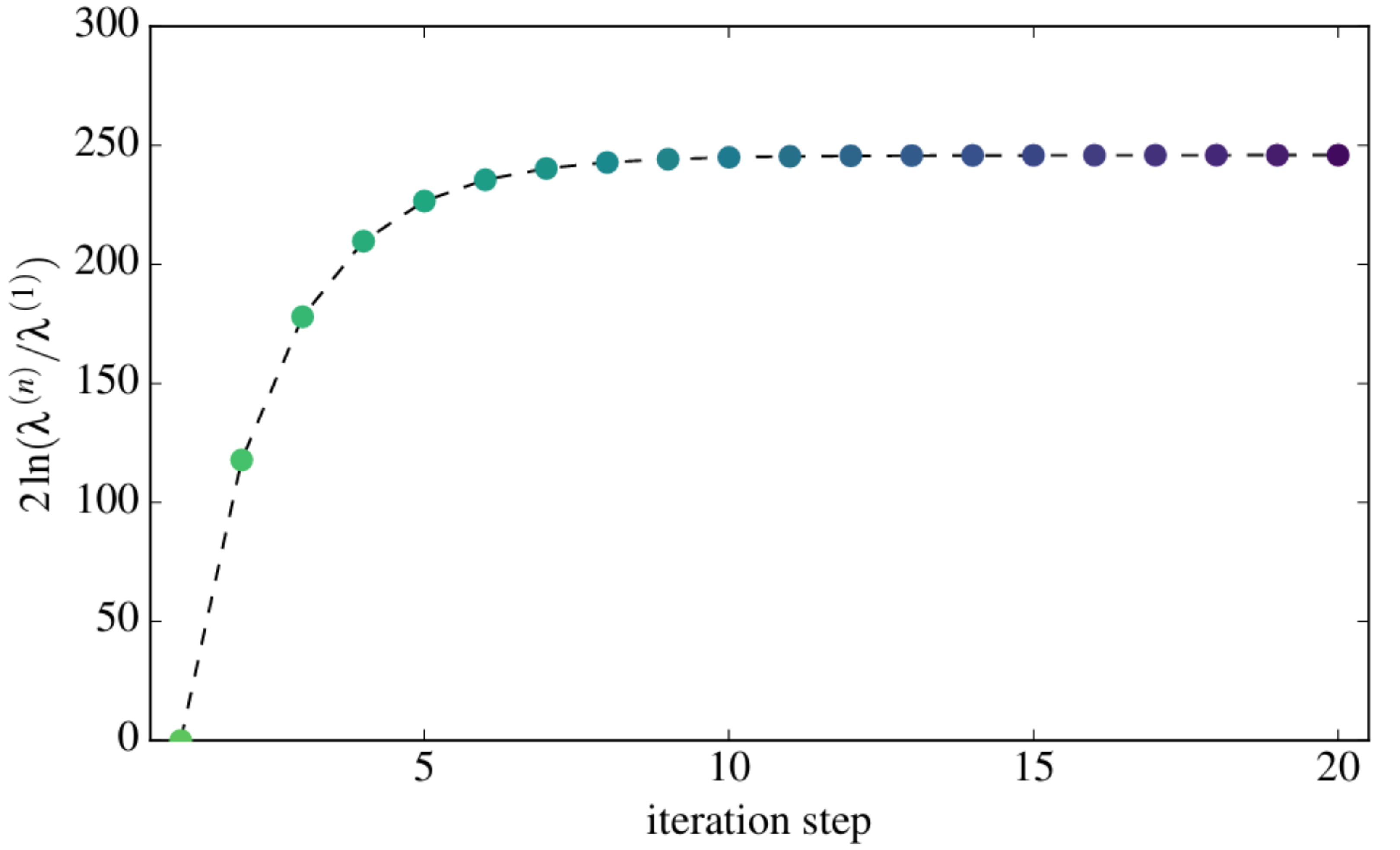

HAWC measures 1/3 of dipole amplitude with 1st iteration only and other *standard* methods

limited field of view
correlation between multipole modes

2

let's inject a
tilted dipole anisotropy

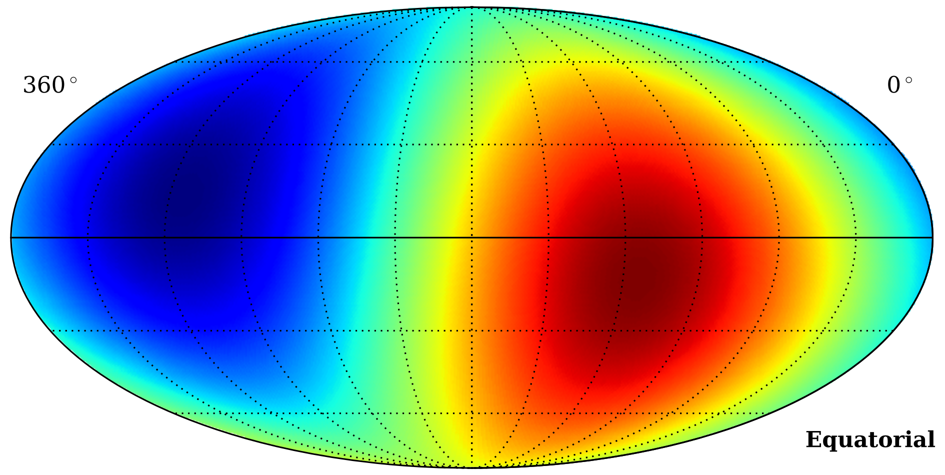

this is the dipole seen
on northern hemisphere

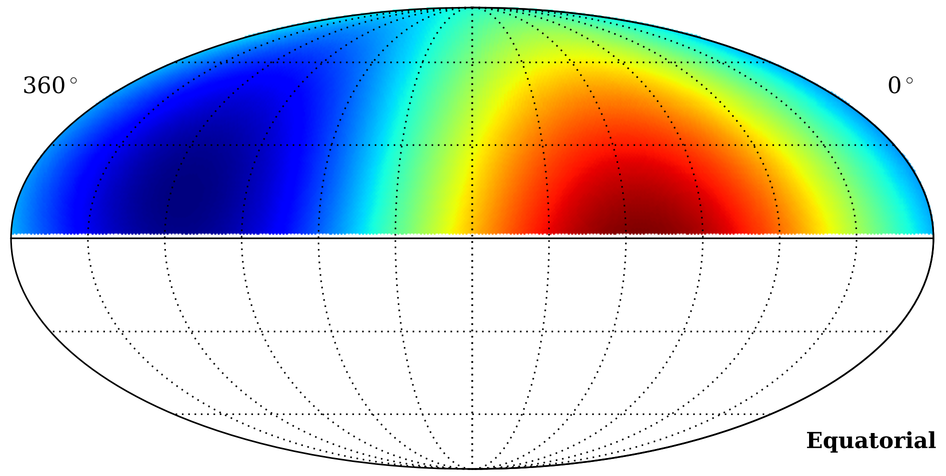

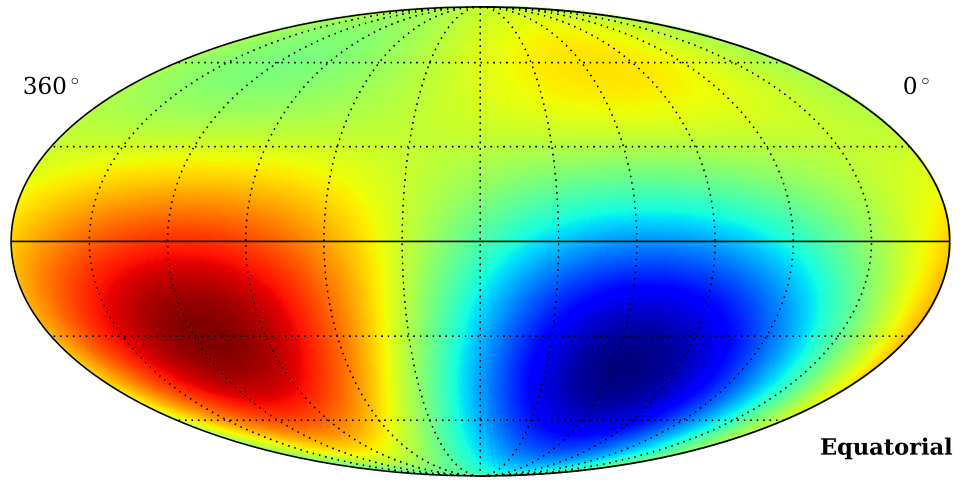

this is the
reconstructed dipole
on northern hemisphere

equatorial component

this is the dipole seen
on southern hemisphere

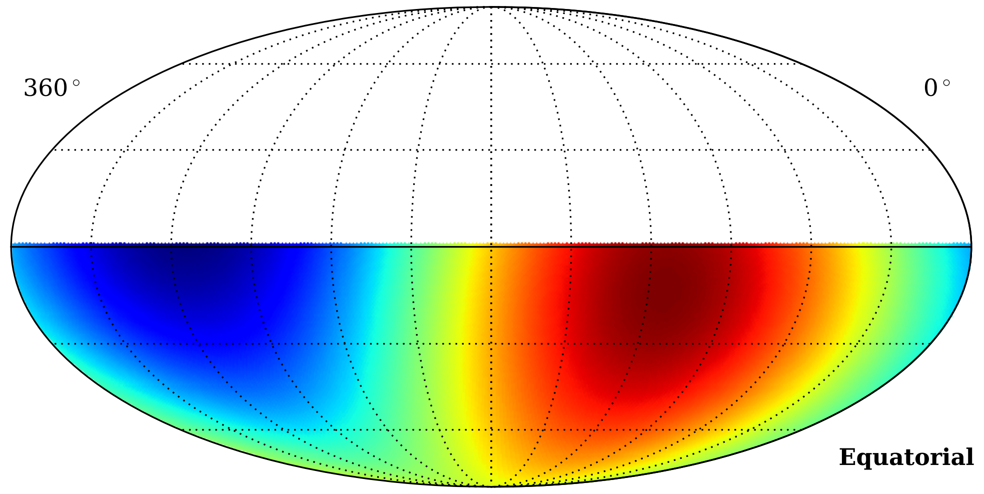

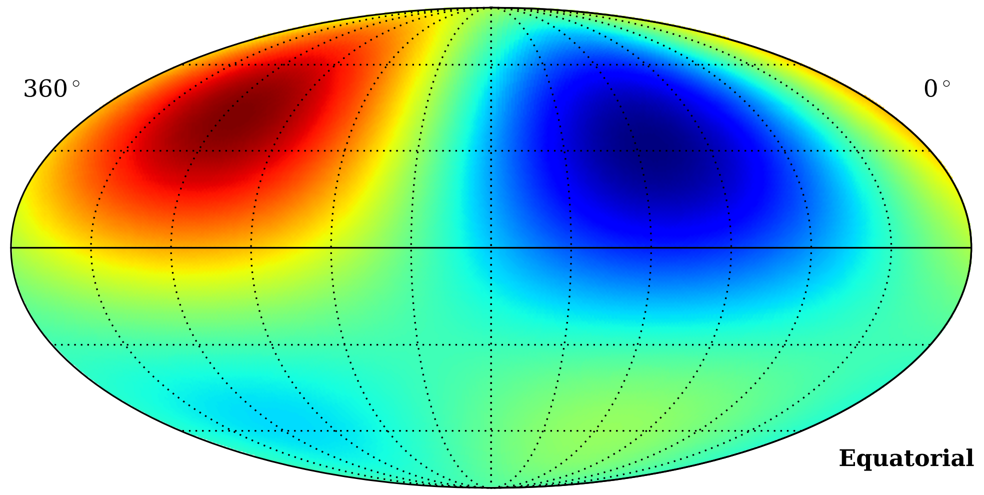

this is the
reconstructed dipole
on southern hemisphere

equatorial component

dipole

dipole

~quadrupole

limited field of view
correlation between multipole modes

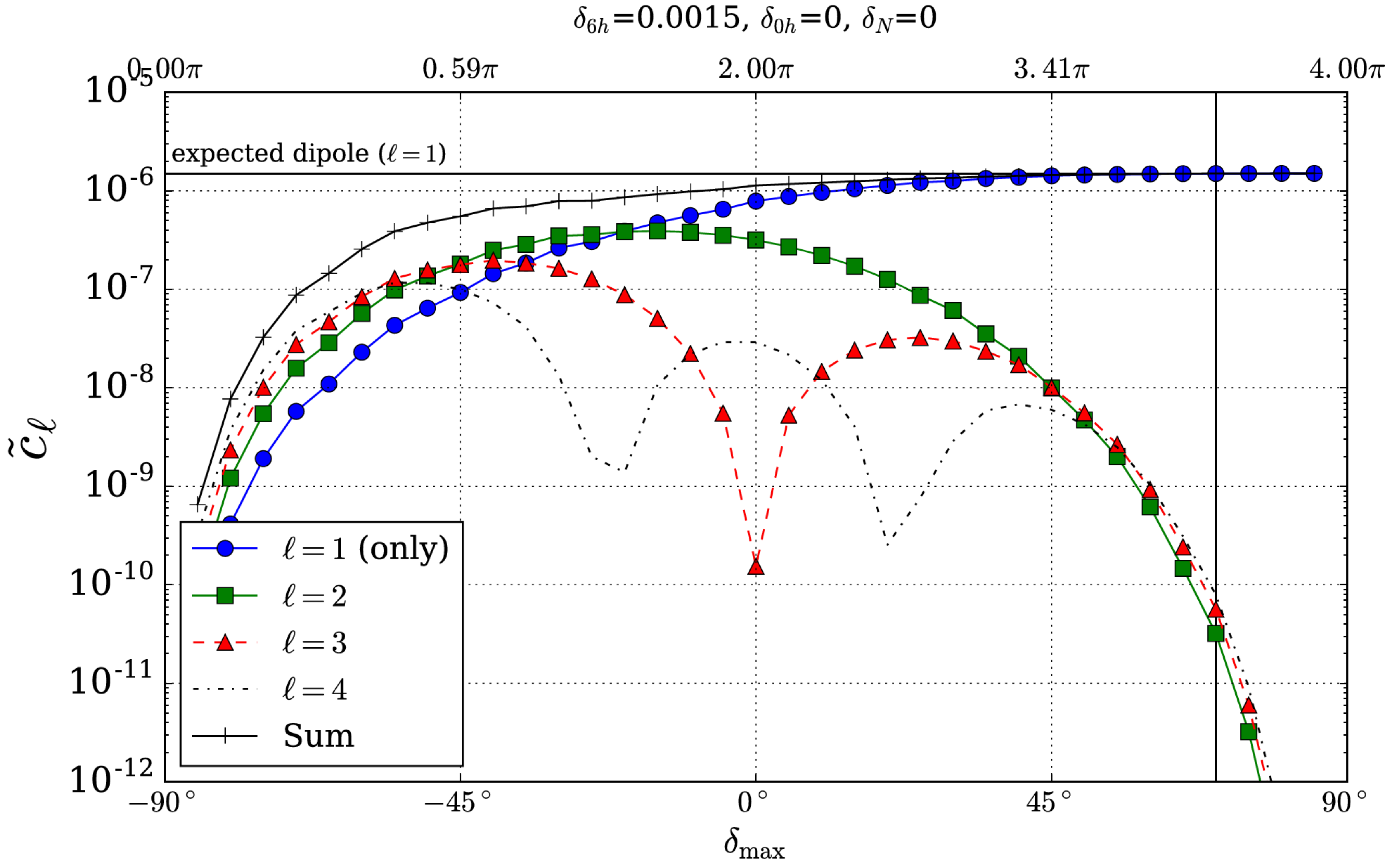

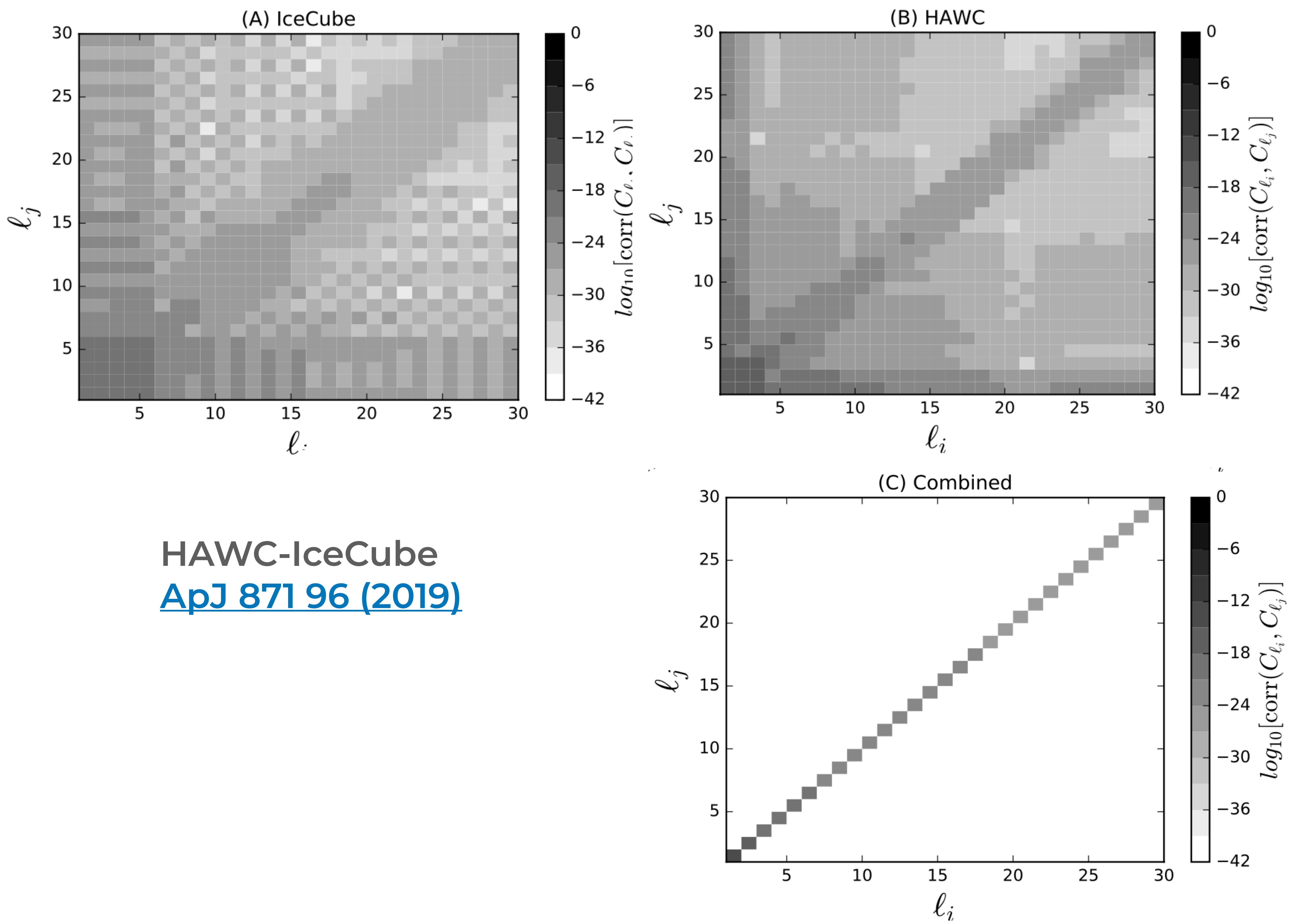

HAWC-IceCube
[ApJ 871 96 (2019)]

Multipole components are subject to **correlations**

caused by **partial sky coverage** since there is a degeneracy between different ℓ-modes.

A pure dipole can result in an artificial quadrupole due to partial sky coverage.

limited field of view

full-sky observations mitigate FOV bias

10 TeV

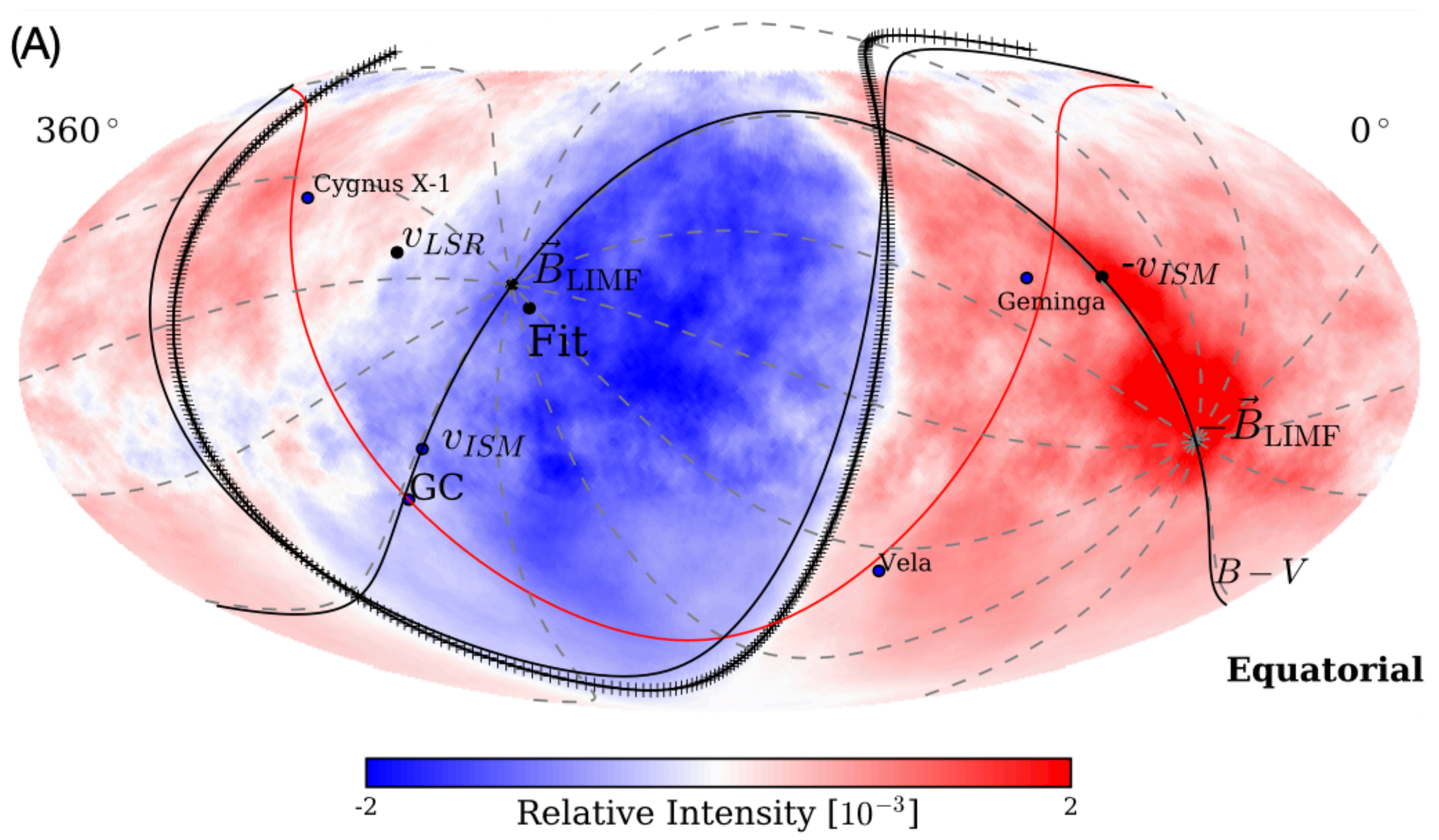

without ℓ = 1, 2, 3

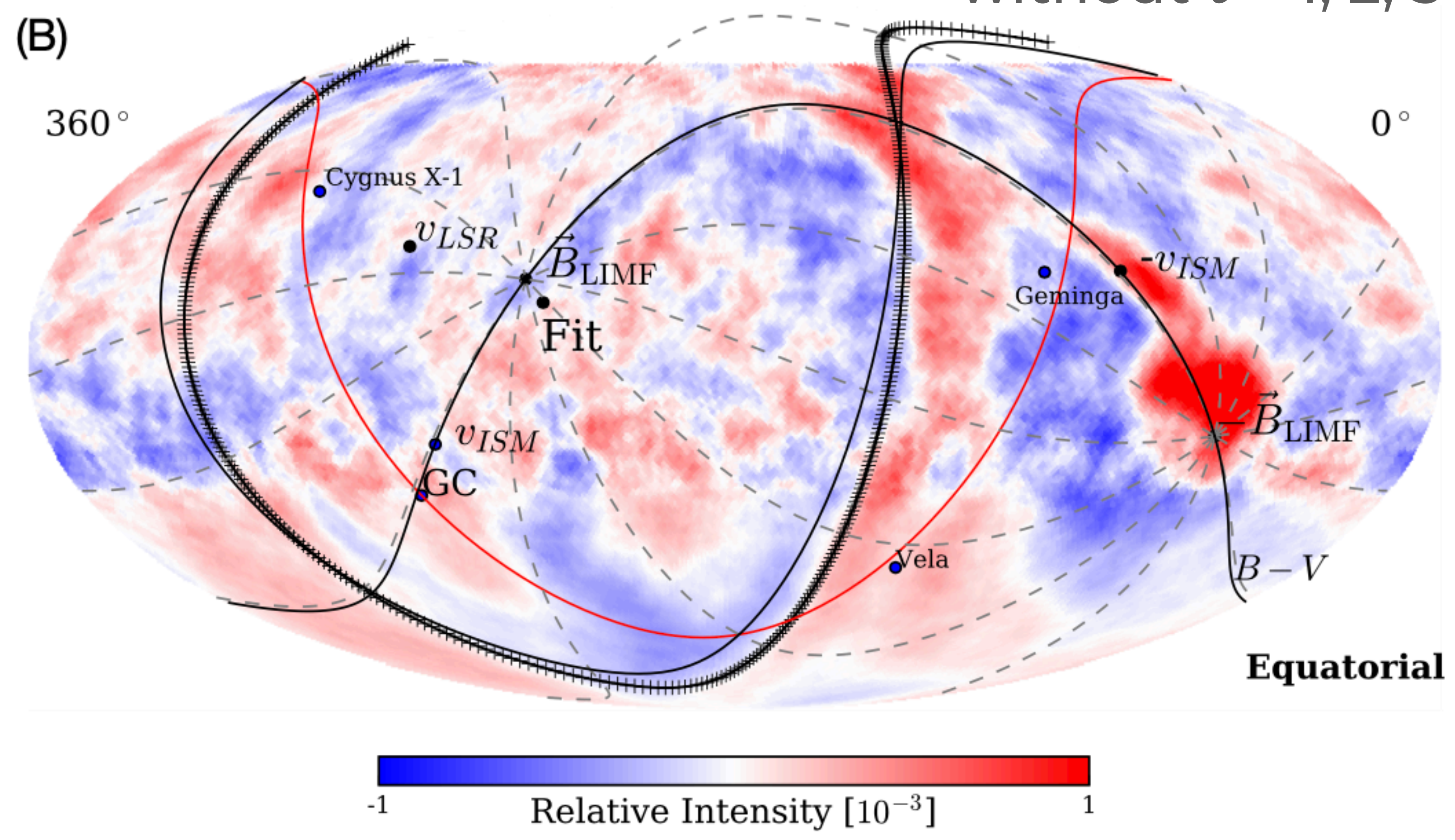

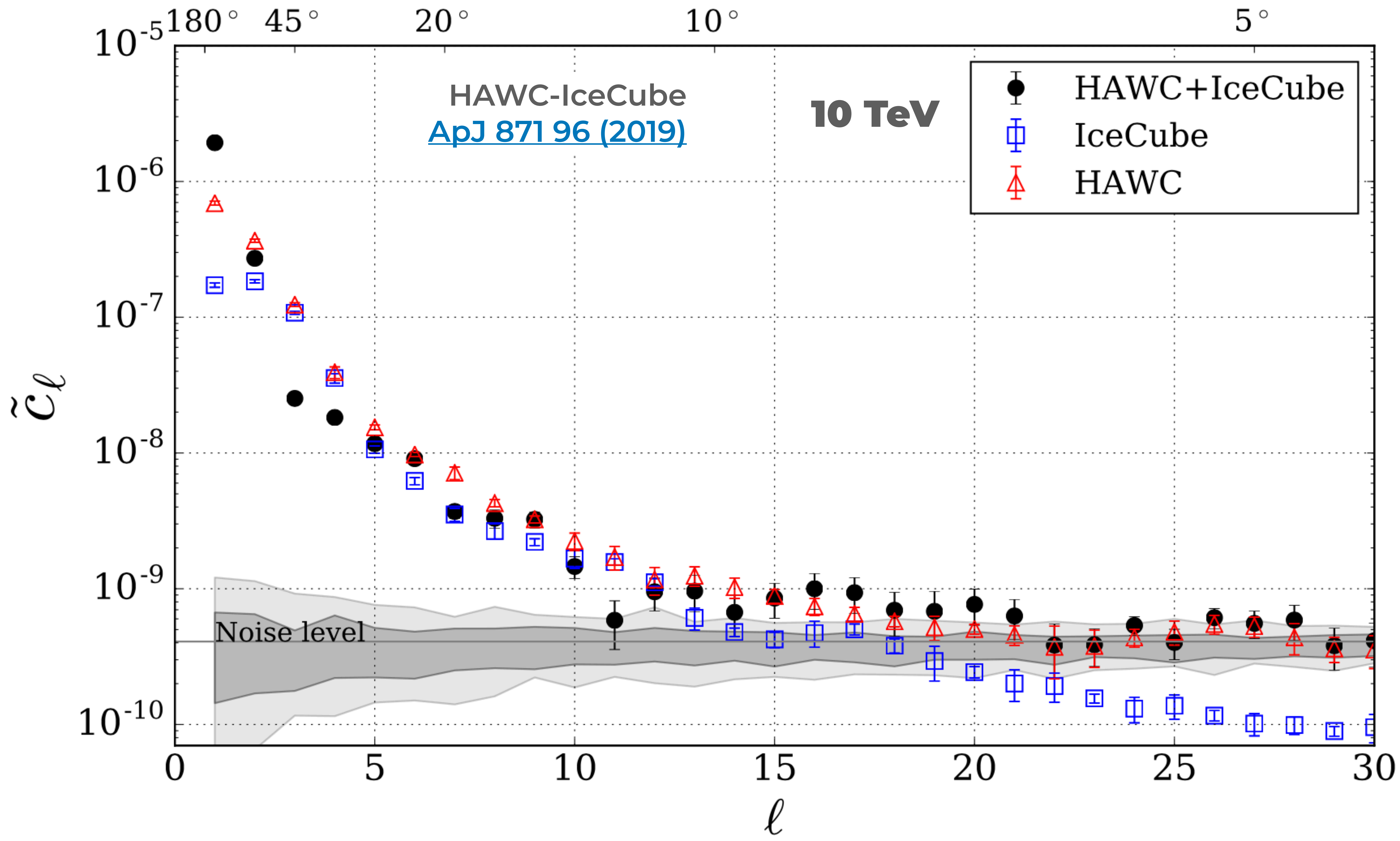

Full sky measurements are the only way to recover the *real anisotropy*

loss of large-scale power leads to erroneous physical interpretations

response function
resolutions and uniformities

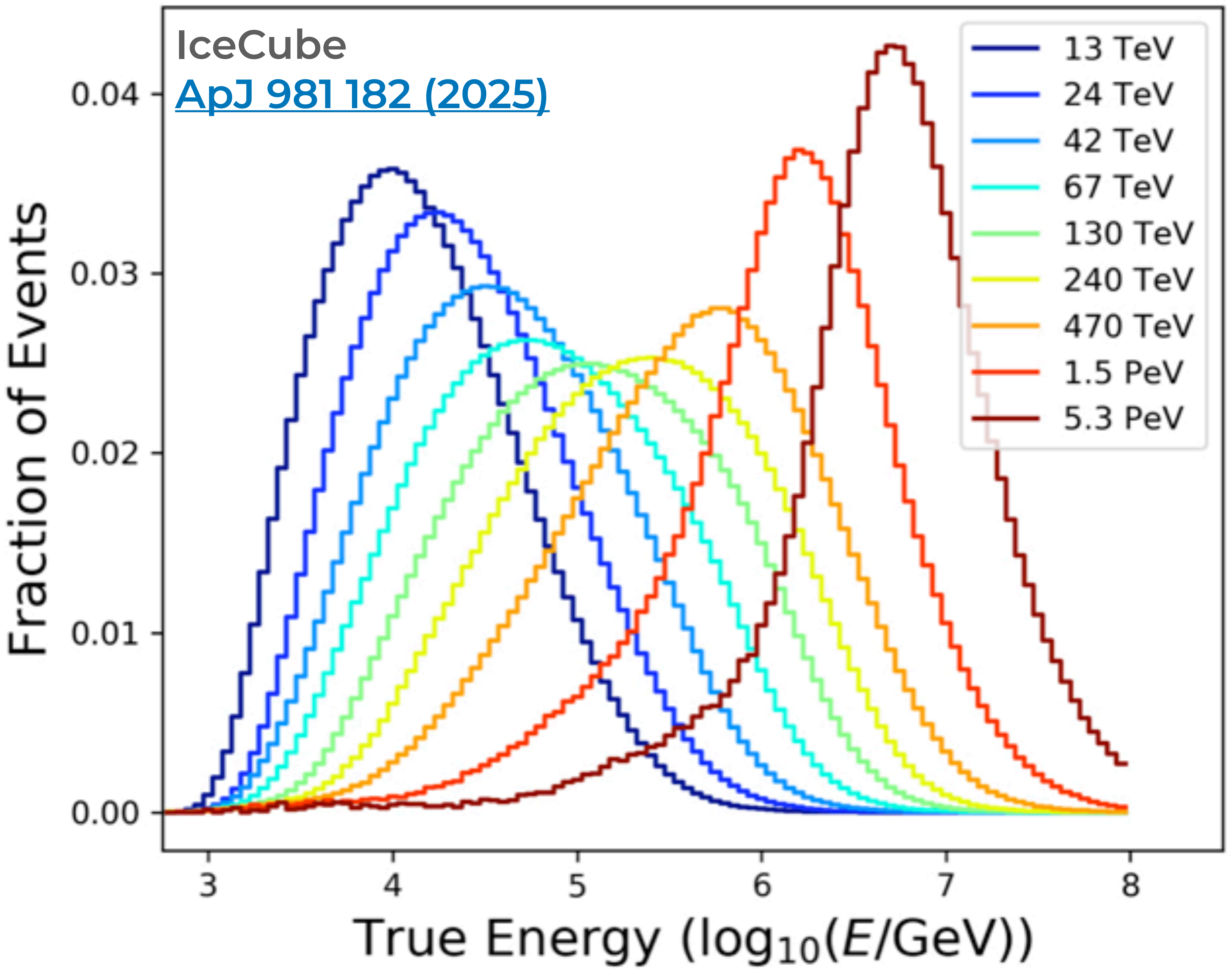

finite energy resolution

overlap between energy samples

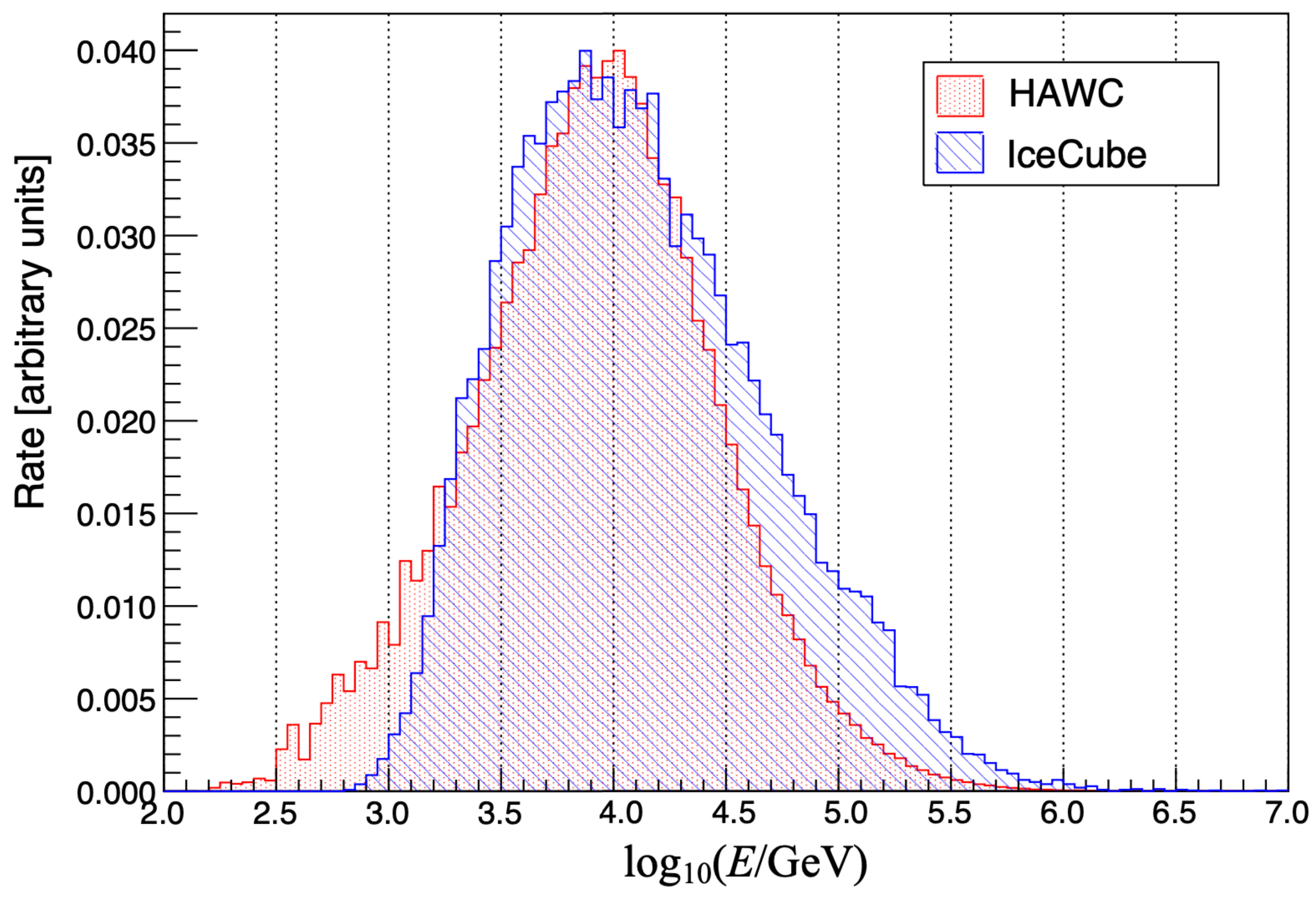

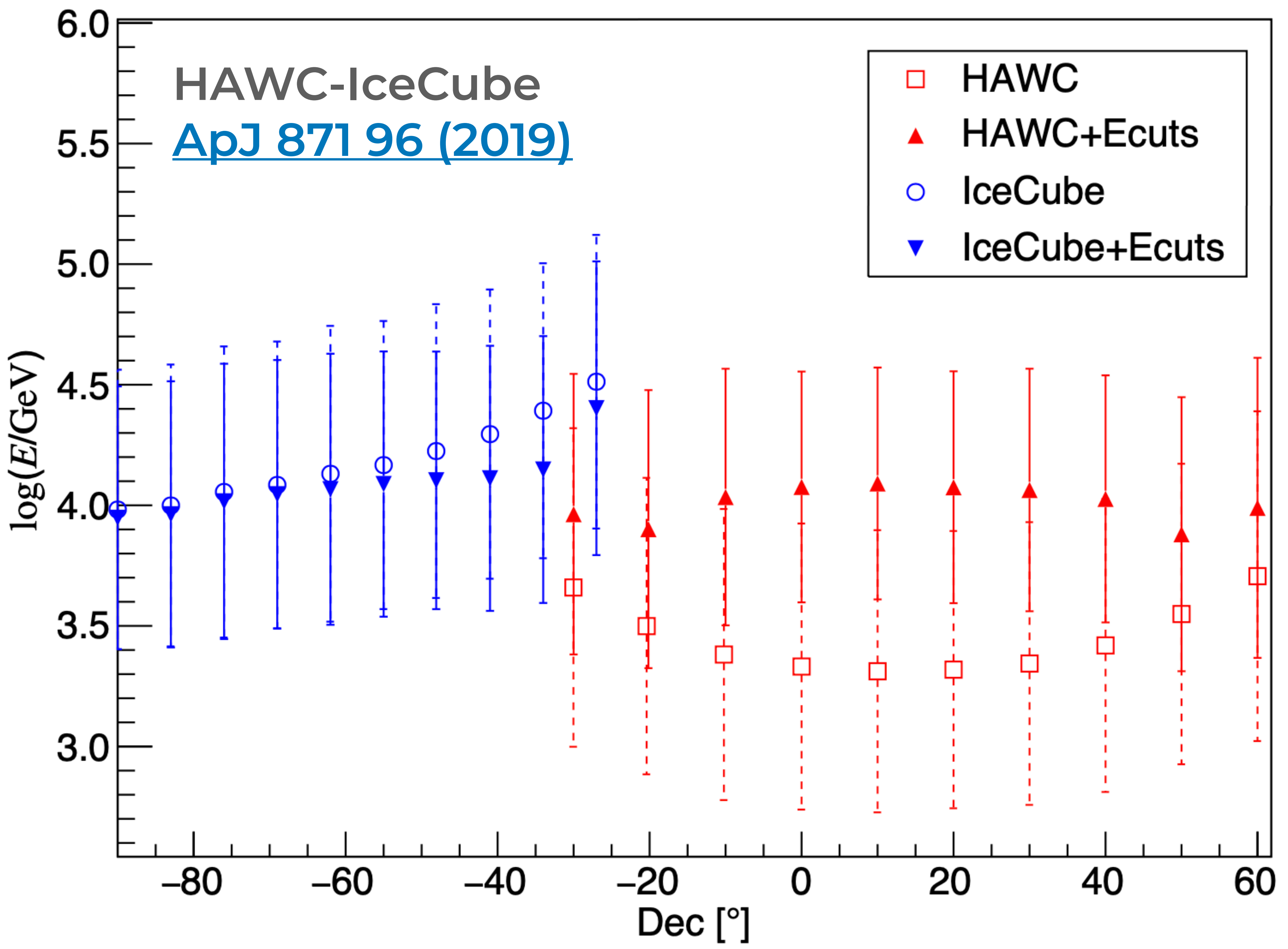

uniform **energy response function across the sky**

otherwise results show **mixed anisotropy** structures from different energies at **various declination bands**

mass composition
and rigidity scaling

observed cosmic rays have mixed mass composition: it's not only protons

different experiments have different **mass sensitivities**

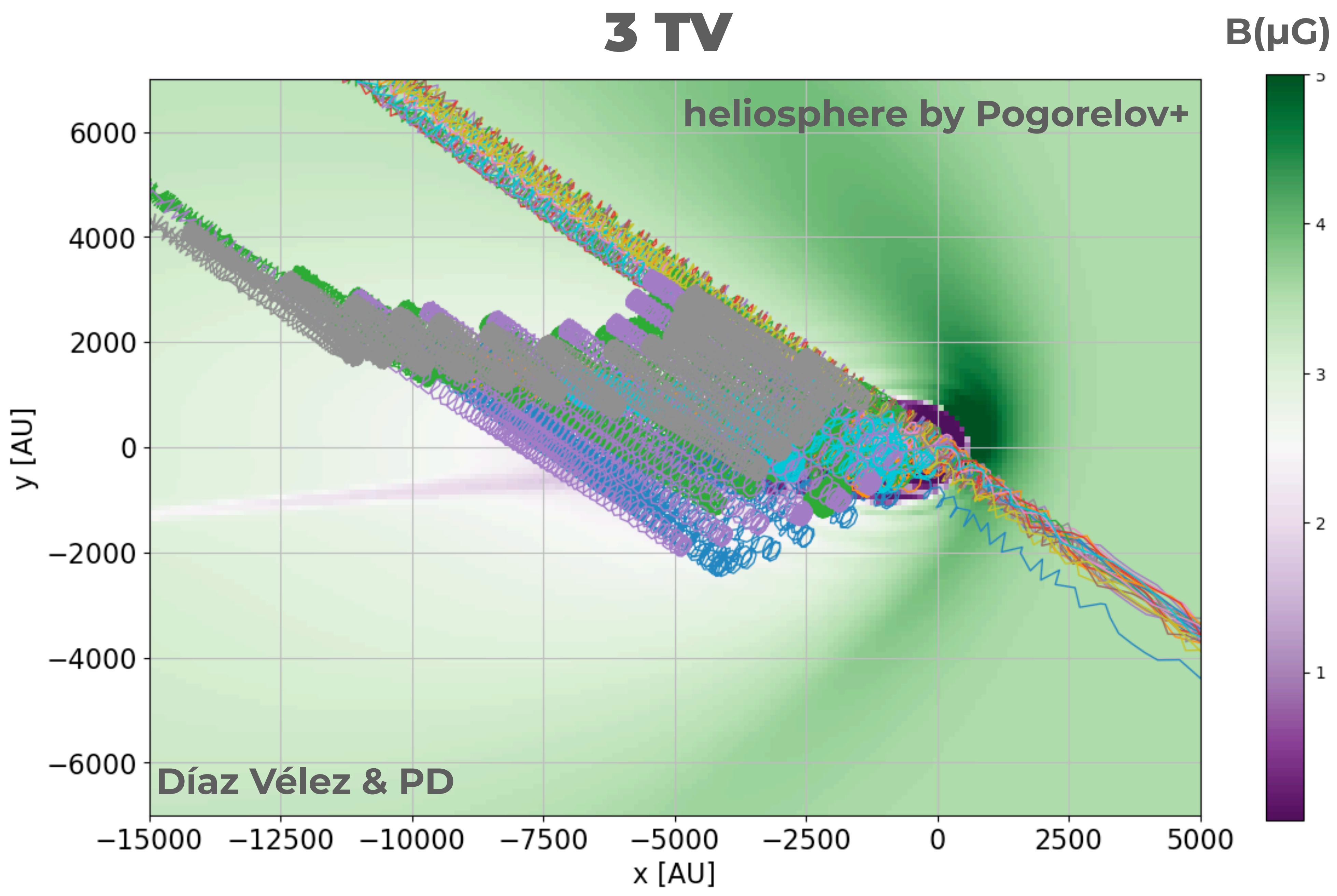

dipole component results from the combined mixed composition anisotropies which depends on energy

does anisotropy scale with rigidity, or does each species have its peculiar anisotropy?

conclusions

- **Promote inter-experiment collaborations:** not just stitching maps

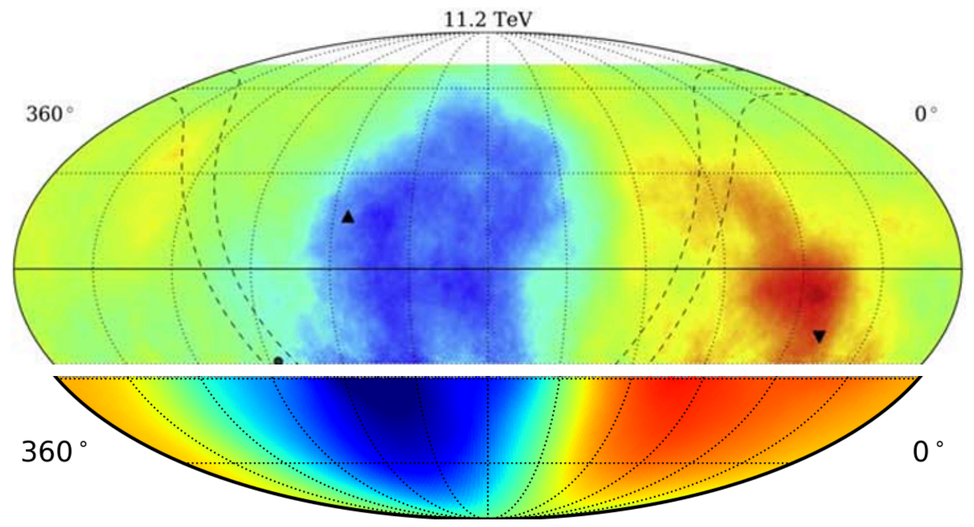

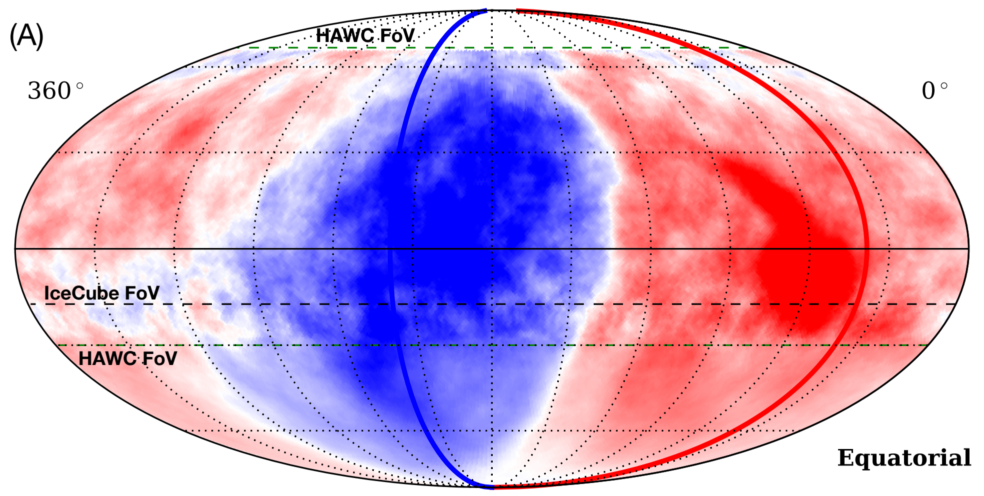

- **Encourage collaborations with theorists/modelers**
  - how to understand and correctly use the observations
  - how to prepare observations for the most appropriate model comparisons

- **Understand the role of the heliosphere < 100s TV**
  - develop models for interpreting cosmic rays

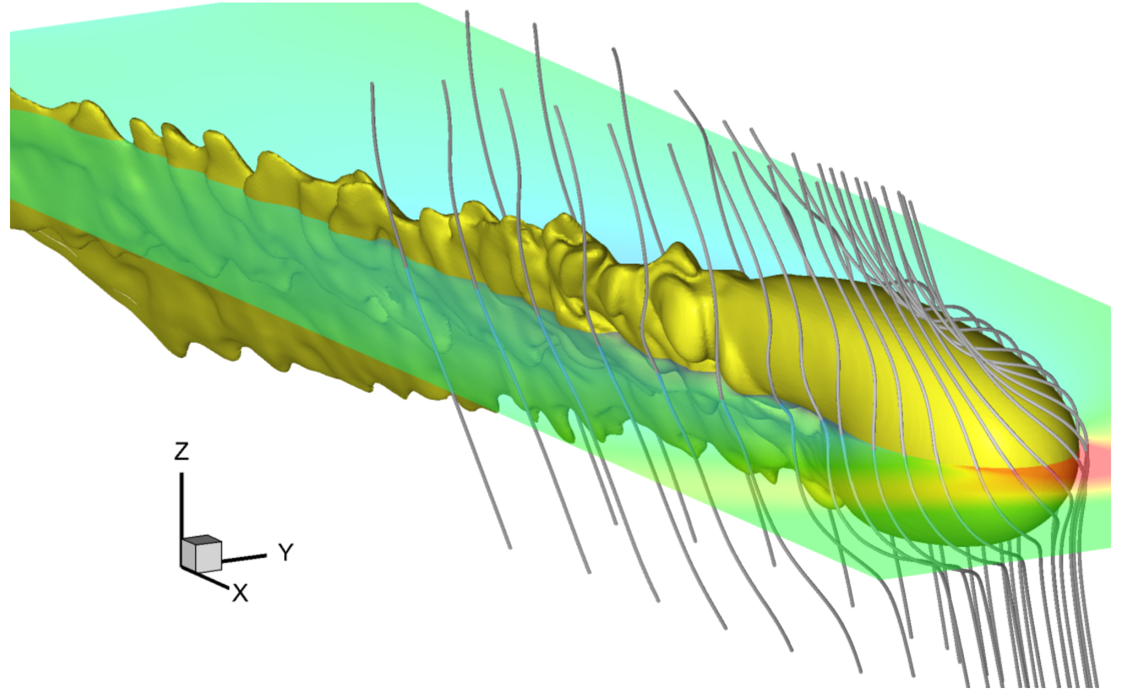

谢谢

Thank you

additional slides

cosmic-ray anisotropy

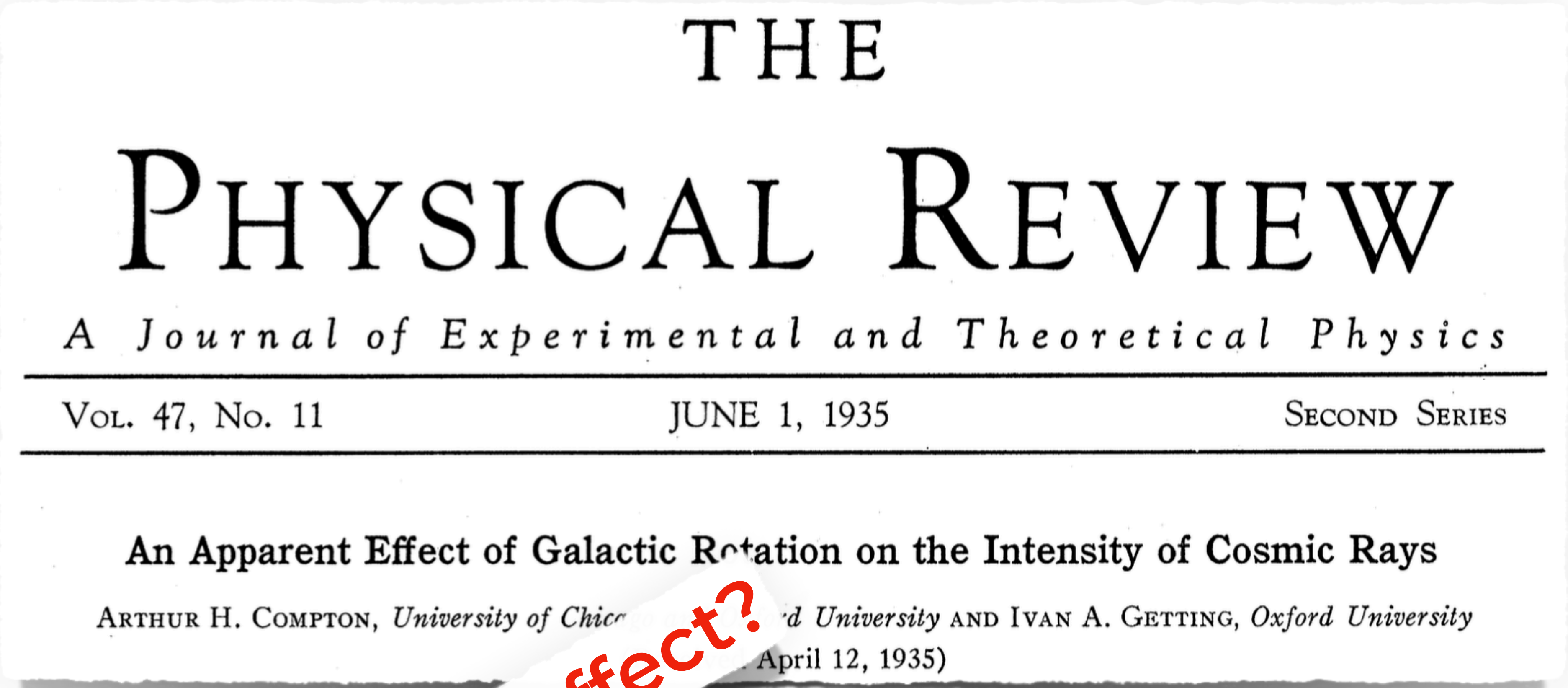

galactic rotation effect?

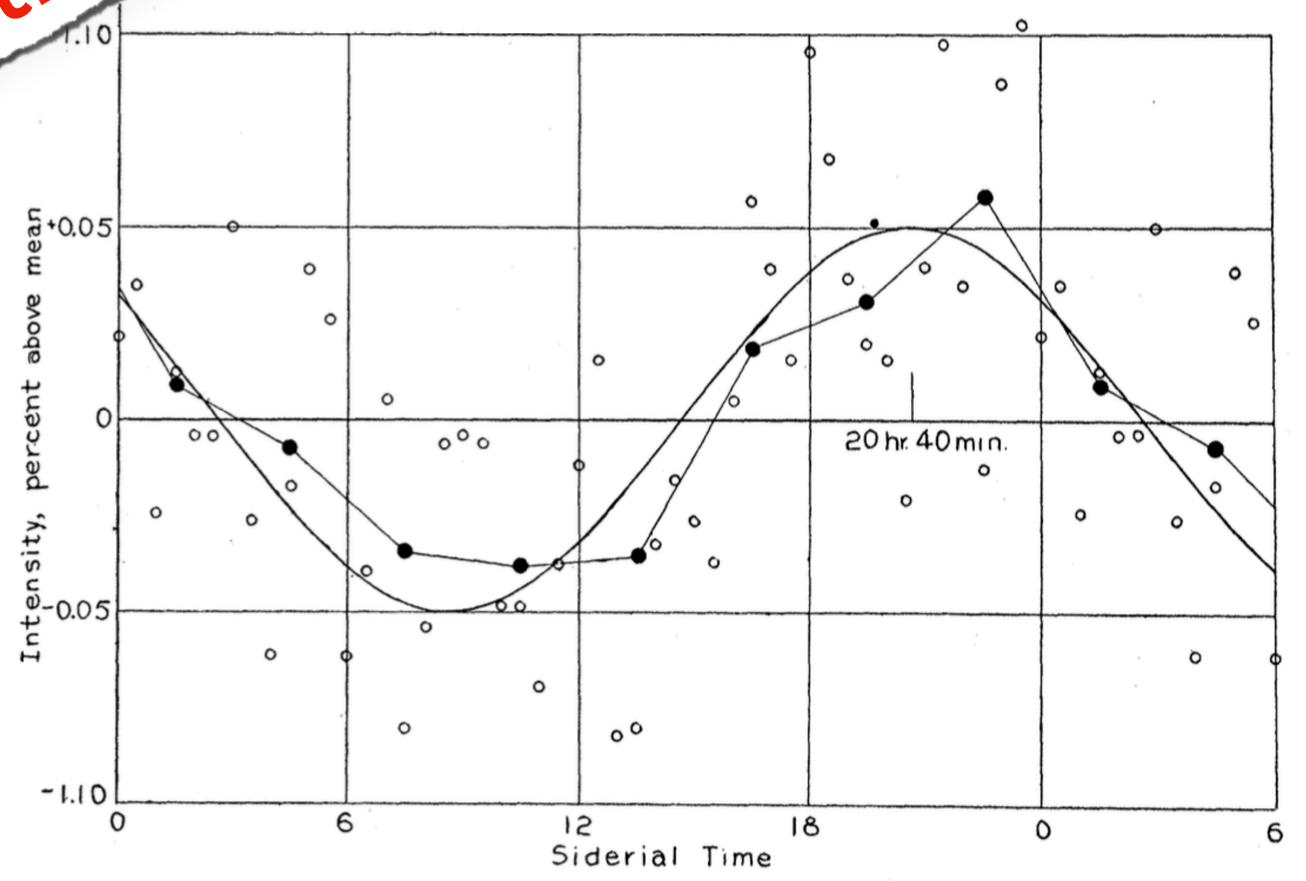

Fig. 2. Percentage variation in intensity of the cosmic rays with sidereal time. Curve, predicted effect due to galactic rotation. Data, Hess and Steinmaurer; open circles, half-hour means; solid circle, 3-hour means.

galactic co-rotation?

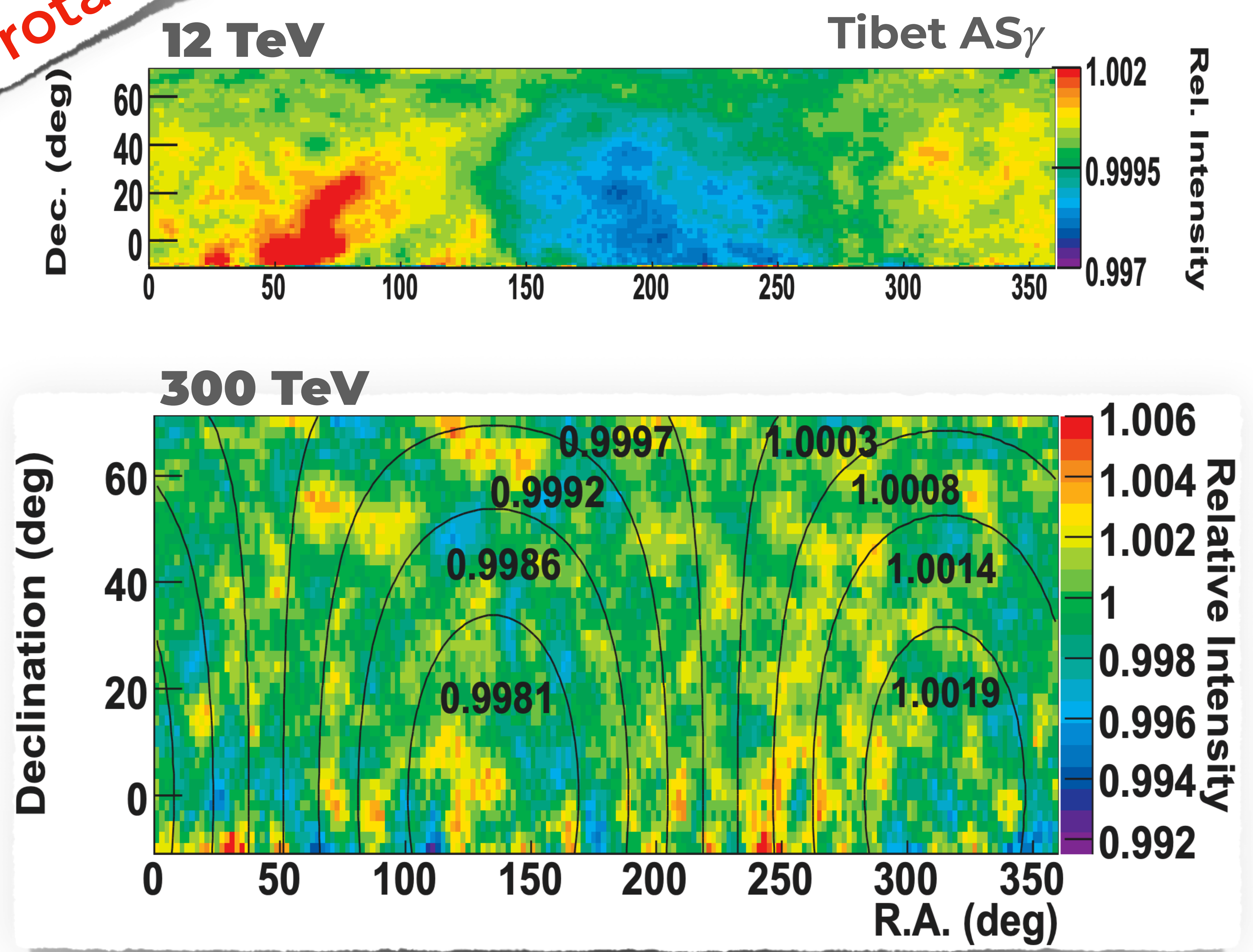

What does it take to provide interpretations that are as unbiased as possible?

where we are now

IceCube-Gen2

tech design report

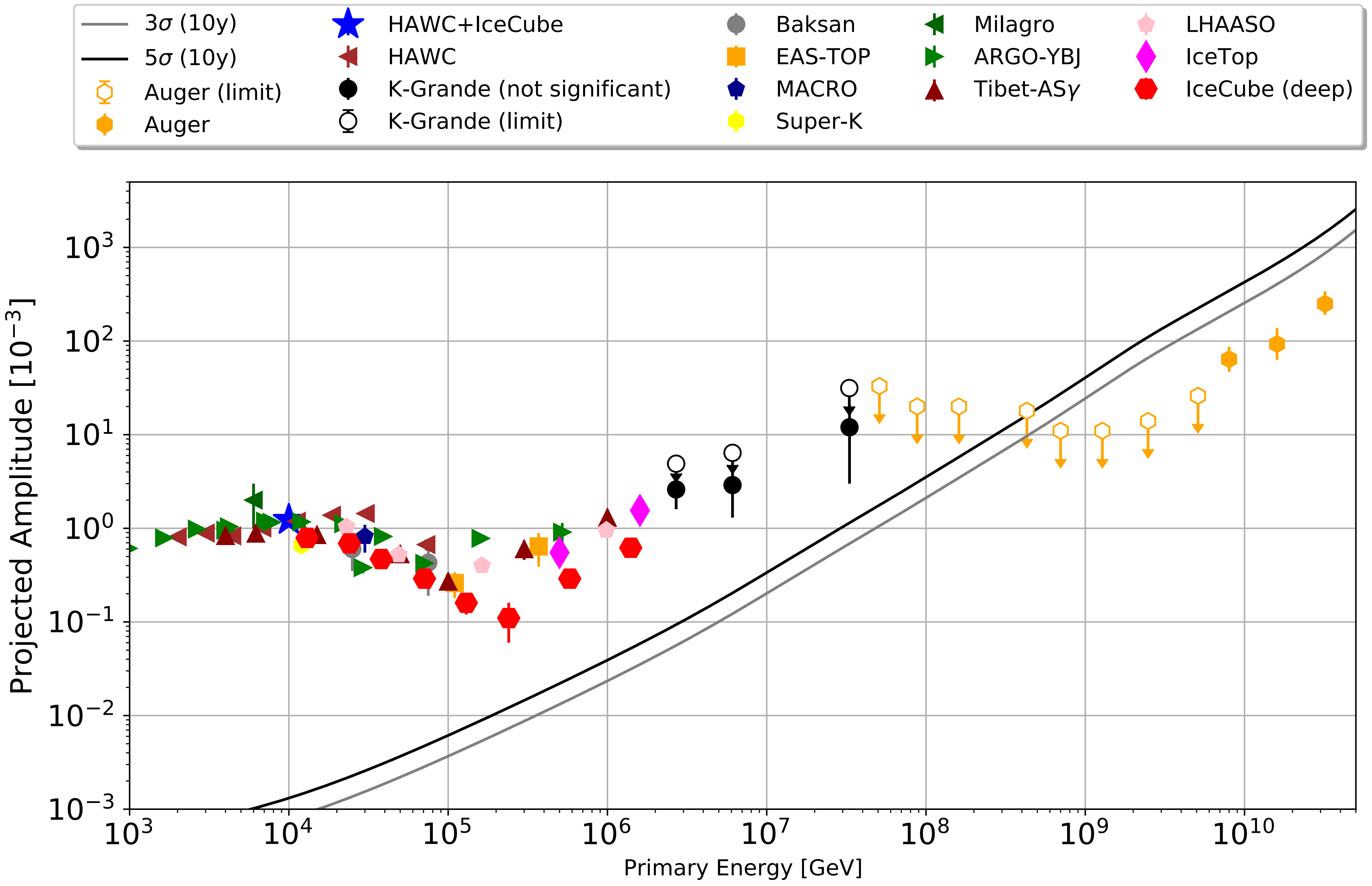

Figure 27: Sensitivity of cosmic-ray anisotropy measurements with IceCube-Gen2 with 10 years worth of data. The expected three and five sigma sensitivities to the equatorial plane component of the dipole anisotropy are shown. IceCube-Gen2 will be far the most sensitive detector for the PeV energy range, extending IceCube's energy range of anisotropies by more than an order of magnitude in energy. In particular, statistically non-significant measurements of the dipole amplitude by KASCADE-Grande [327], if true, can be confirmed at five sigma level. Note that KASCADE-Grande and Auger [328] results are shown with measurements (full symbols) and 90% CL upper limits (empty symbols) [327–341].

consequences of measuring anisotropy

HAWC
ApJ 865 57 (2018)

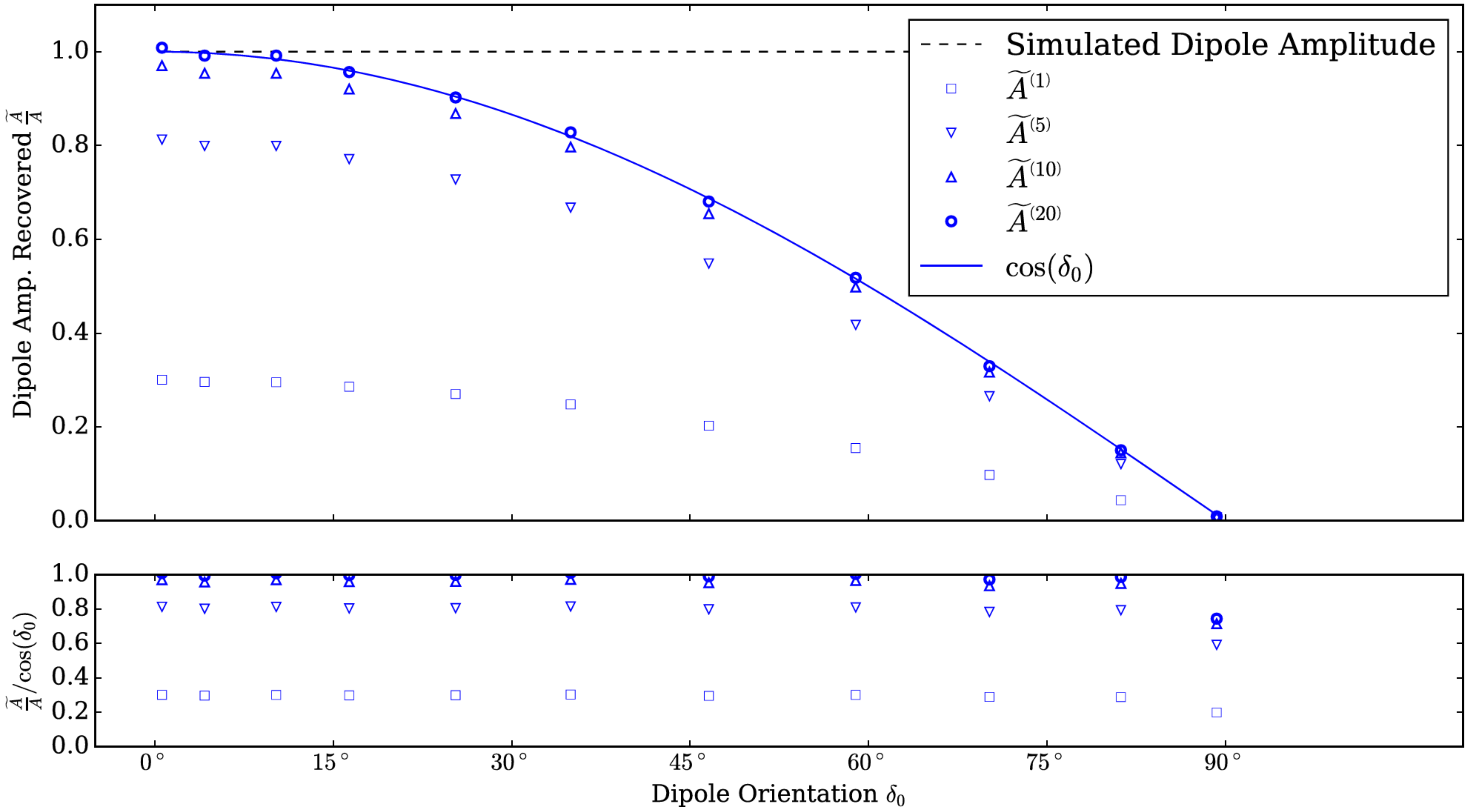

effect of the **north-south blindness**

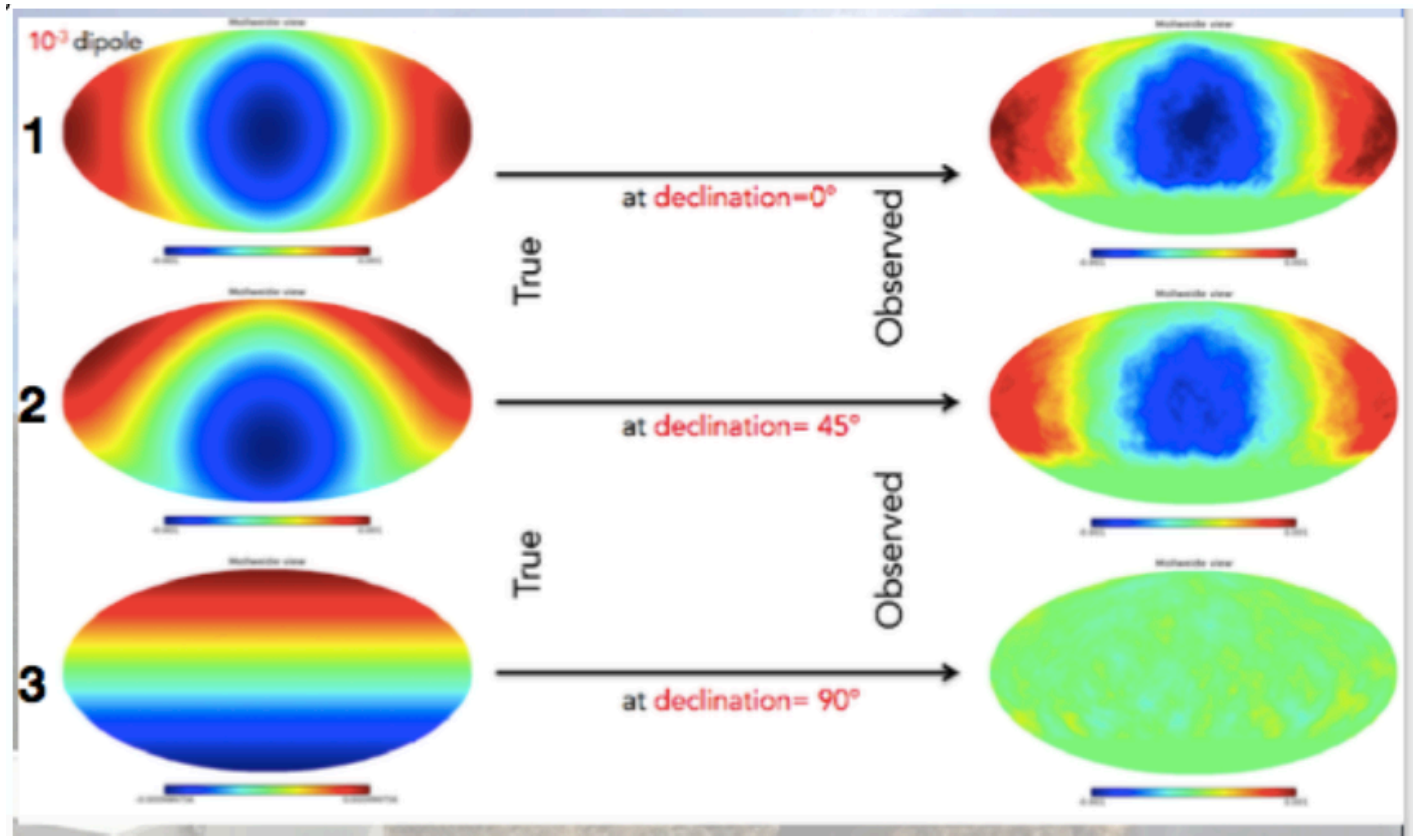

Simulated dipole reconstructed with LLH method

Vertical dipole component cannot be measured (when using data-driven reference map estimation)

Iterative LLH method compensates for the limited field of view (light to dark red)

Geometric correction needed due to limited sky coverage

IceCube
ApJ 981 182 (2025)

measuring the dipole component

relative intensity expanded in spherical harmonic functions

$$\delta I(\mathbf{u}_i) = \sum_{\ell=1}^{\infty} \sum_{m=-\ell}^{\ell} a_{\ell m} Y_{\ell m}(\mathbf{u}_i)$$

with partial sky coverage the $Y_{\ell m}$ are correlated except for the $m = \ell$ terms

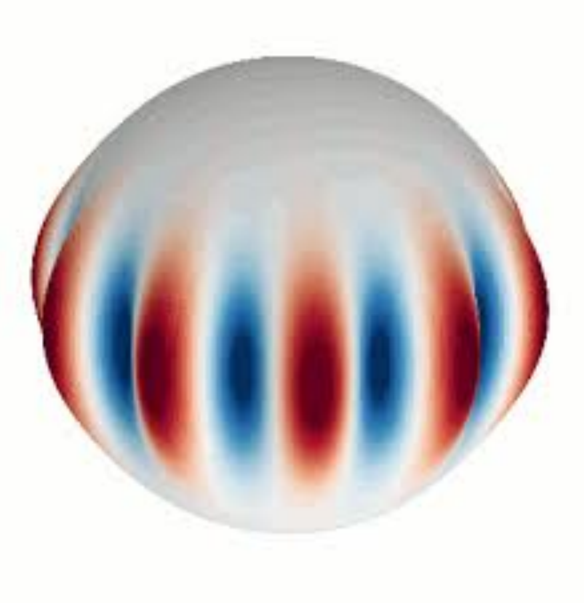

we use these functions for a **2D** fit of sky maps

$$F(\alpha_i, \delta_i) = \sum_{n=m=\ell=1}^{3} A_n \cos^n(\delta_i) \cos(n\alpha_i + \phi_n)$$

to be compared with the *standard* **1D** dipole fits

$$\tilde{F}(\alpha_i) = \frac{1}{\sin\delta_{\max} - \sin\delta_{\min}} \int_{\delta_{\min}}^{\delta_{\max}} F(\alpha_i, \delta) \cos\delta \, d\delta$$

$$= \sum_{n=1}^{3} \tilde{A}_n \cos(n\alpha_i + \tilde{\phi}_n)$$

IceCube
ApJ 981 182 (2025)

measuring the dipole component

for the dipole component this 1D function is

$$\tilde{F}(\alpha_i) = \frac{A_1}{\sin\delta_{\text{max}} - \sin\delta_{\text{min}}} \int_{\delta_1}^{\delta_2} \cos^2\delta \cos(\alpha_i + \phi_1) d\delta$$

$$= \frac{\delta_{\text{min}} - \delta_{\text{max}} + \cos\delta_{\text{min}}\sin\delta_{\text{min}} - \cos\delta_{\text{max}}\sin\delta_{\text{max}}}{2(\sin\delta_{\text{min}} - \sin\delta_{\text{max}})} A_1 \cos(\alpha_i + \phi_1)$$

$$= \tilde{A}_1 \cos(\alpha_i + \tilde{\phi}_1)$$

with **geometric correction factor** equal to

that depends on experiment's field of view in Dec.

$$A_1^\dagger \equiv \frac{2(\sin\delta_{\text{min}} - \sin\delta_{\text{max}})}{\delta_{\text{min}} - \delta_{\text{max}} + \cos\delta_{\text{min}}\sin\delta_{\text{min}} - \cos\delta_{\text{max}}\sin\delta_{\text{max}}} \tilde{A}_1$$

dipole anisotropy component

a local source

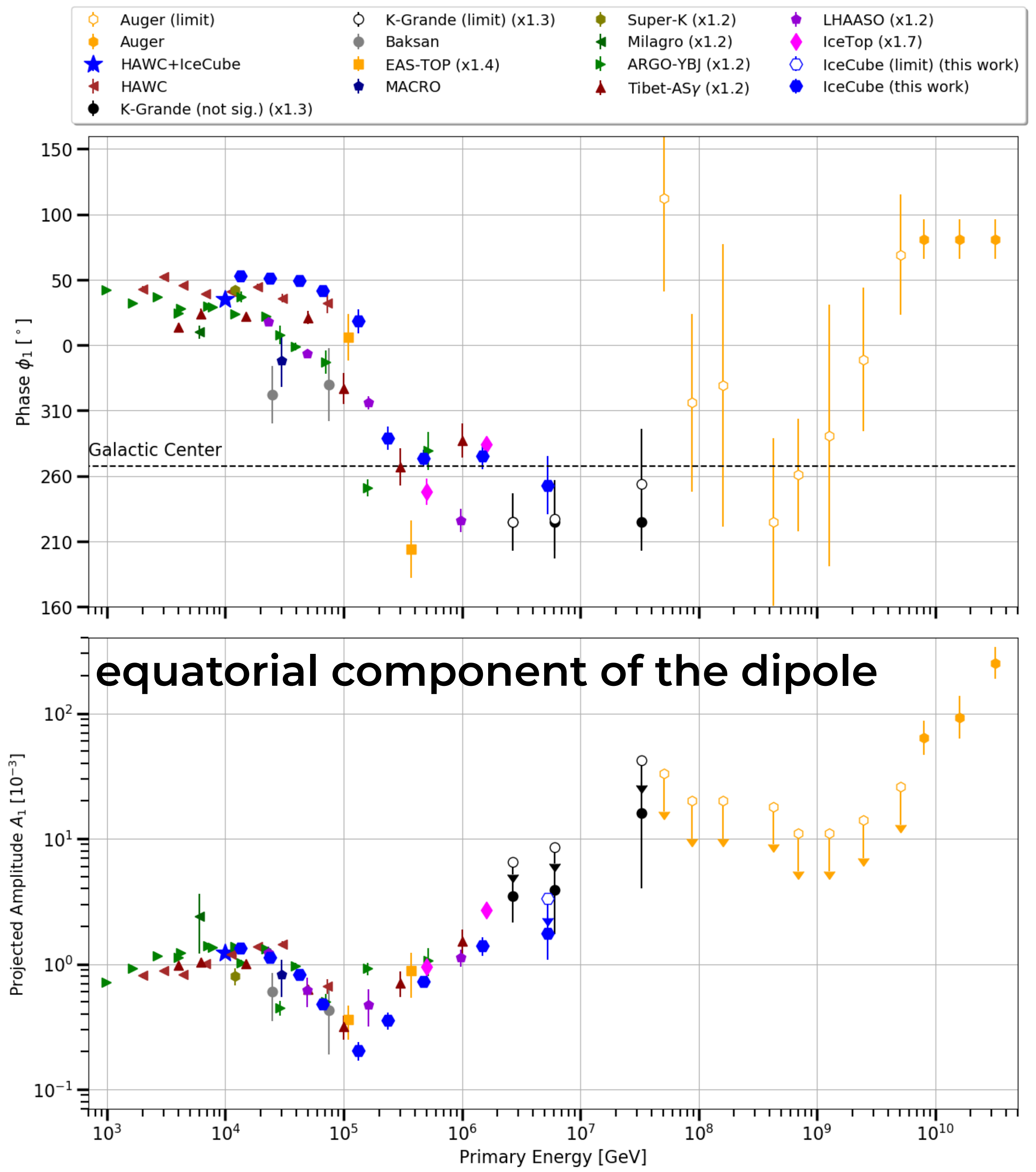

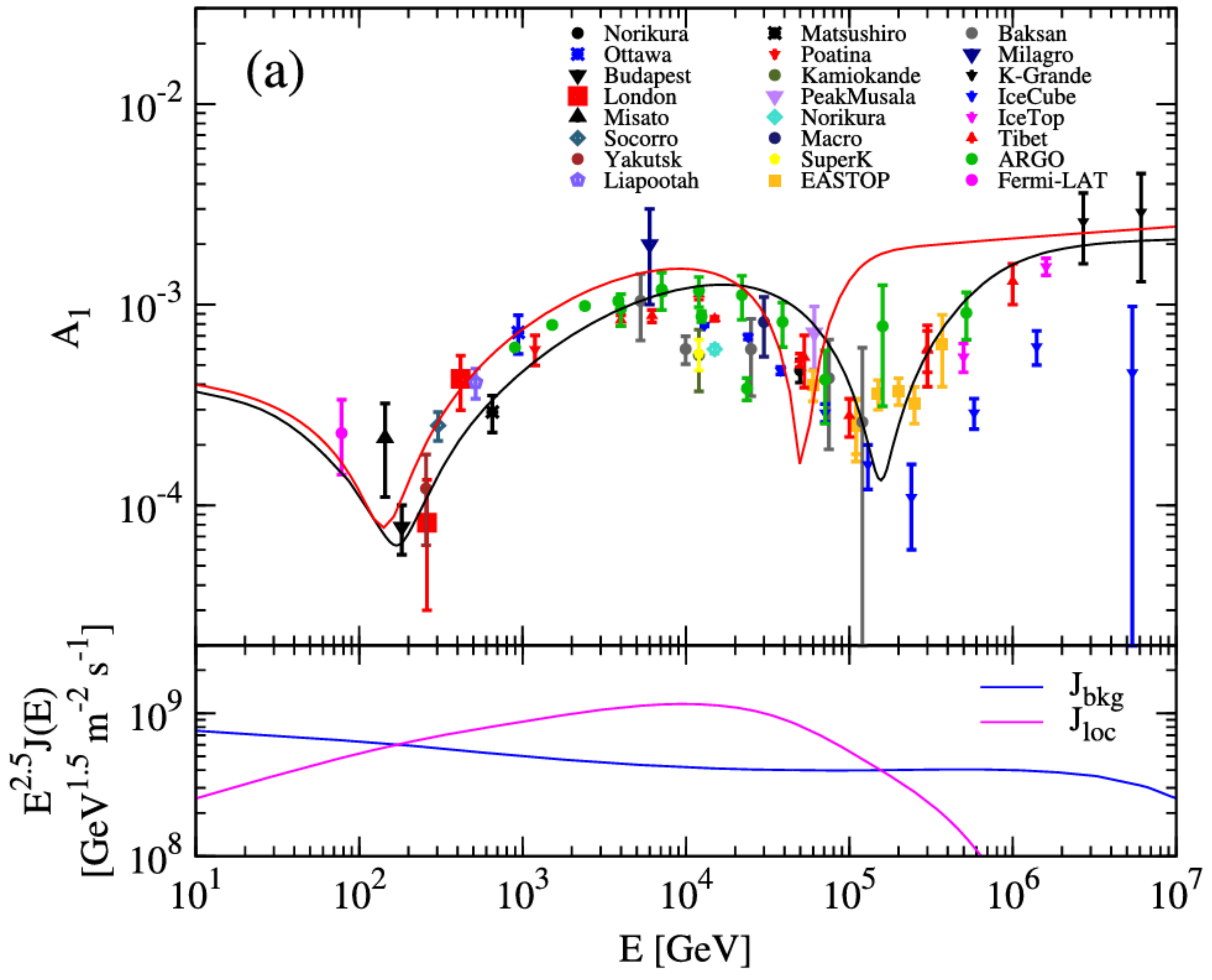

Qiao+ (2023)

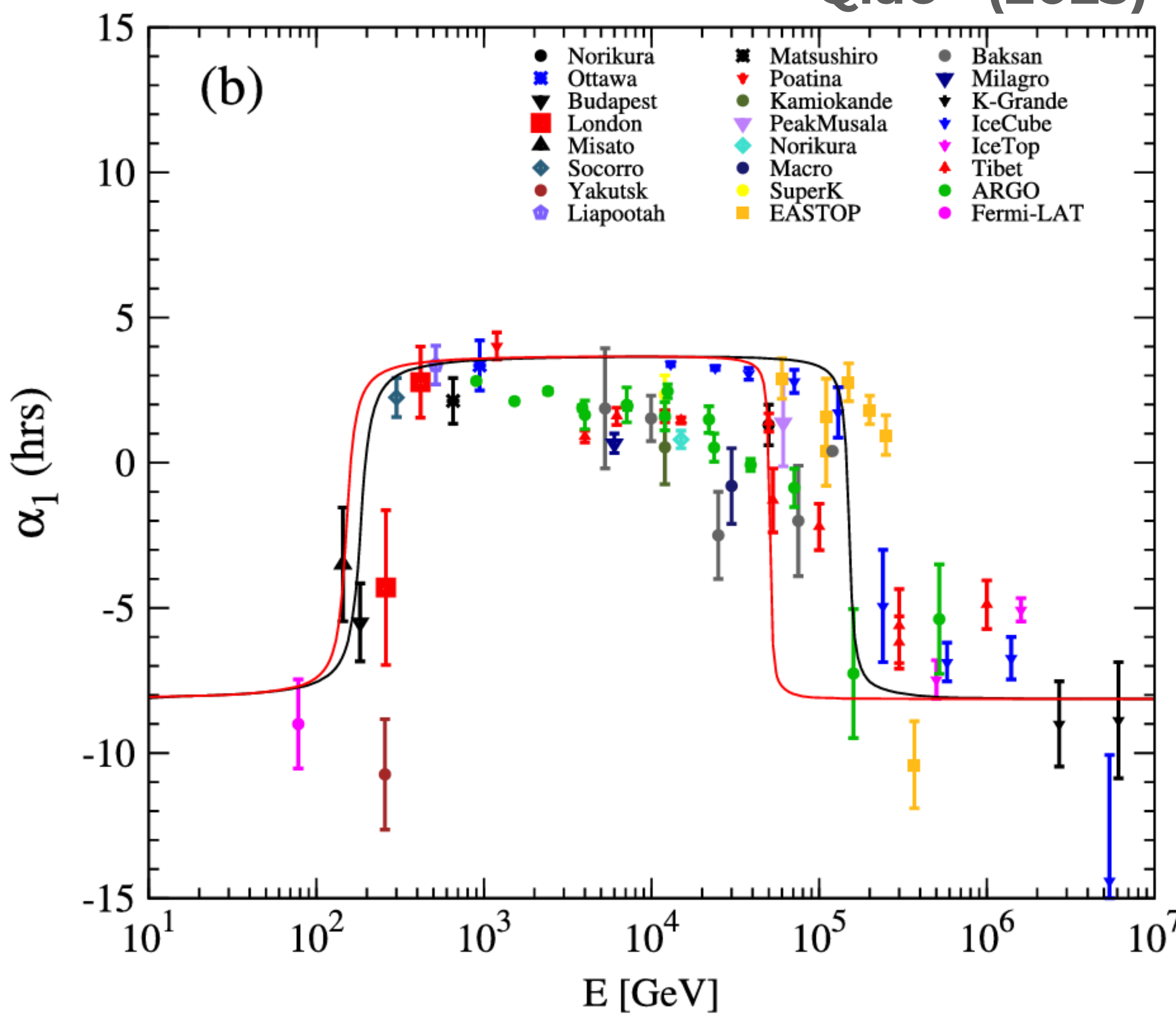

alighment along the IBEX ISM magnetic field

nearby source background source protons all-CRs

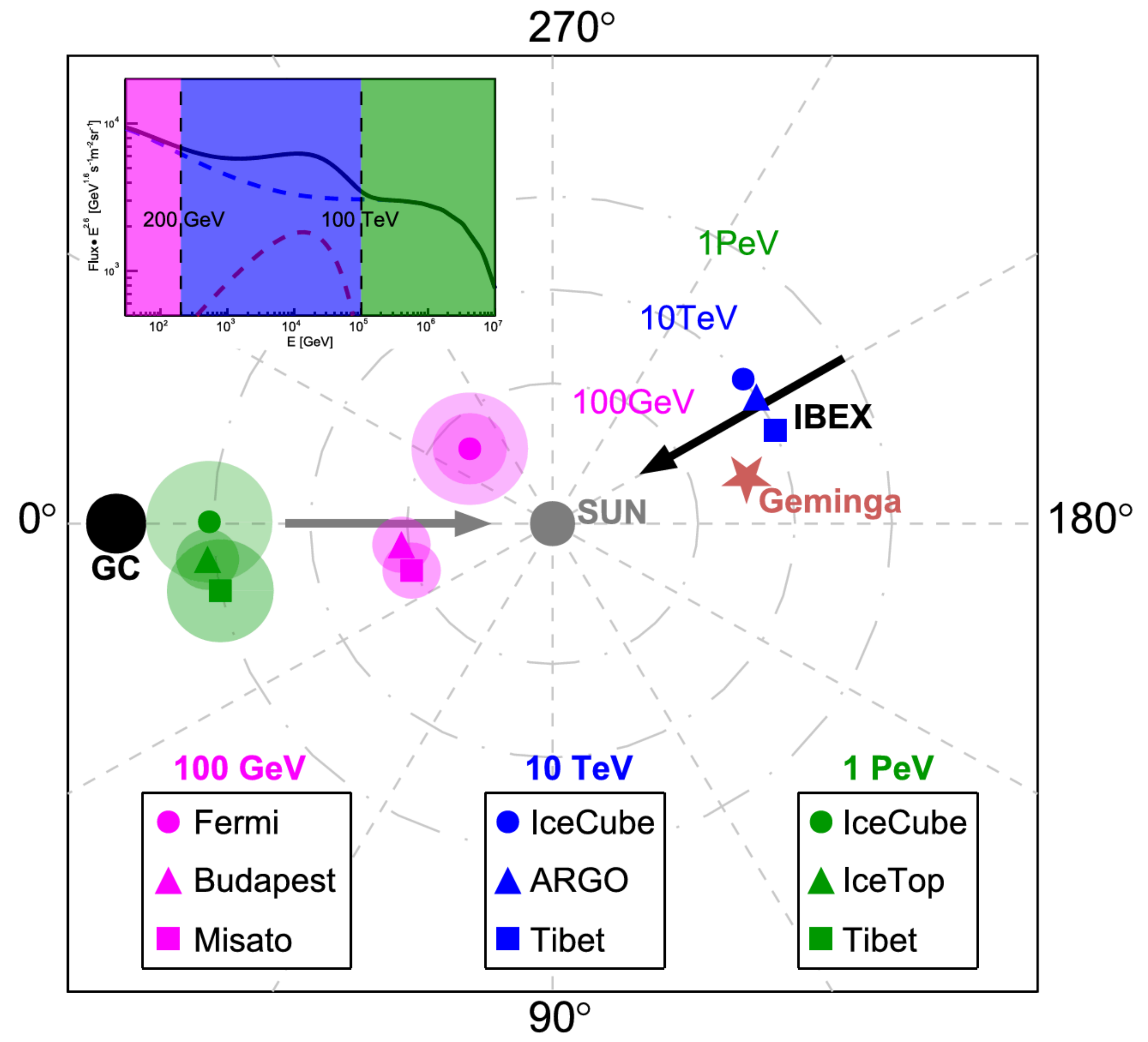

illustration of the evolution of CR energy spectrum and anisotropy in the presence of a local source.

dipole anisotropy component

a local source

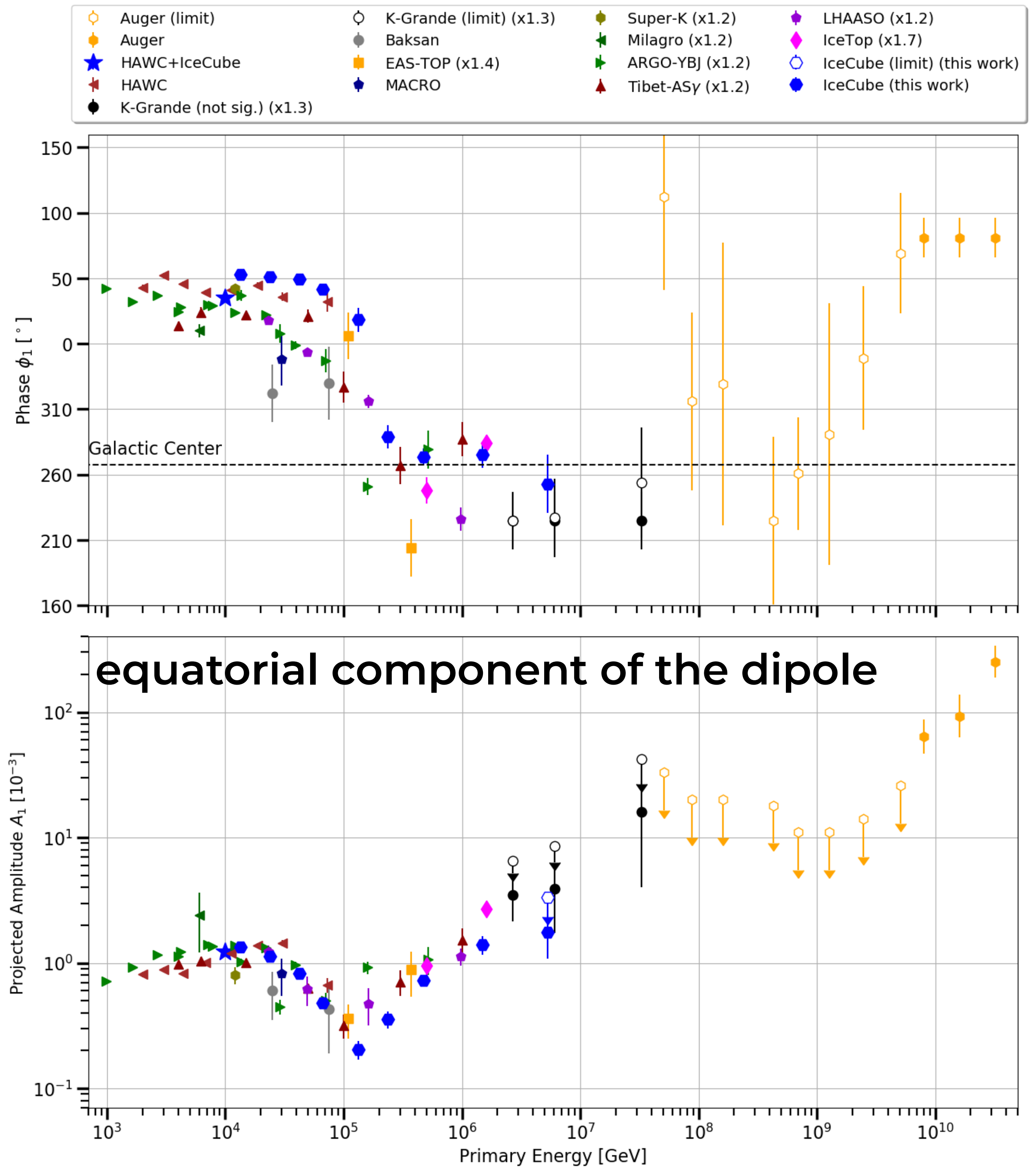

anisotropic diffusion

diffusion coefficient

lower in inner halo

Geminga

local source to determine **spectral anomaly**

and counterbalance galactic anisotropy

below 100 TeV energy scale

Li+ (2024)

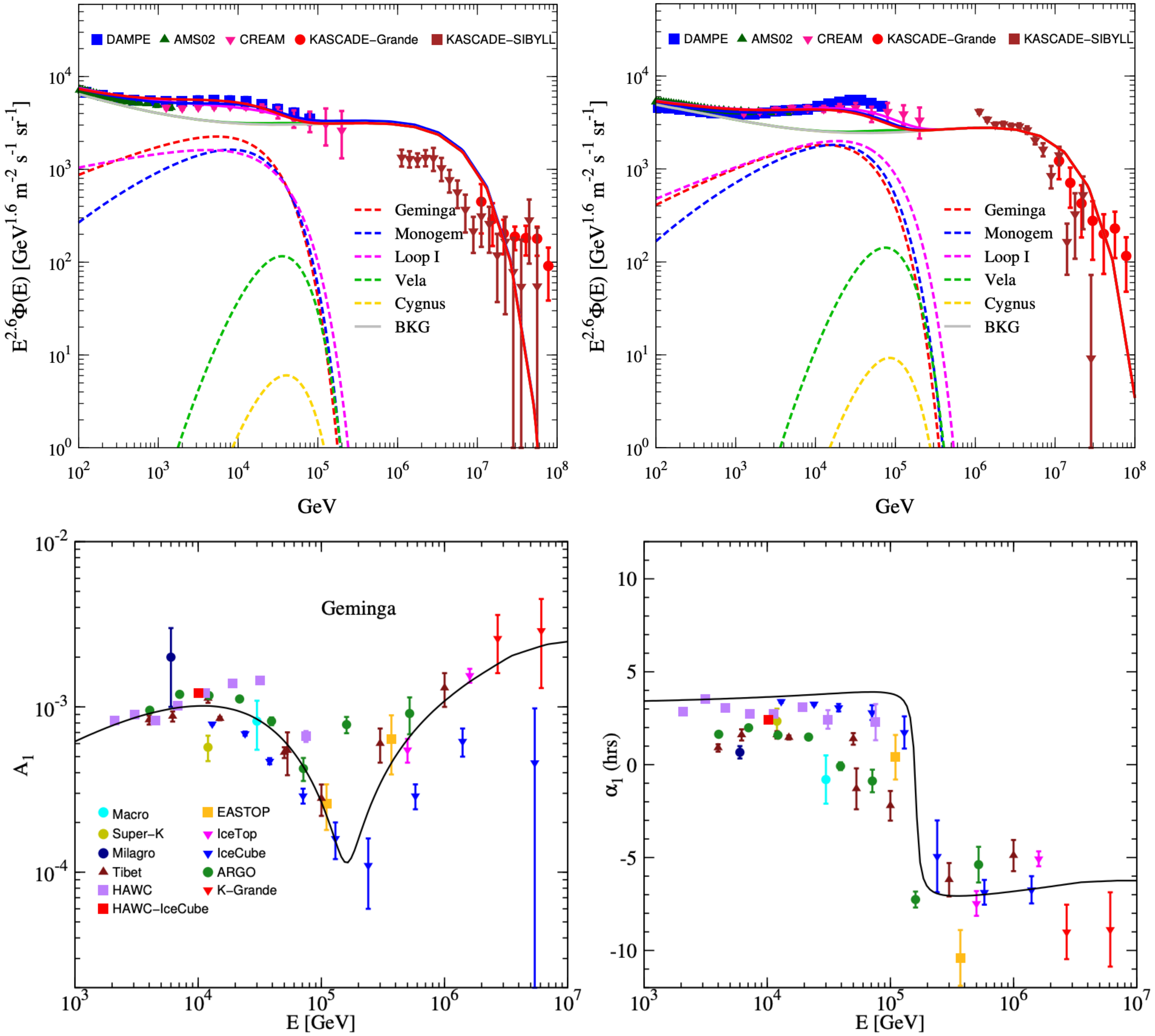

medium/small-scale anisotropy
fingerprint of local turbulence

Kuhlen, Phan, Mertsch (2022)

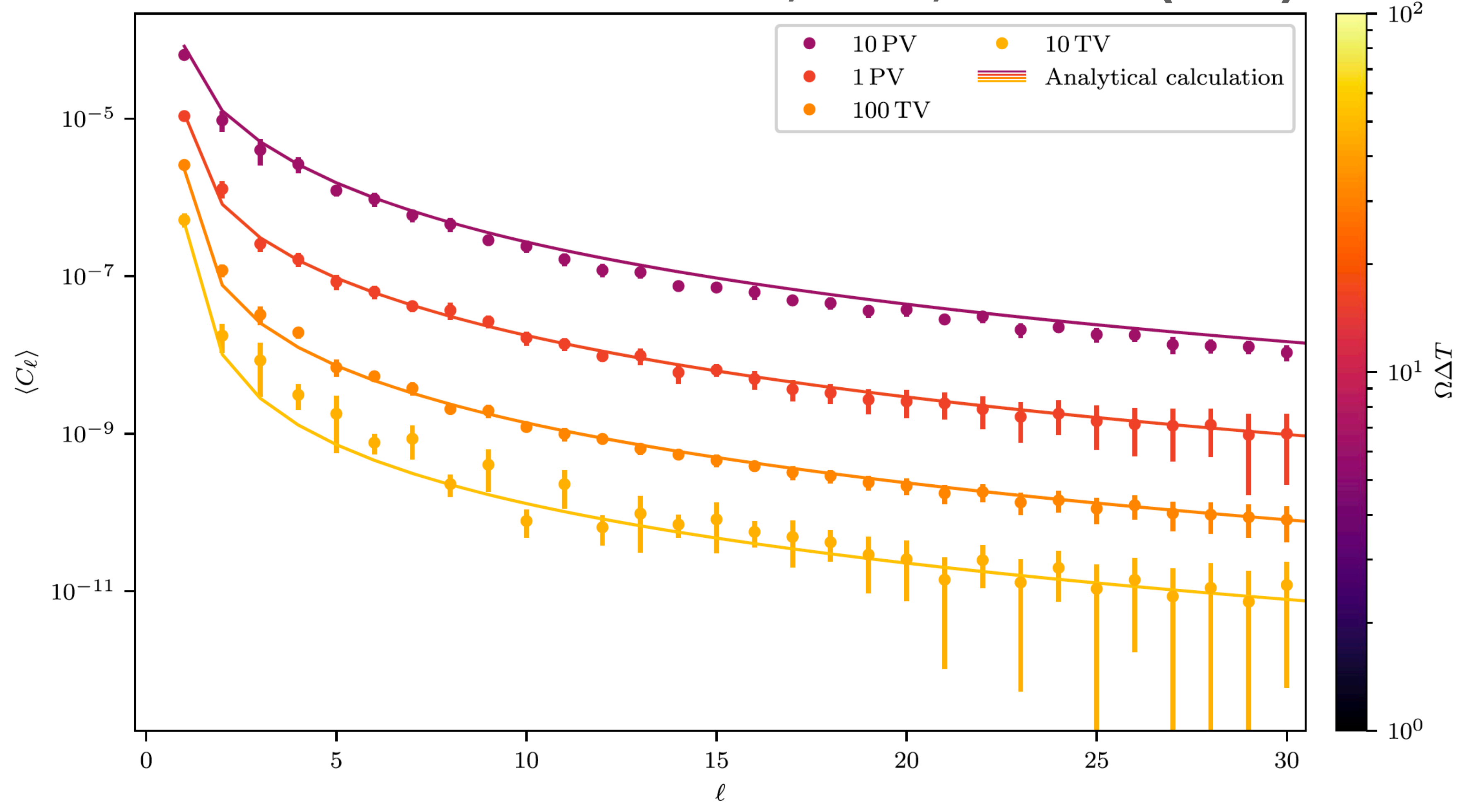

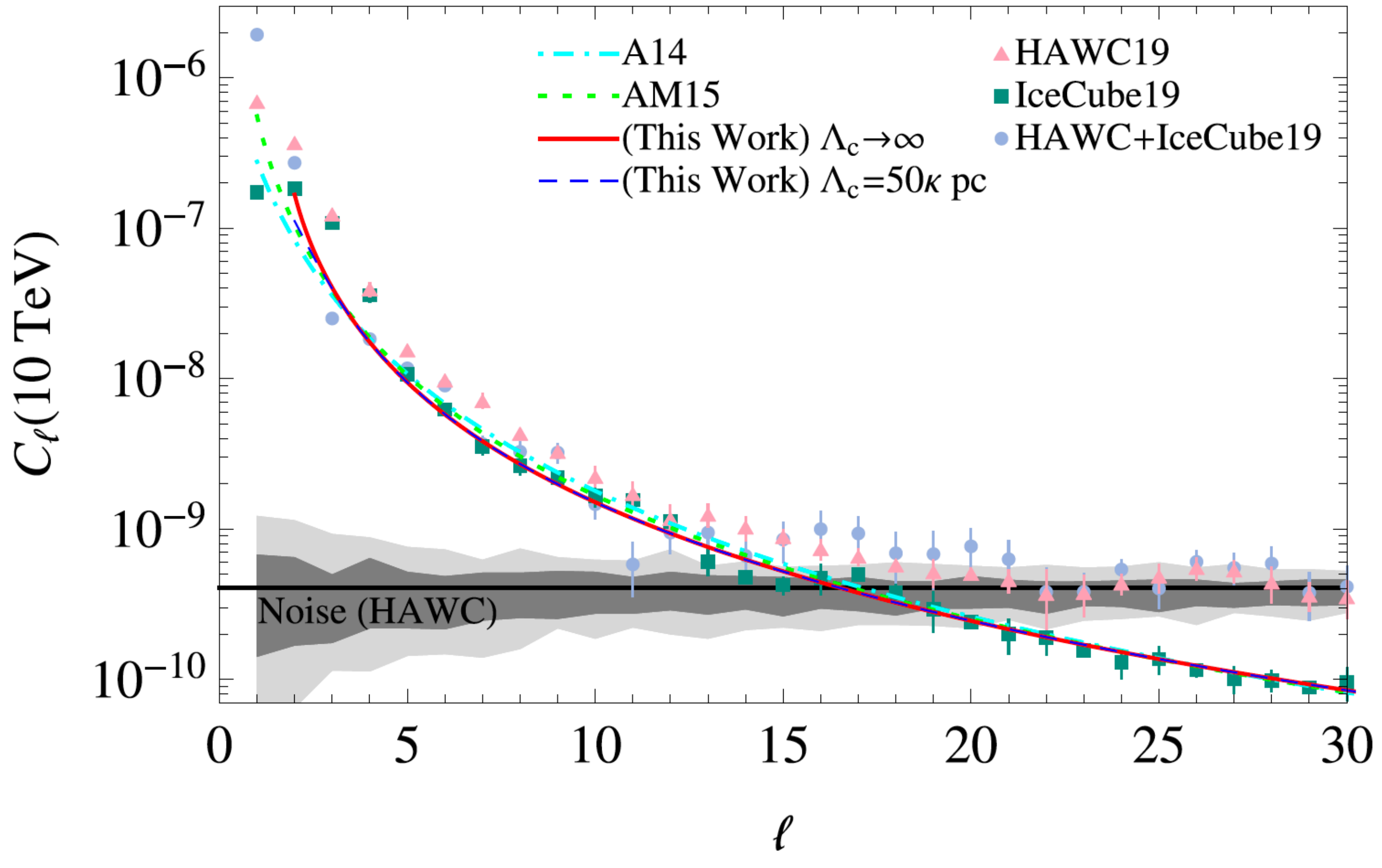

Zhang & Liu (2024)

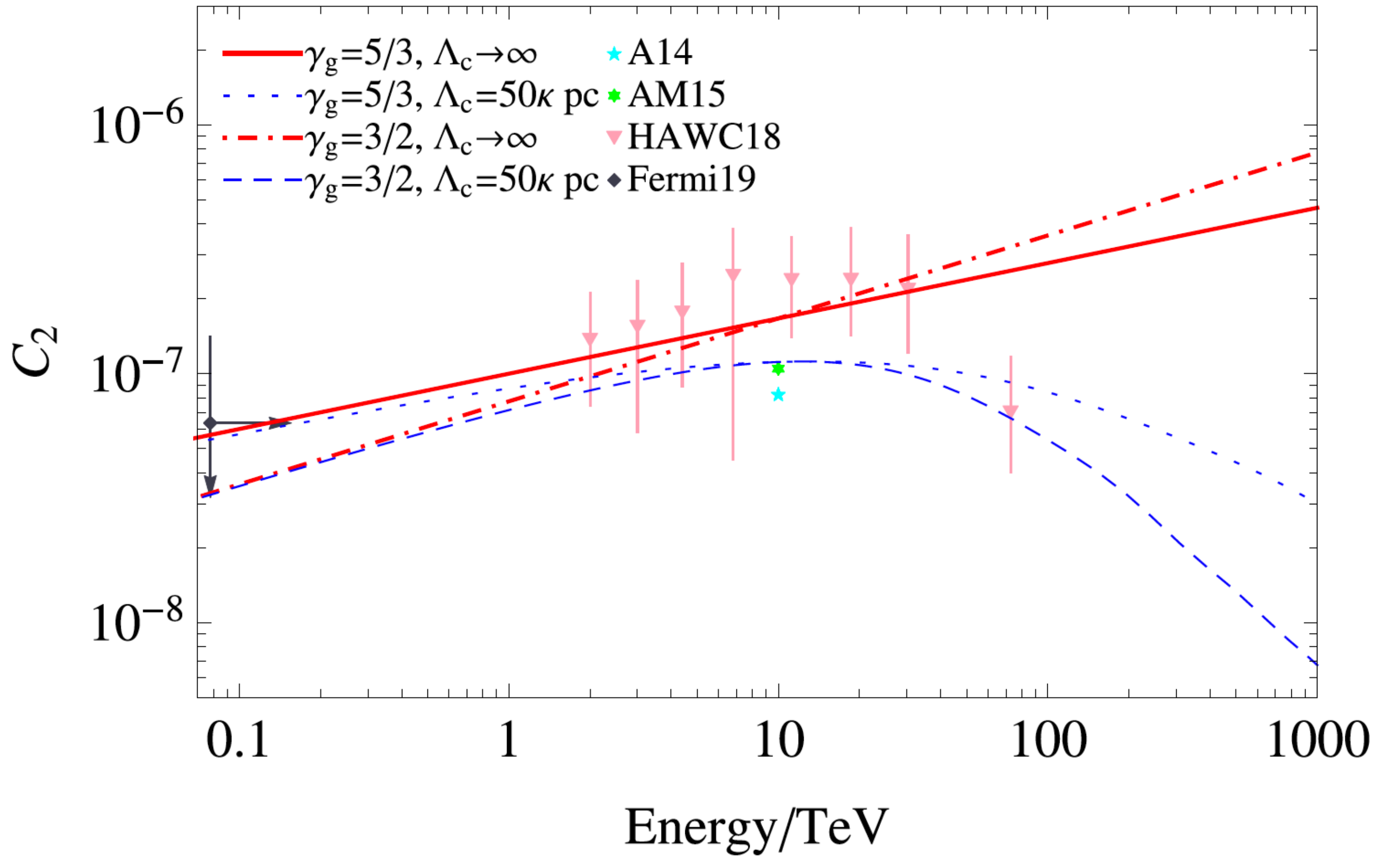

long-baseline numerical calculation in *synthetic turbulence*

angular power spectrum from "correlations of particles experiencing the same turbulent magnetic field."

uniform plasma convection gives rise to the Compton-Getting effect

turbulent plasma convection generates perturbations at various angular scales

"With the idea that particle distributional fluctuations can be related to fluid local nonuniformity, we have demonstrated that turbulent convection may give rise to remarkable small-scale anisotropies of the distribution."

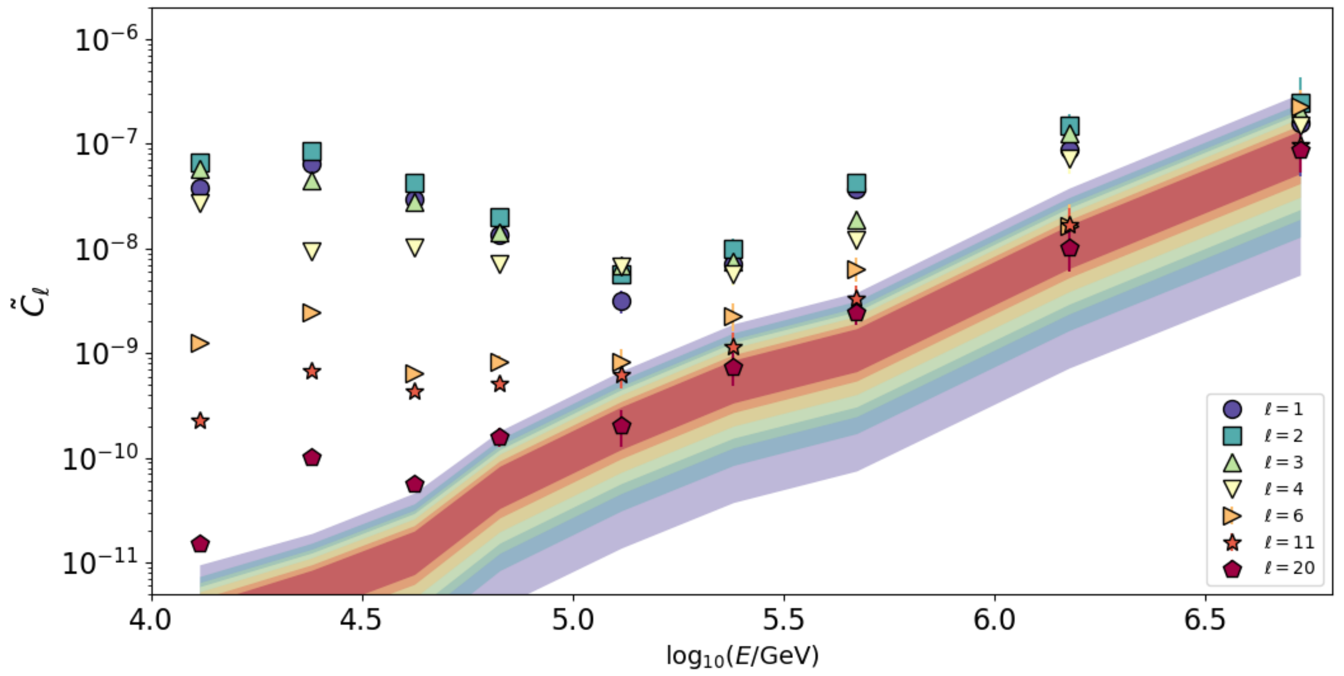

IceCube
ApJ 981 182 (2025)

medium-scale anisotropy
fingerprint of local turbulence

propagation effects on **anisotropic** spectrum of Goldreich-Sridhar type Alfvén waves

isotropic distribution of fast magnetosonic modes with a power spectrum compatible with Cho & Lazarian (2002)

isotropic diffusion (in QLT) generates a dipole anisotropy and cannot explain observations

Giacinti & Kirk (2017)

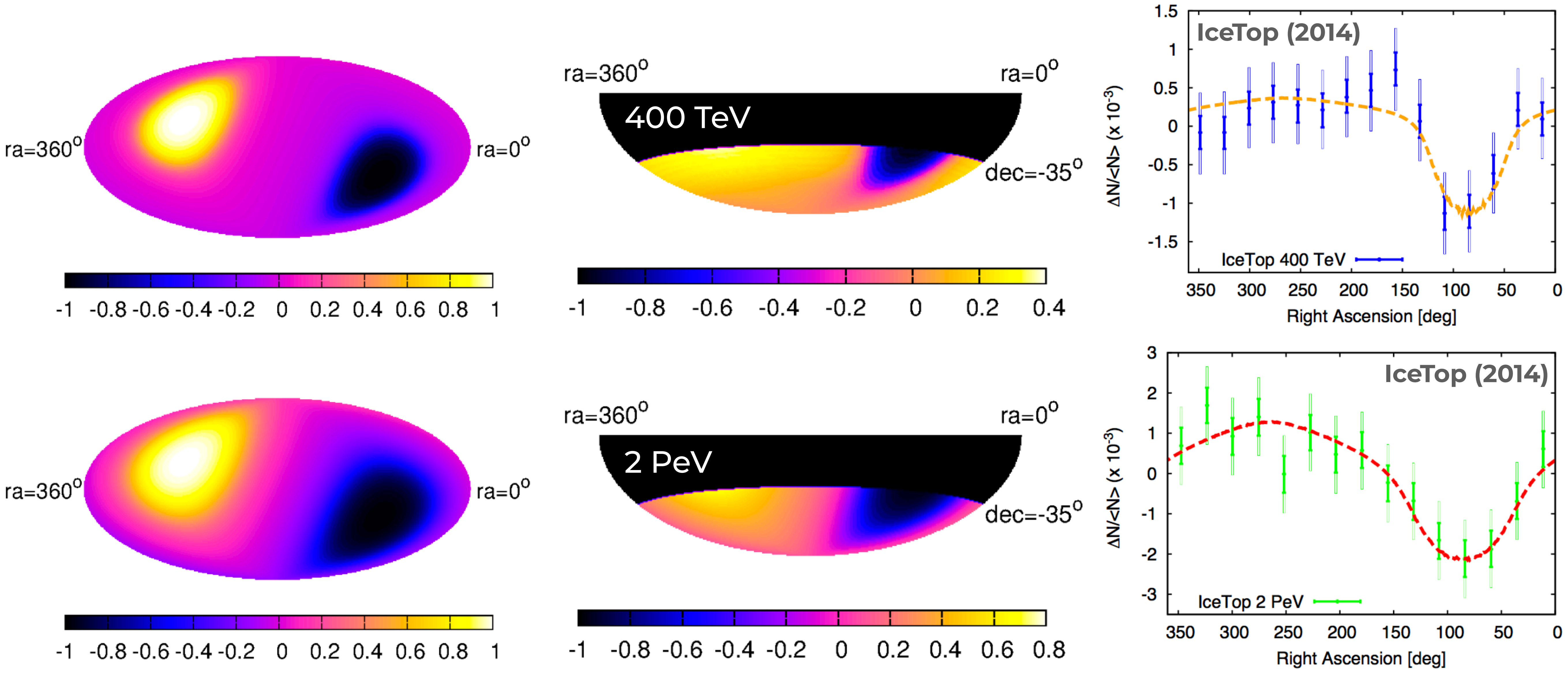

our magnetic backyard
influence of the heliosphere

López Barquero + PD+ (2017)

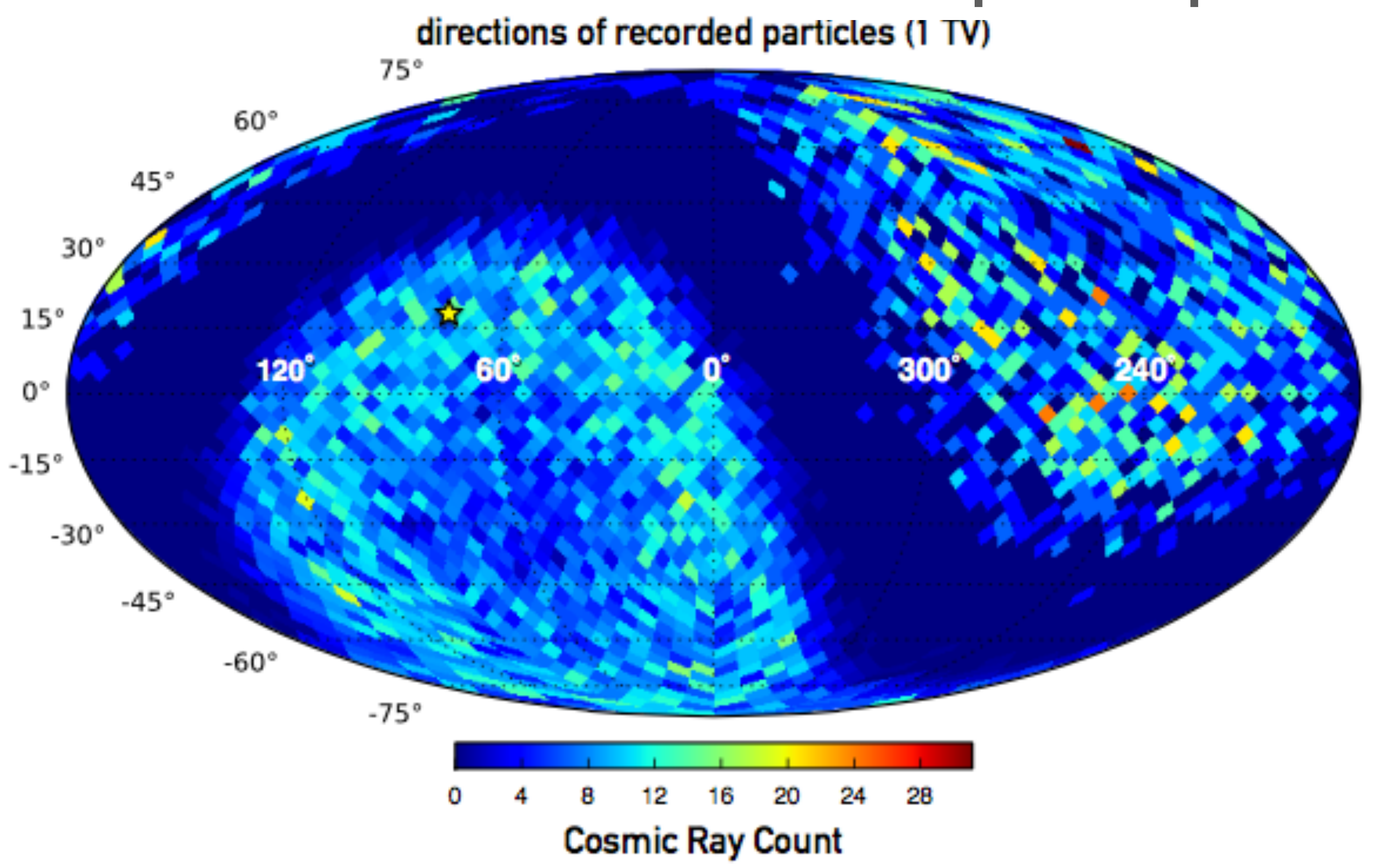

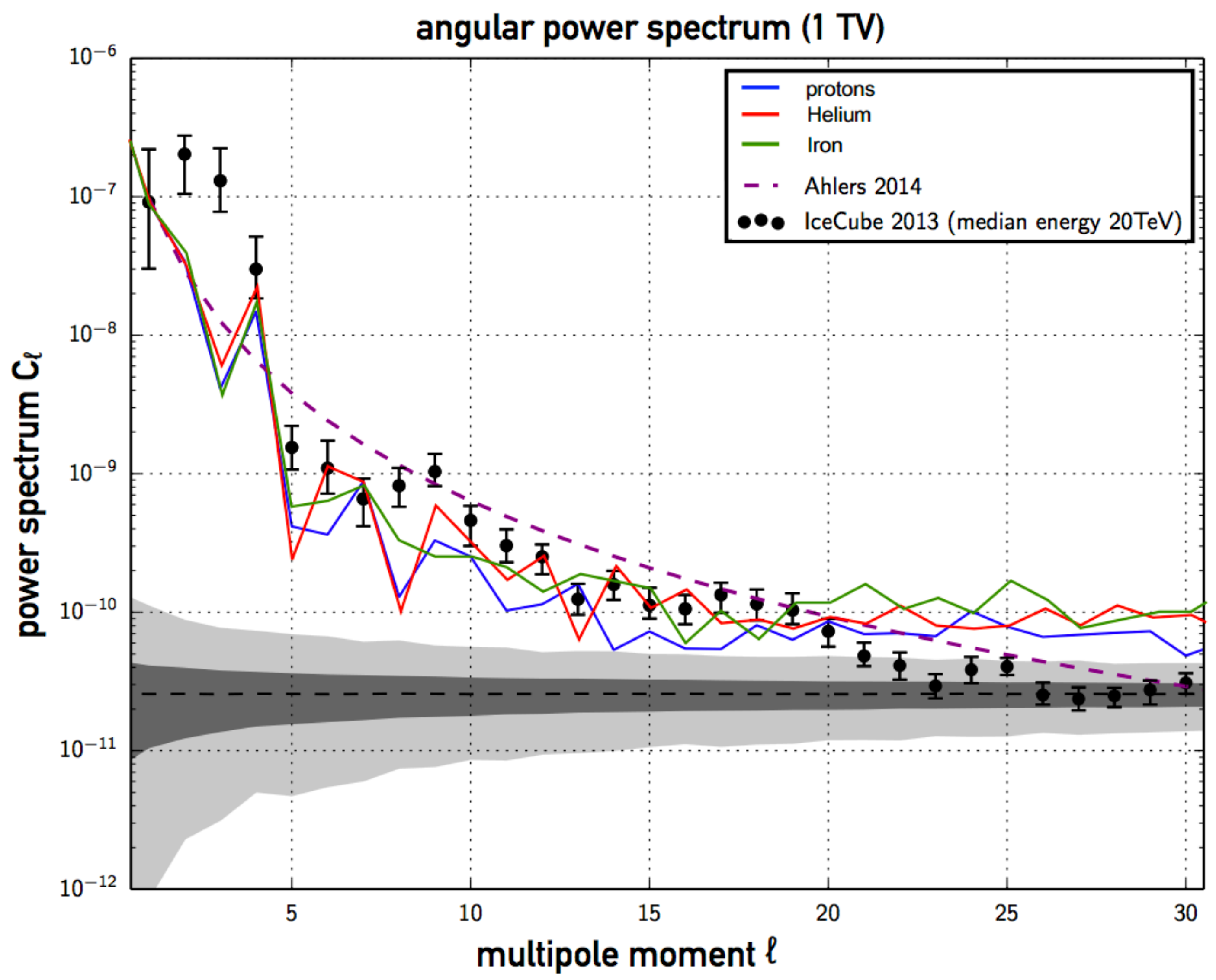

forward propagation
injection @ 6000 AU - target @ 200 AU

takes into account pitch-angle ranges with trajectories **bouncing back** into space

uniform pitch-angle distribution **redistributed** into different angular components

particles injected in the region **upstream of the ISM flow** back-scatter into the **downstream** region due to the ***heliospheric magnetic bubble***

our magnetic backyard

influence of the heliosphere

Schwadron, PD+ (2014)

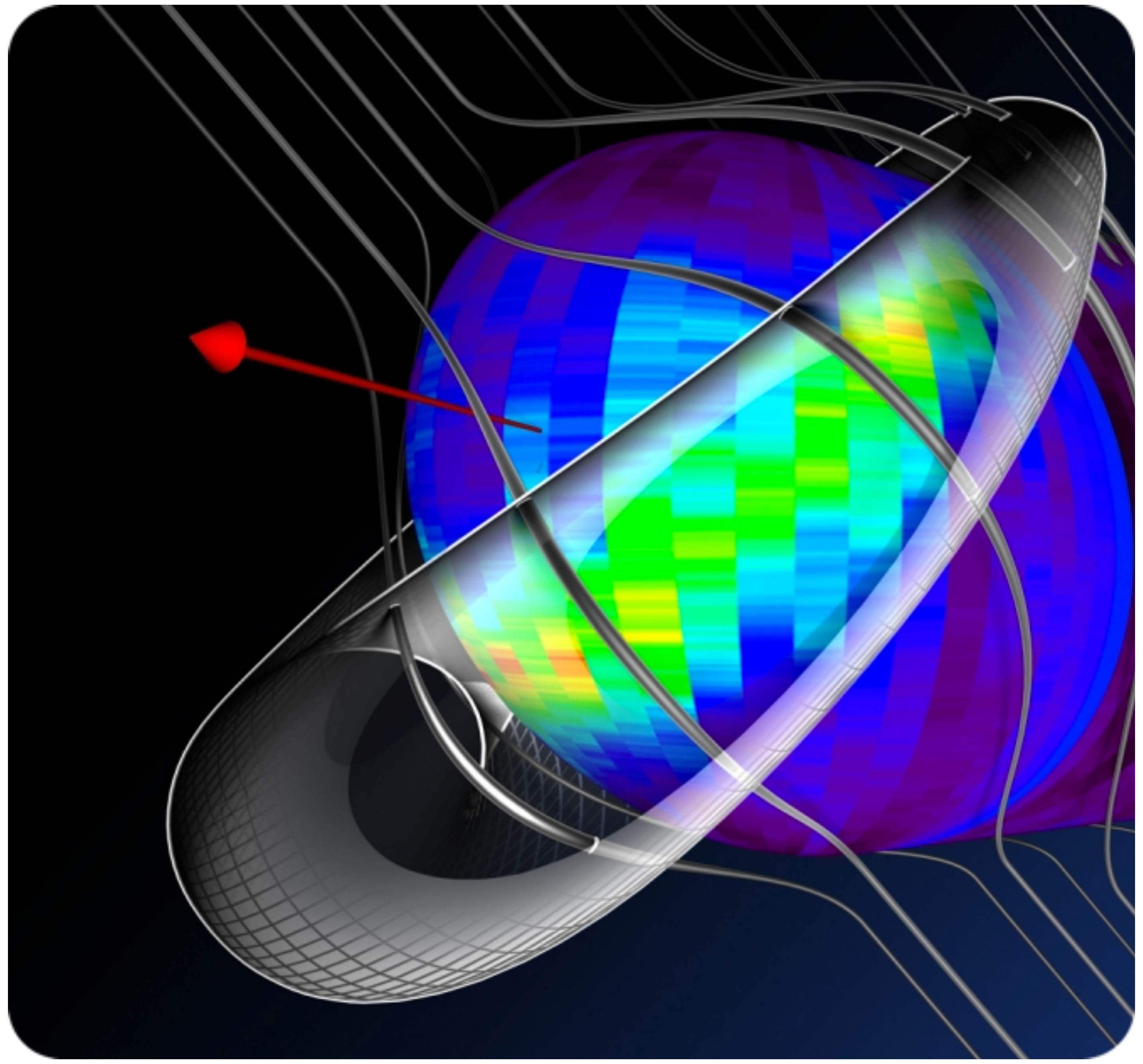

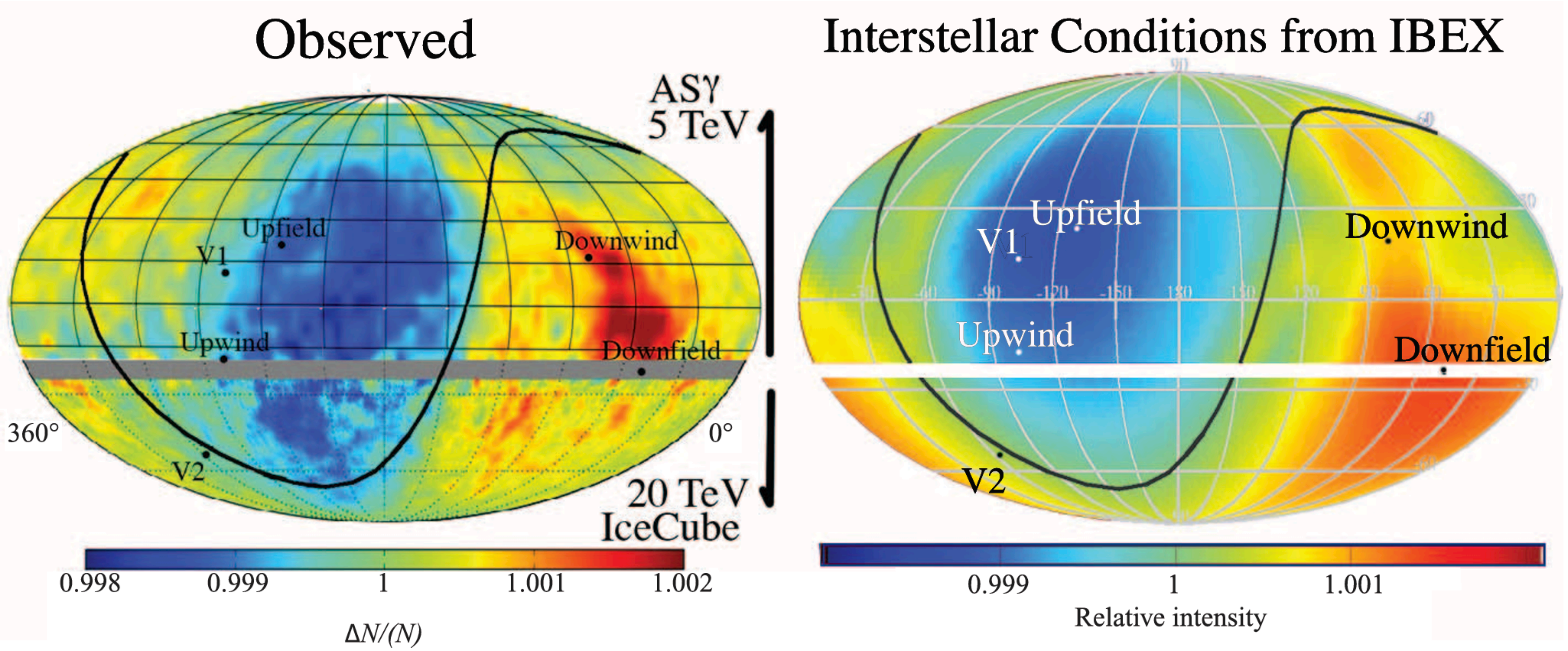

Fig. 2. TeV cosmic-ray anisotropies compared with predictions. Comparison between observed (**left**) and modeled (**right**) cosmic-ray relative intensities across the sky (J2000 coordinates). Black curves show the magnetic equator with a magnetic field direction derived from the center of the IBEX ribbon. On the left, the region below 25°S latitude is the anisotropy map from IceCube with a median energy of 20 TeV (*18*) and above 20°S latitude is the anisotropy map from ASγ with 5-TeV median energy (*15*). Similarly, the modeled map (right) at 20 TeV is shown below 25°S latitude and at 5 TeV above 20°S latitude. Both portions of the maps are smoothed over 3° to 5°. Labels indicate upwind and downwind directions (*2*), the current locations of Voyager 1 (V1), and Voyager 2 (V2) directions, and the "upfield" and "downfield" directions. Downfield is along the LISM magnetic field determined by IBEX in the direction closest to the interstellar velocity, and upfield is in the opposite direction. Plots are in equatorial coordinates with 0 hours at the right and increasing longitudes toward the left.

5 limited field of view

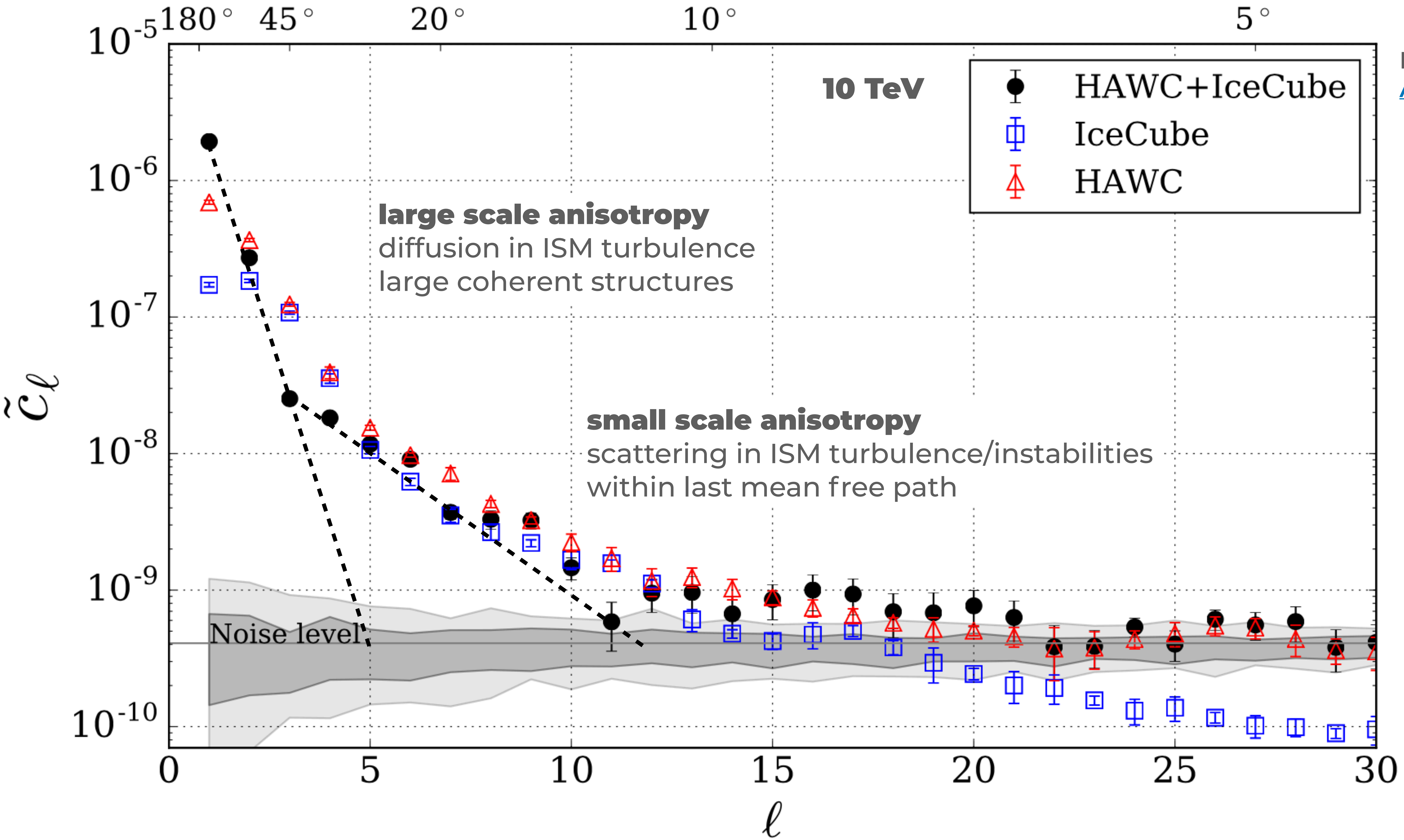

HAWC
ApJ 871 96 (2019)

Bian, Giacinti, Reville (2025)

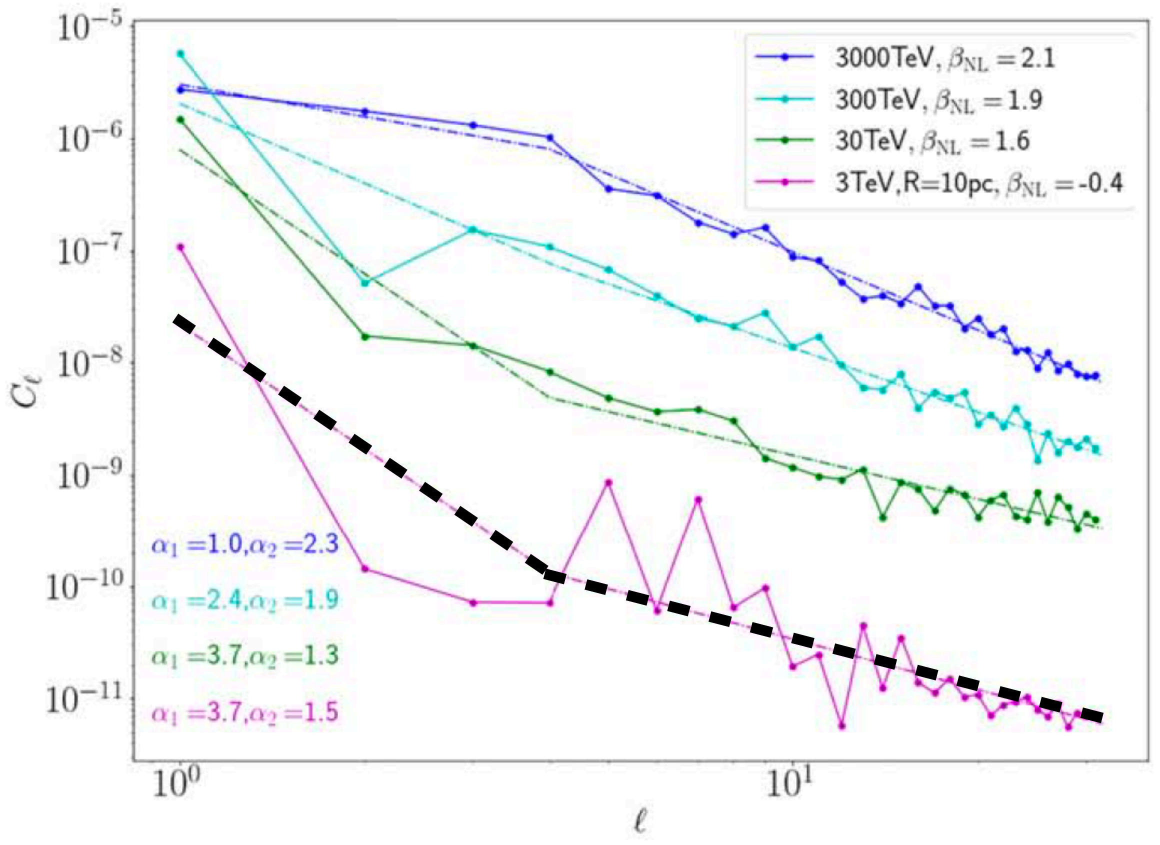

limited field of view

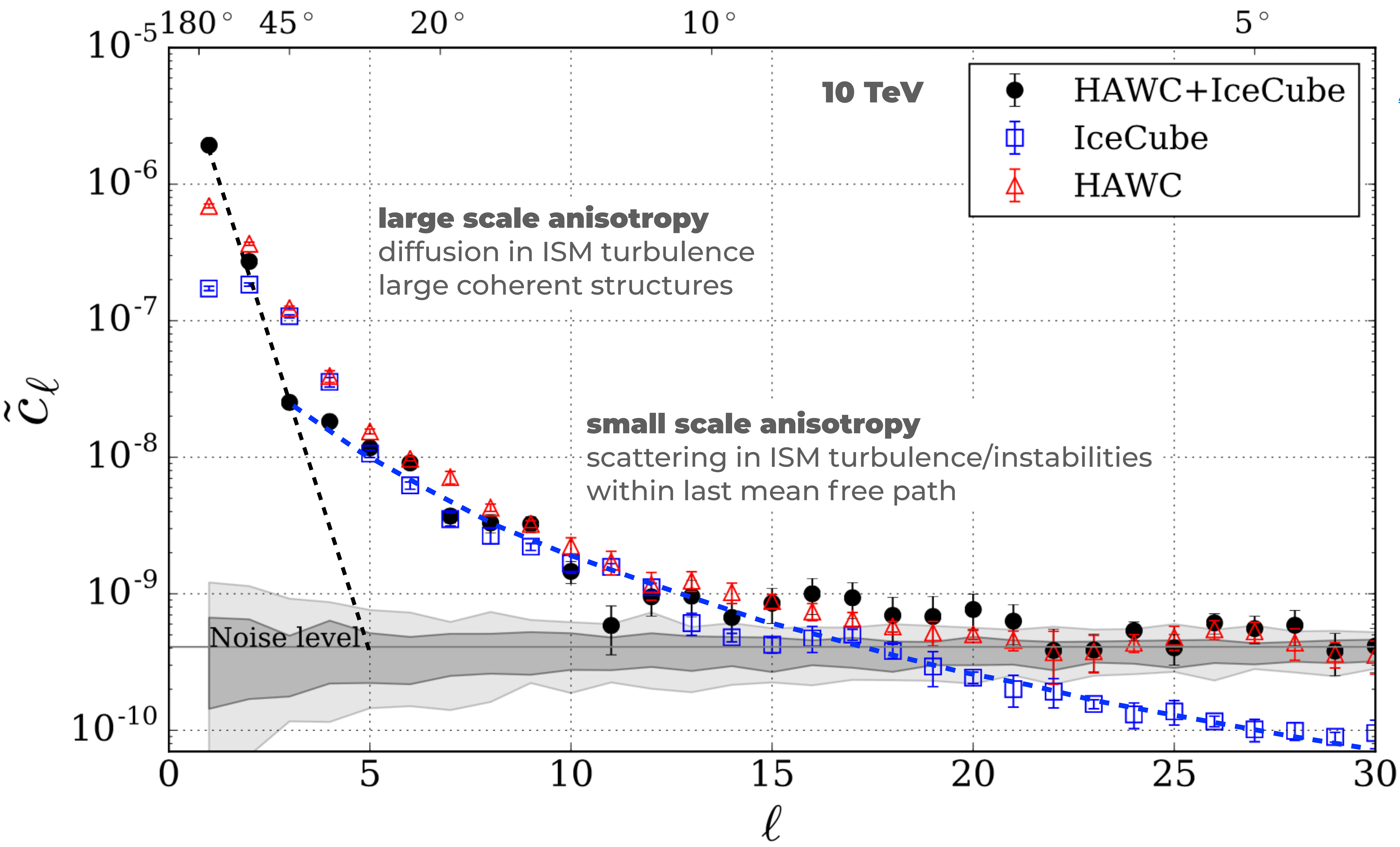

HAWC
ApJ 871 96 (2019)

Ahlers (2013) - Ahlers & Mertsch (2015)

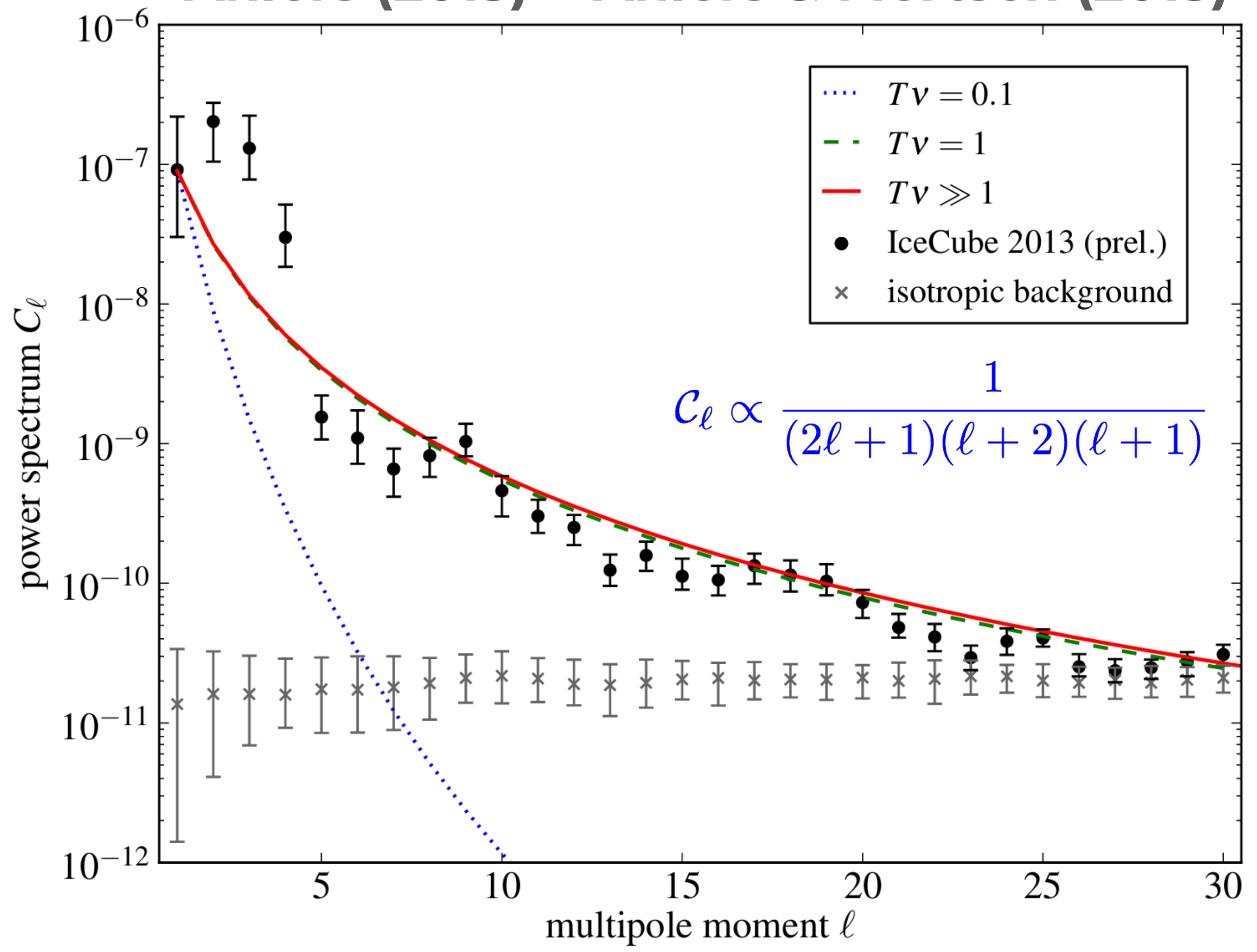

observed anisotropy

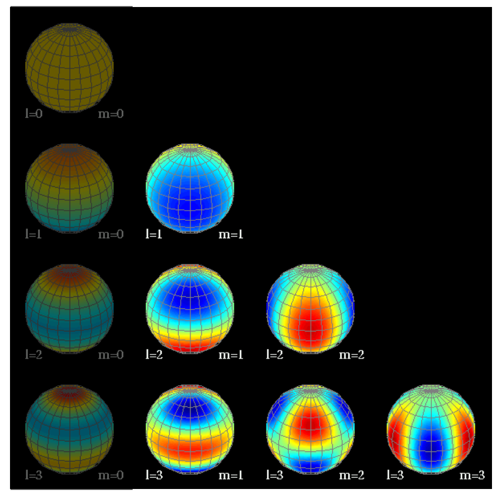

spherical harmonic analysis

missing *vertical* component (m = 0)

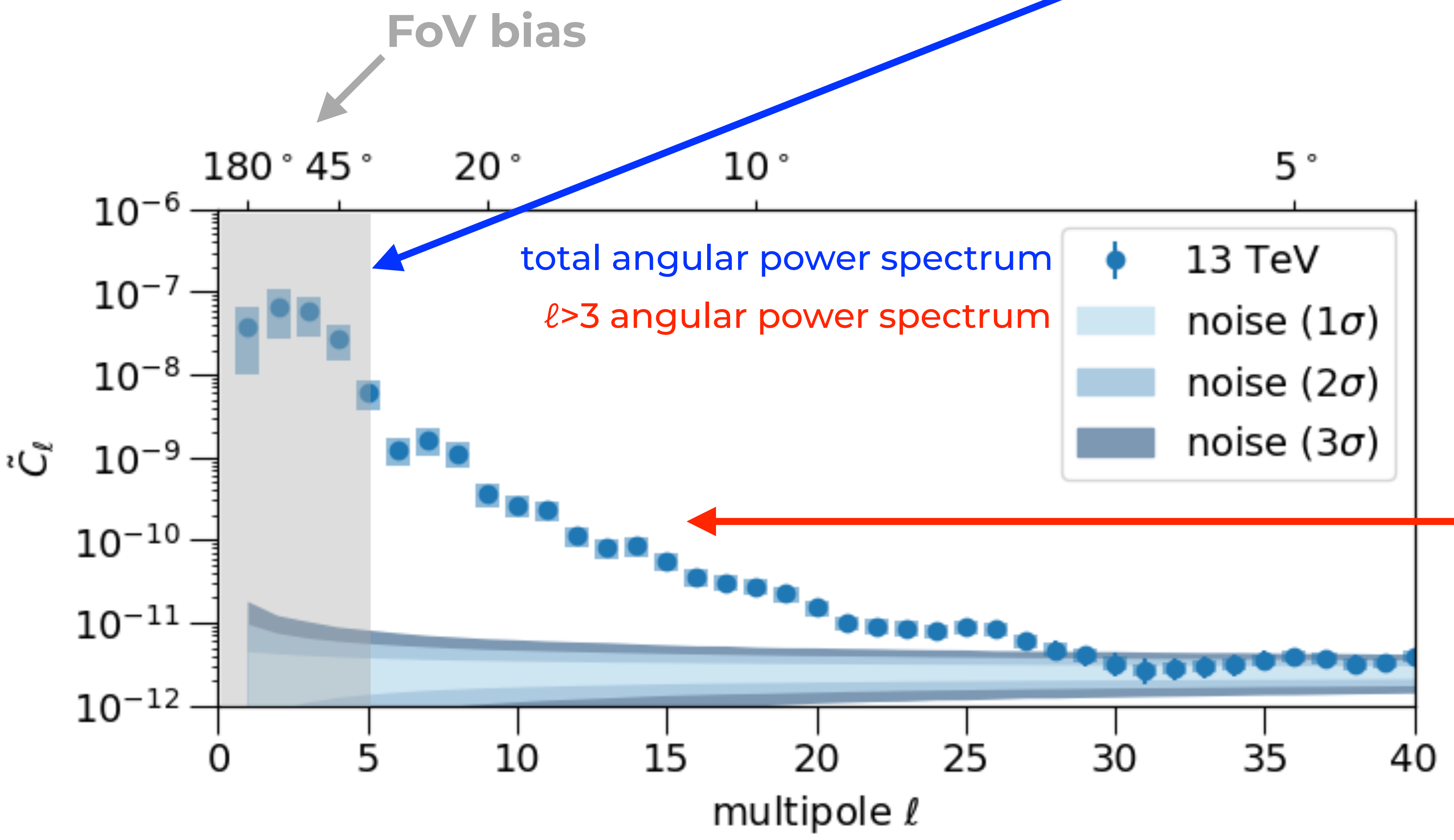

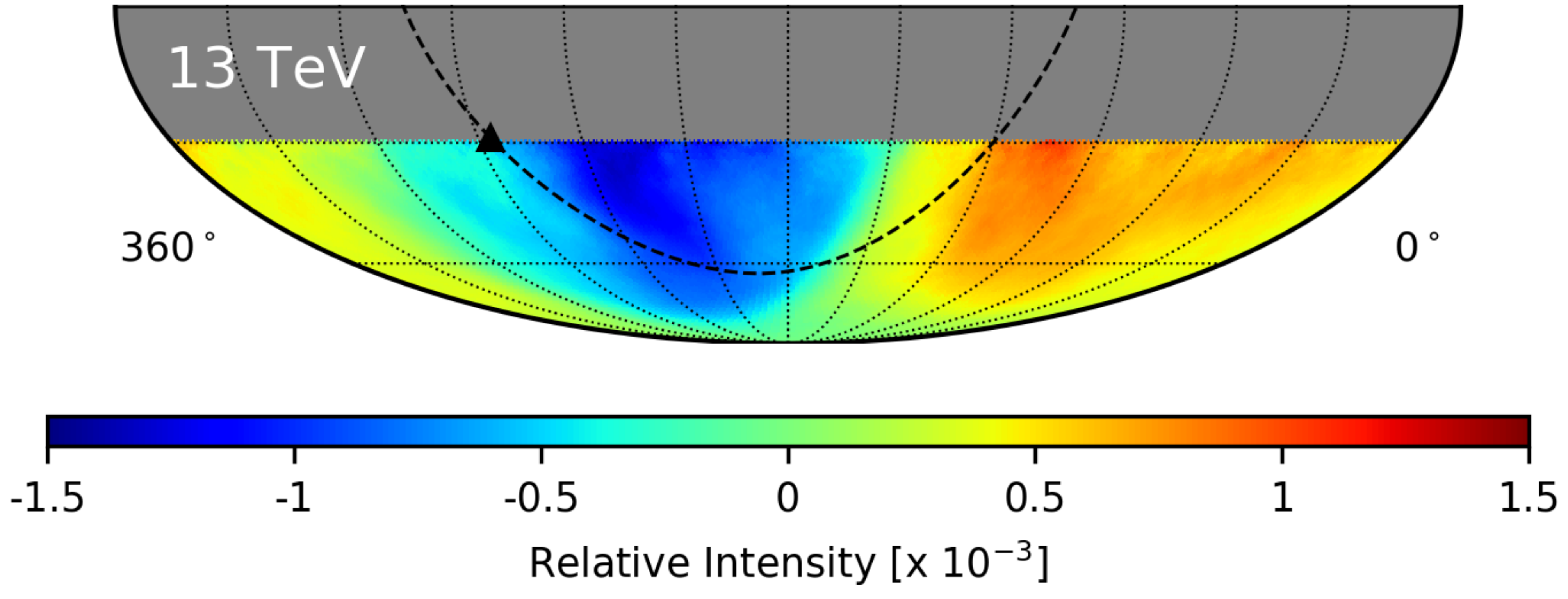

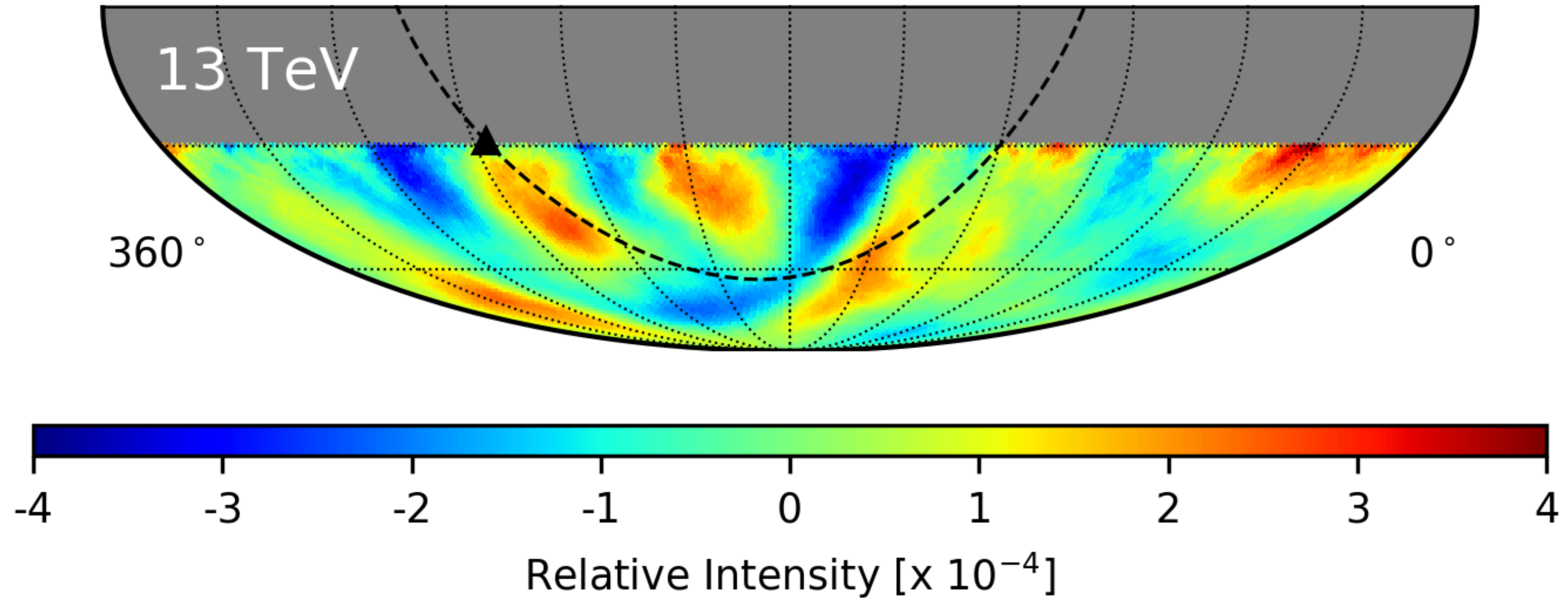

time variations?

IceCube
ApJ 981 182 (2025)

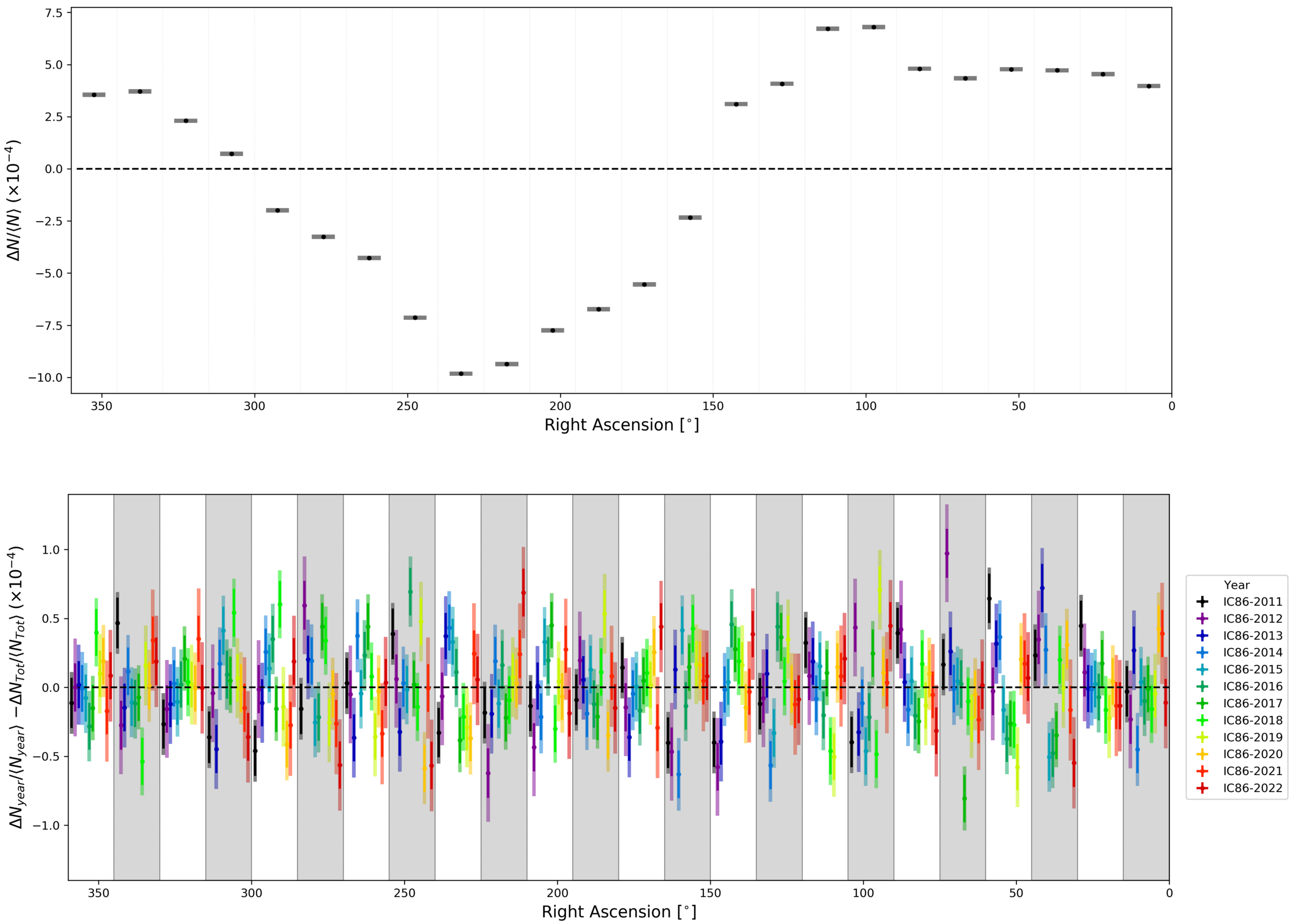

AMANDA + IceCube

33RD INTERNATIONAL COSMIC RAY CONFERENCE, RIO DE JANEIRO 2013
THE ASTROPARTICLE PHYSICS CONFERENCE

Study of the time-dependence of the cosmic-ray anisotropy with AMANDA and IceCube

THE ICECUBE COLLABORATION[1],
[1] *See special section in these proceedings*
santander@icecube.wisc.edu

NOT calendar years

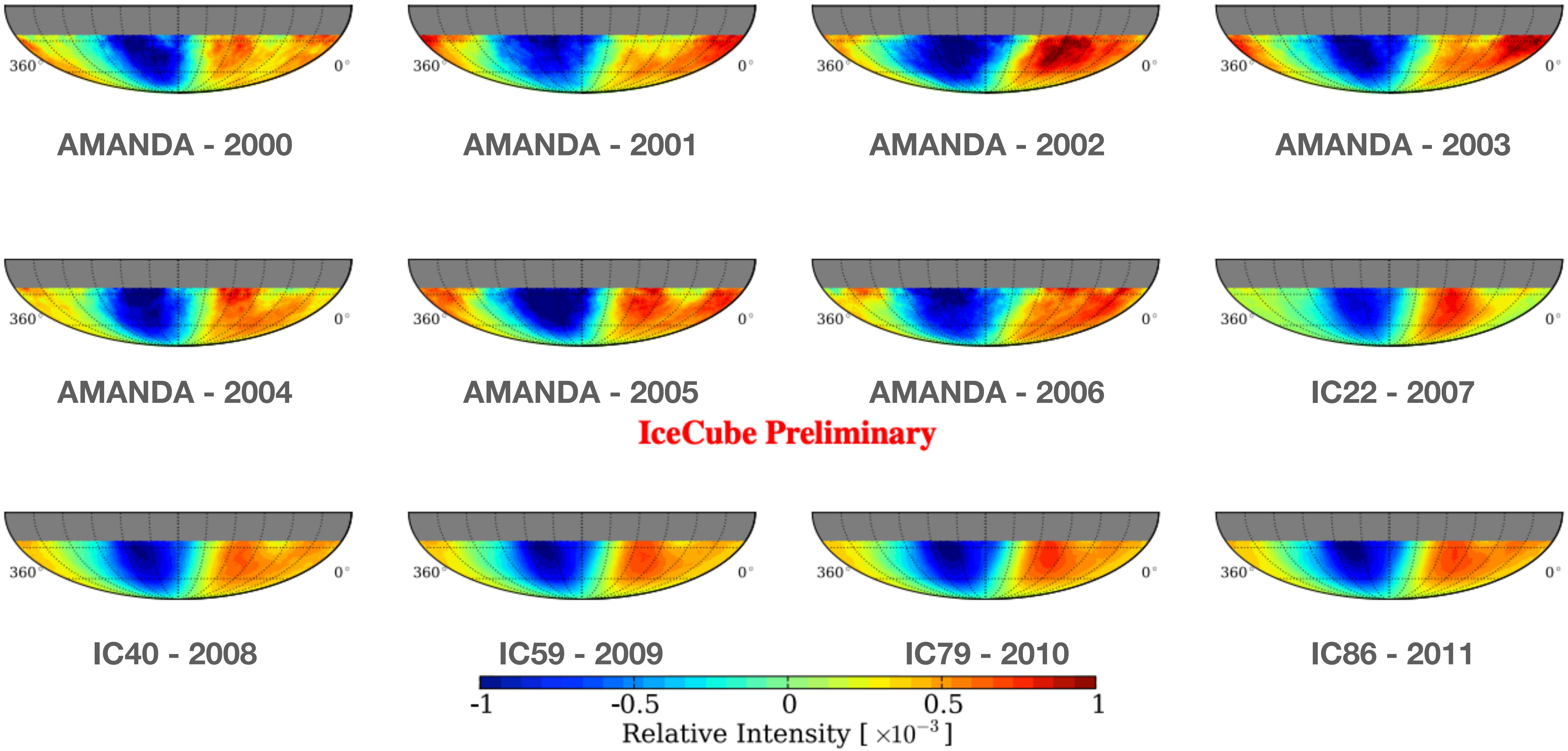

AMANDA + IceCube

NOT calendar years

33RD INTERNATIONAL COSMIC RAY CONFERENCE, RIO DE JANEIRO 2013
THE ASTROPARTICLE PHYSICS CONFERENCE

ICRC 2013

Study of the time-dependence of the cosmic-ray anisotropy with AMANDA and IceCube

THE ICECUBE COLLABORATION[1],
[1] *See special section in these proceedings*
santander@icecube.wisc.edu

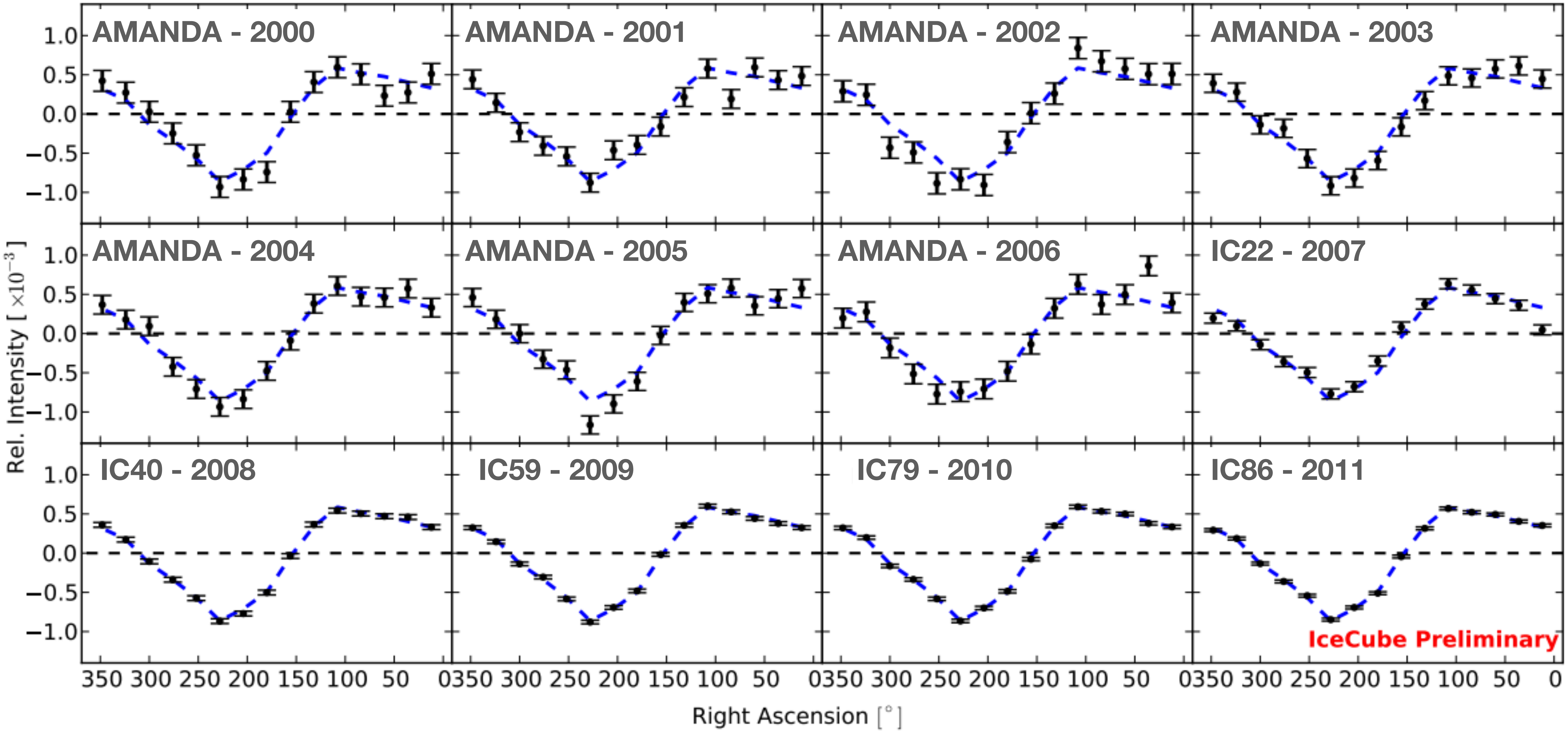

local interstellar magnetic field

Abeysekara et al., ApJ (2019) 871 96

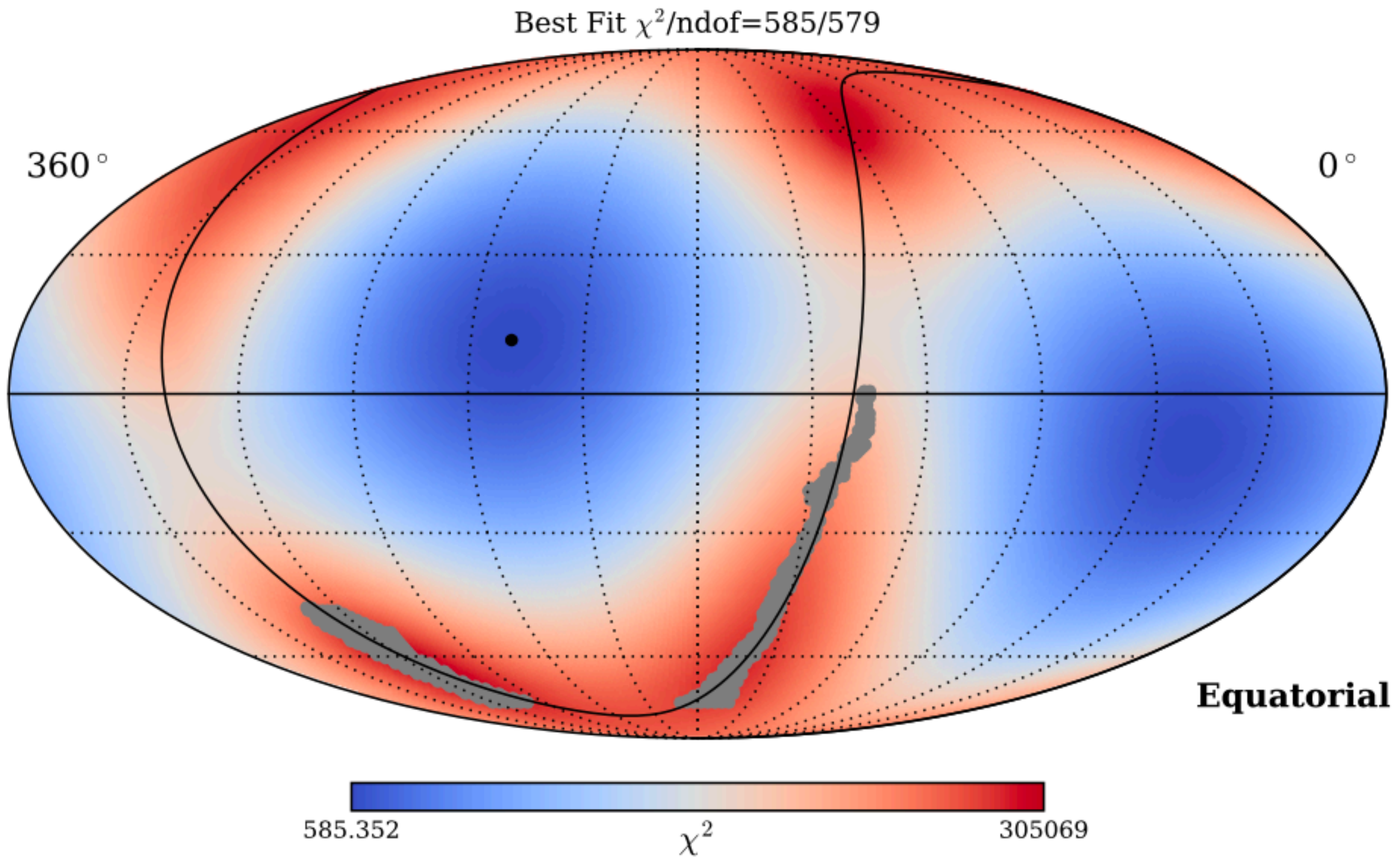

Figure 12. χ^2 distribution map for circular fit to boundary between large-scale excess and deficit regions shown in J2000 equatorial coordinates. The black point corresponds to the minimum χ^2 for the center of the circle and the black curve is the fitted circle. The grey points are the selected pixels for the fit. The best fit has a value of $\chi^2/\text{ndof} = 585/579$.

Local Interstellar Magnetic Field

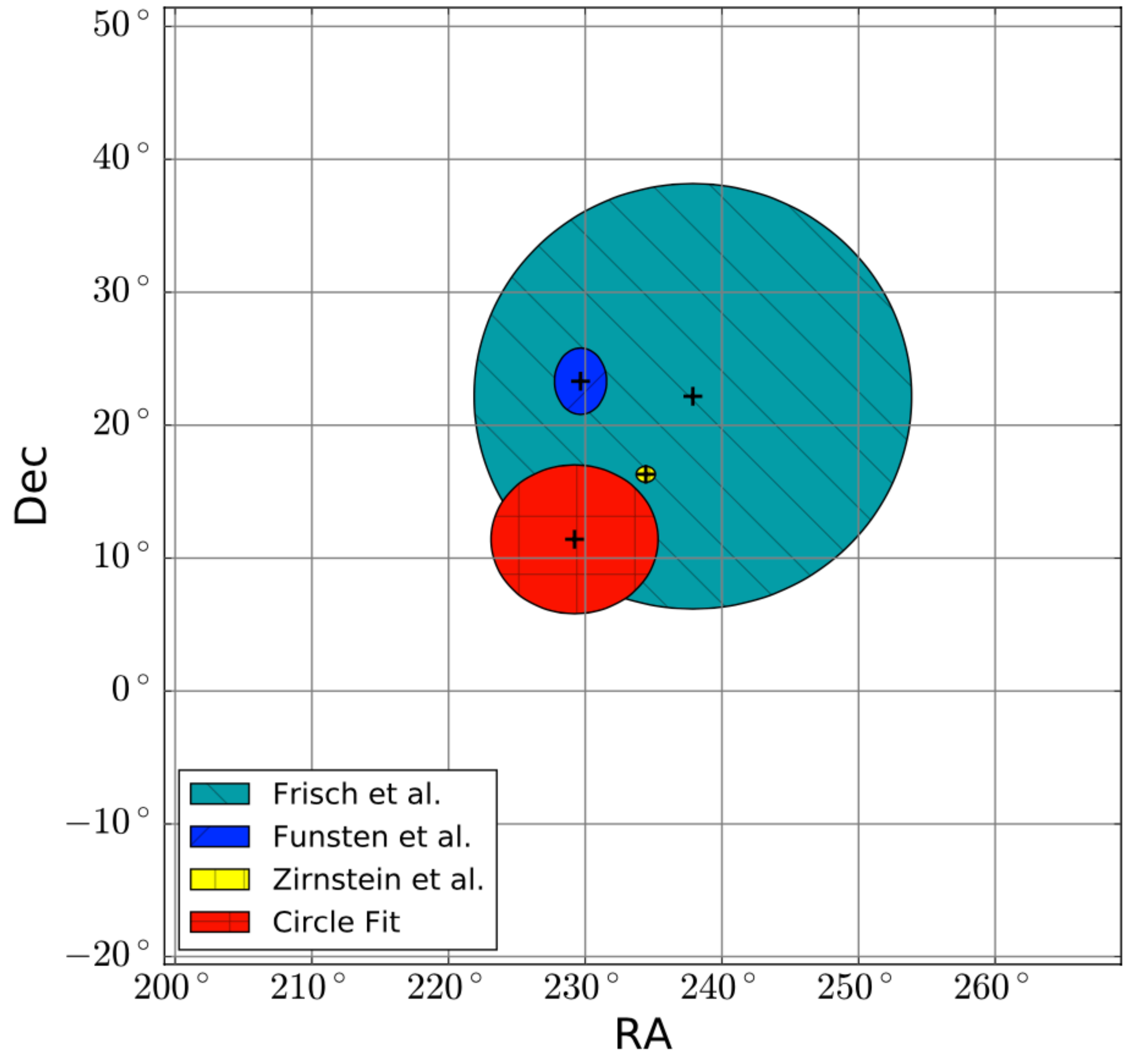

Figure 13. Circular fit to boundary between large-scale excess and deficit regions shown in J2000 equatorial coordinates along with published magnetic field measurements by Funsten et al. (2013) inferred from the emission of energetic neutral atoms (ENA) originating from the outer heliosphere by the Interstellar Boundary Explorer (IBEX) (Zirnstein et al. 2016), and Frisch et al. (2015) obtained from the polarization of stars within 40 pc.

The heliosphere

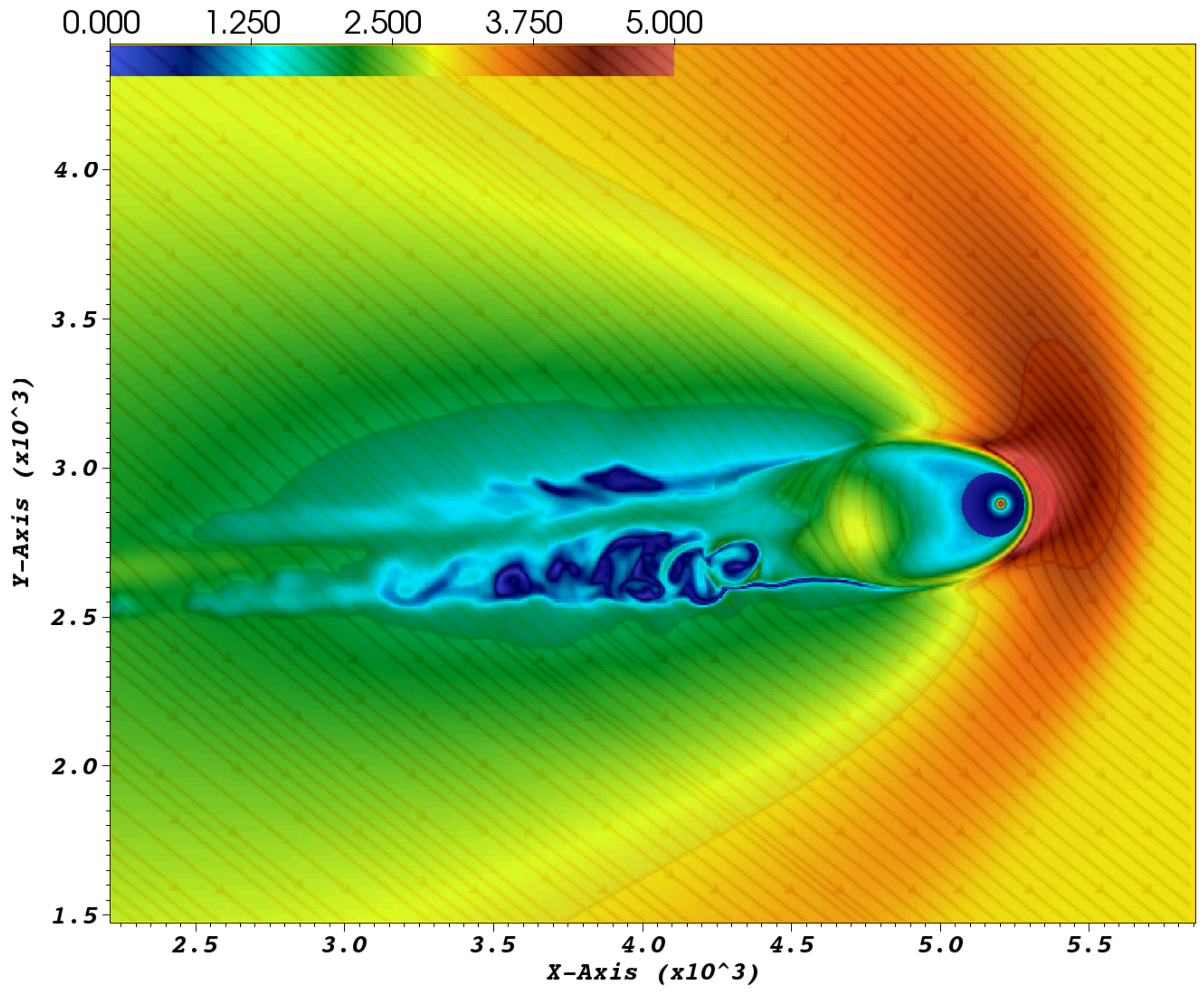

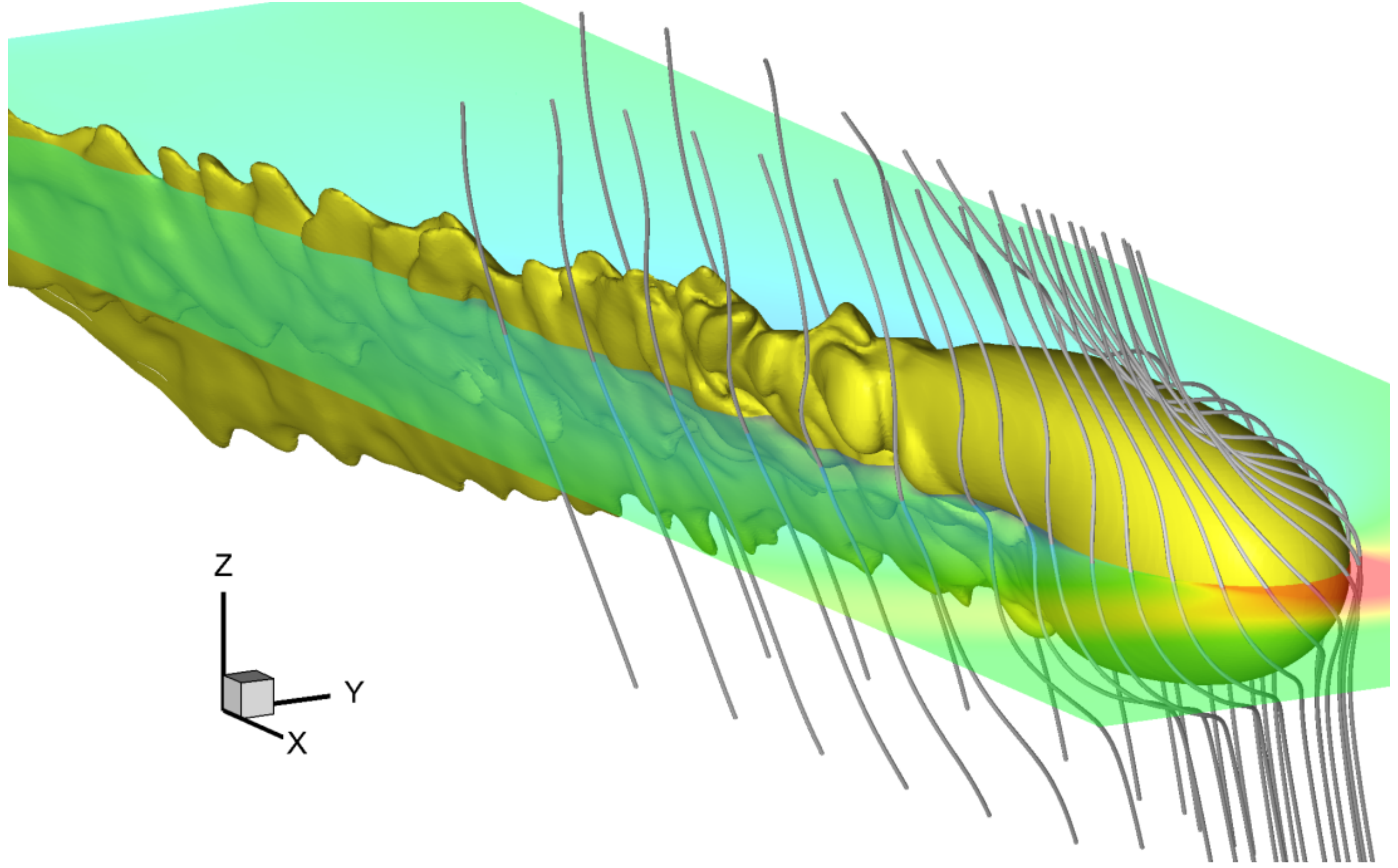

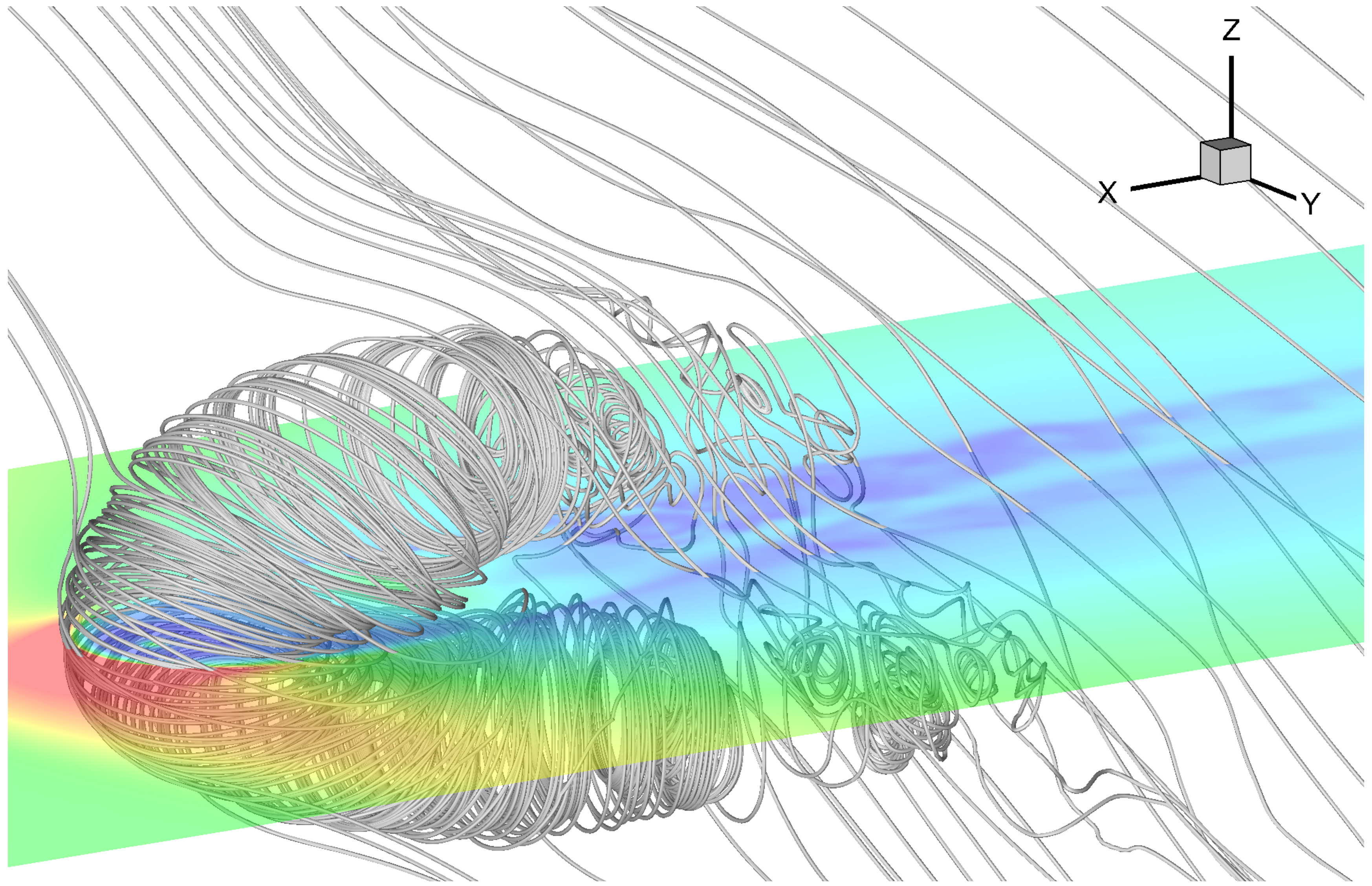

Heliospheric model by
Borovikov, Heerikhuisen, Pogorelov, 2015

The heliosphere

Díaz Vélez & PD

draping of interstellar magnetic field magnetic mirror

10 TV particles can be trapped

residence time can reach ~20 years

strong heliospheric influence

cosmic rays distribution re-shaped when passing through the heliosphere

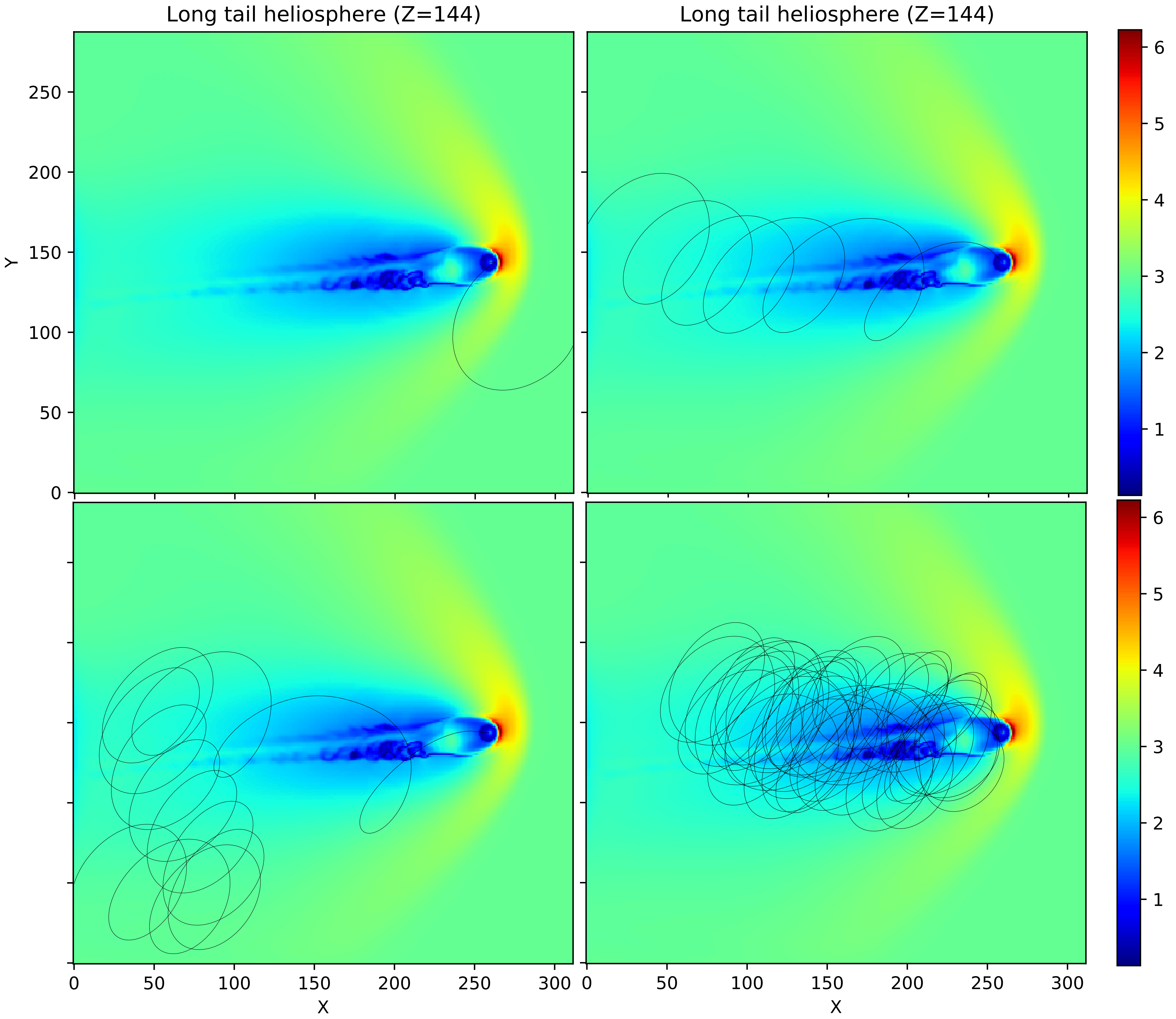

Heliospheric model by
Borovikov, Heerikhuisen, Pogorelov, 2015

The heliosphere

Díaz Vélez & PD

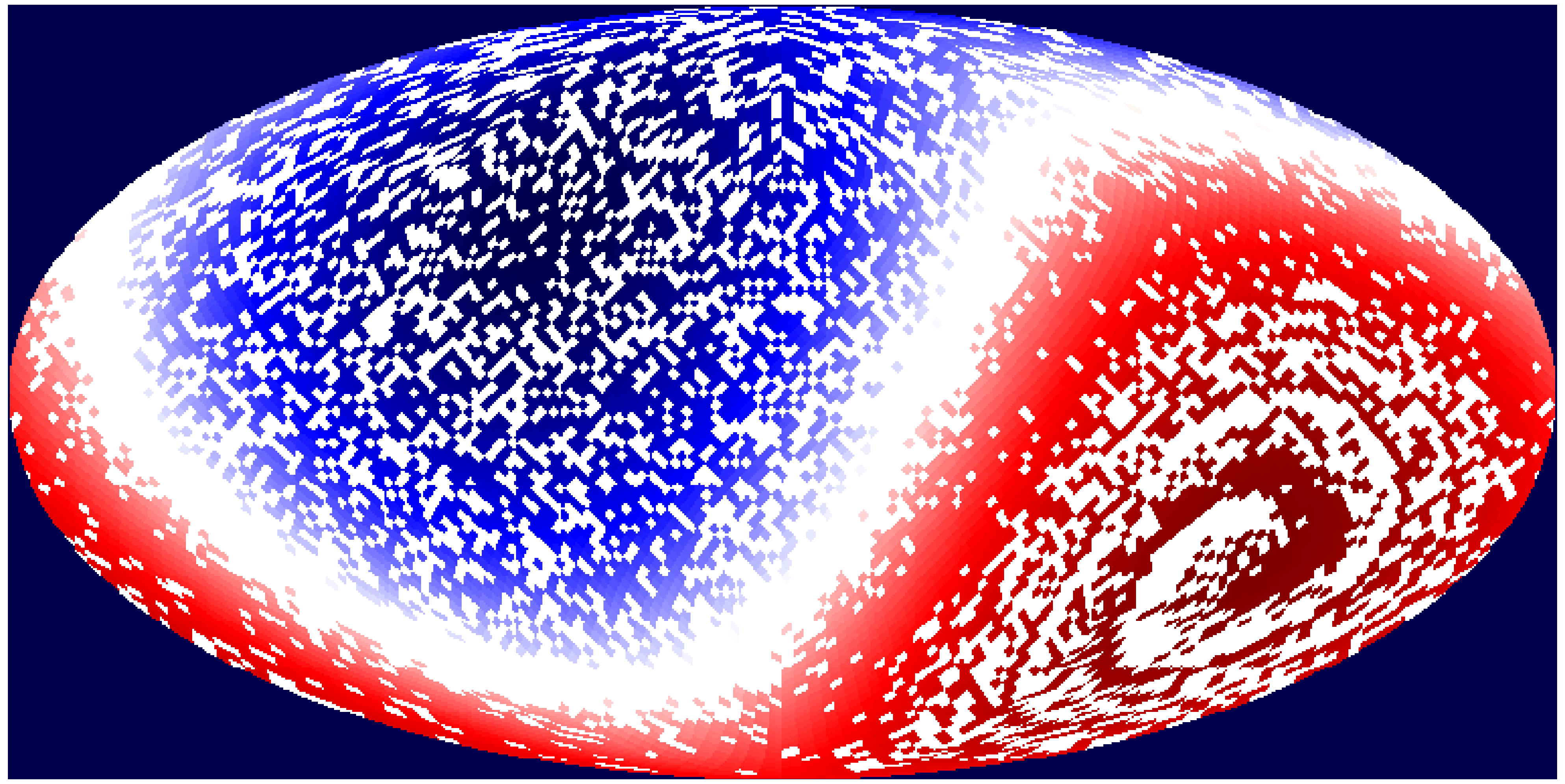

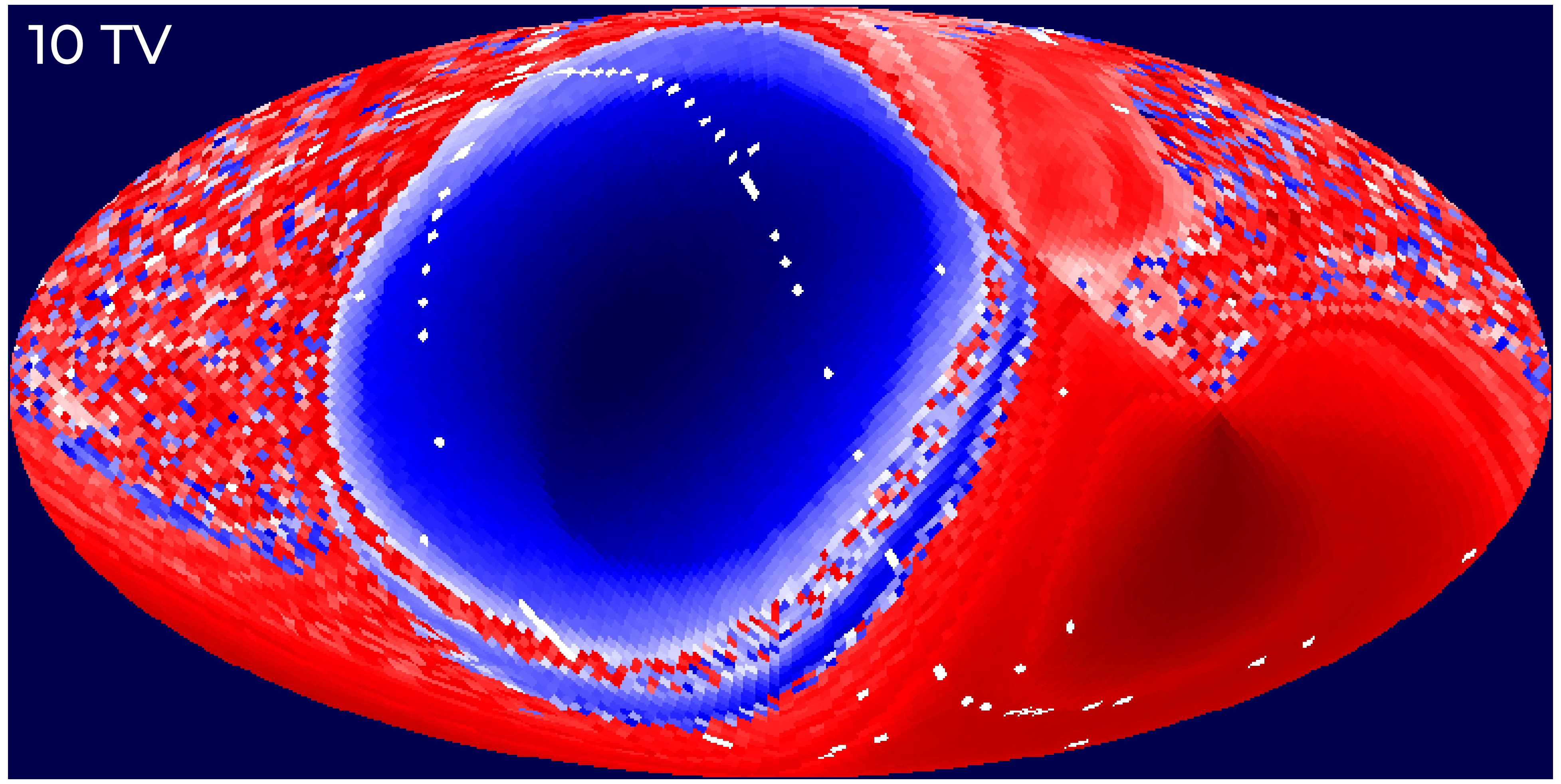

backward propagation
assume dipole pitch-angle distribution in the ISM
(isotropic diffusion)

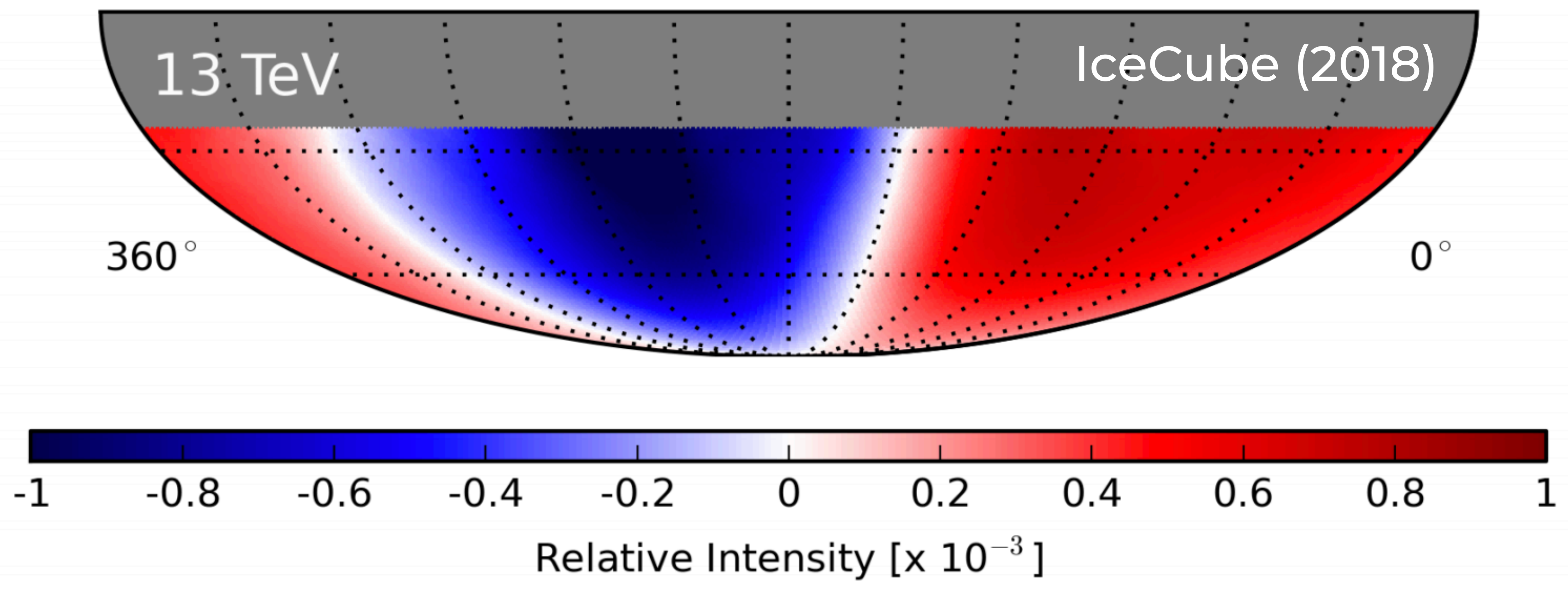

strong heliospheric influence

observed distribution compatible with mostly
dipolar CR density gradient in the ISM
isotropic pitch-angle diffusion

different distribution than the ISM

The heliosphere

Díaz Vélez & PD

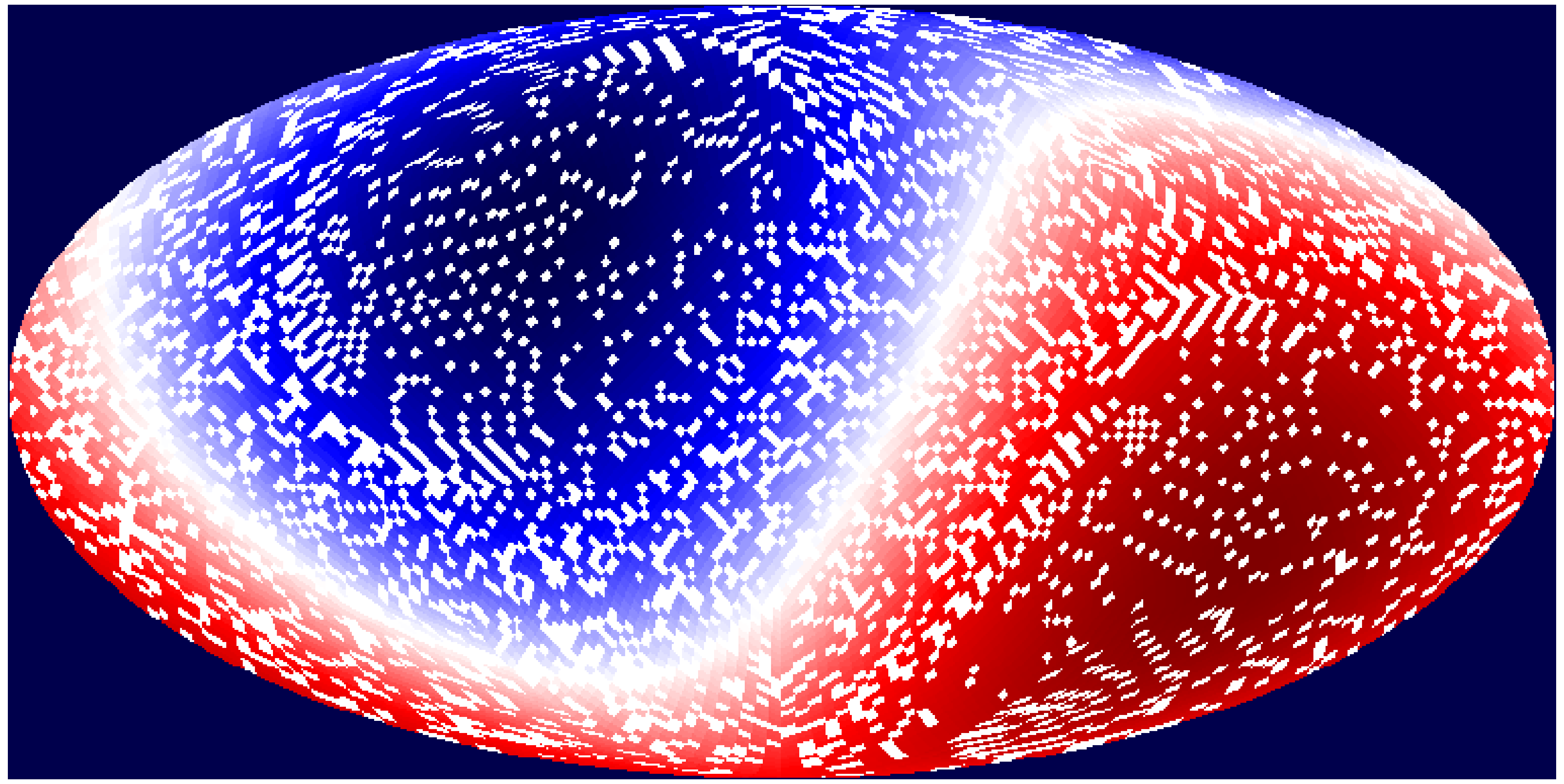

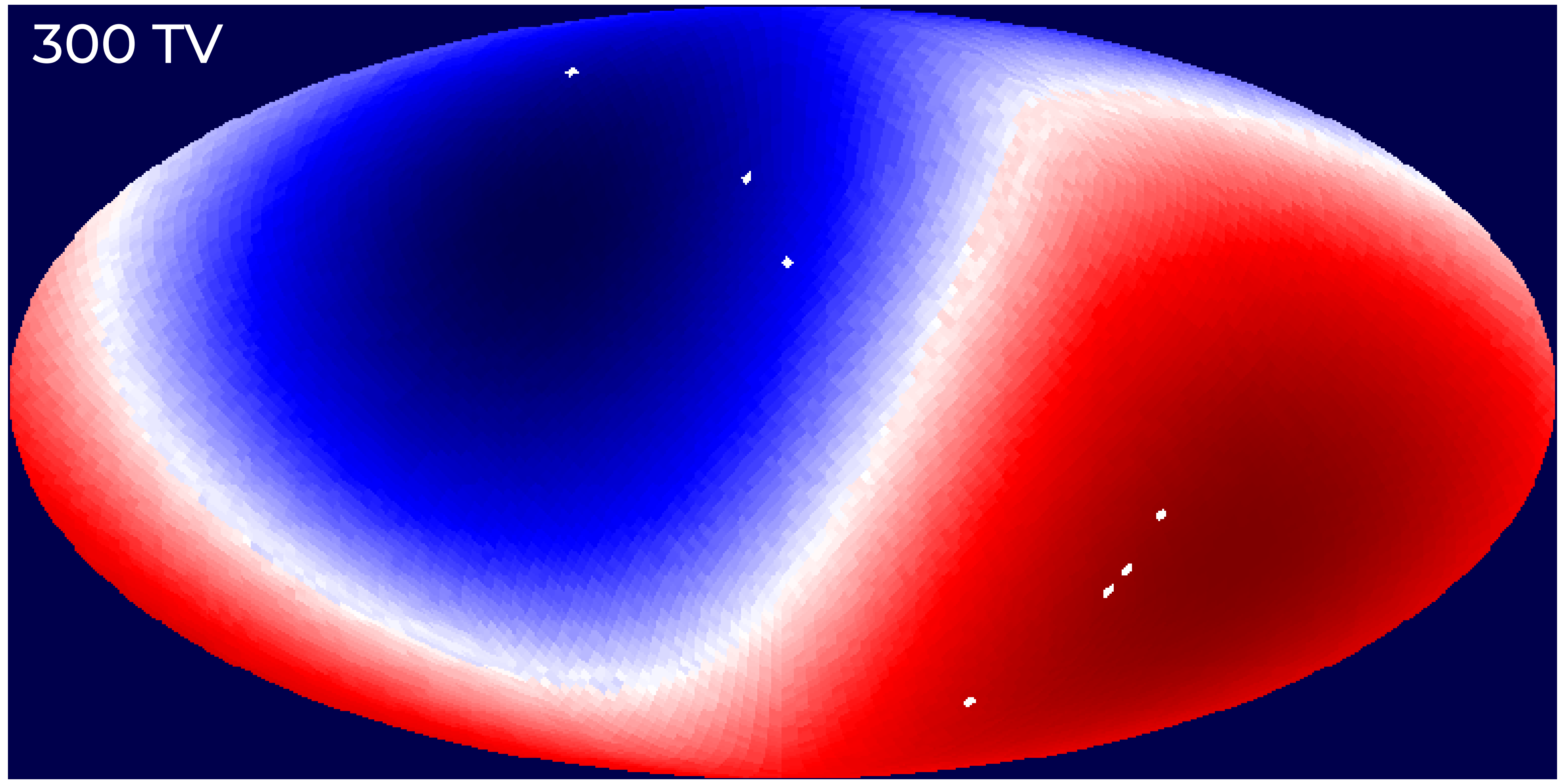

backward propagation
assume dipole pitch-angle distribution in the ISM
(isotropic diffusion)

no heliospheric influence

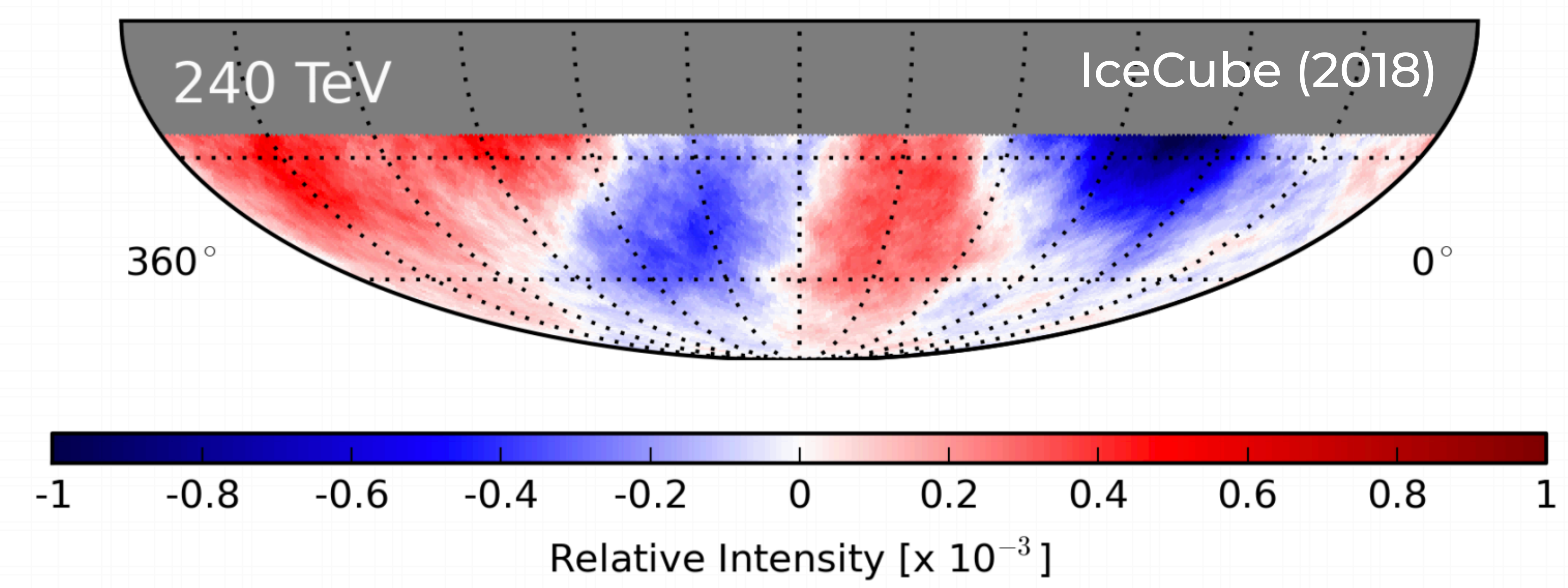

pitch-angle distribution in the ISM cannot be the same as that at 10 TV

pristine distribution from the ISM

future experiment
IceCube-Gen2

IceCube-Gen2

tech design report

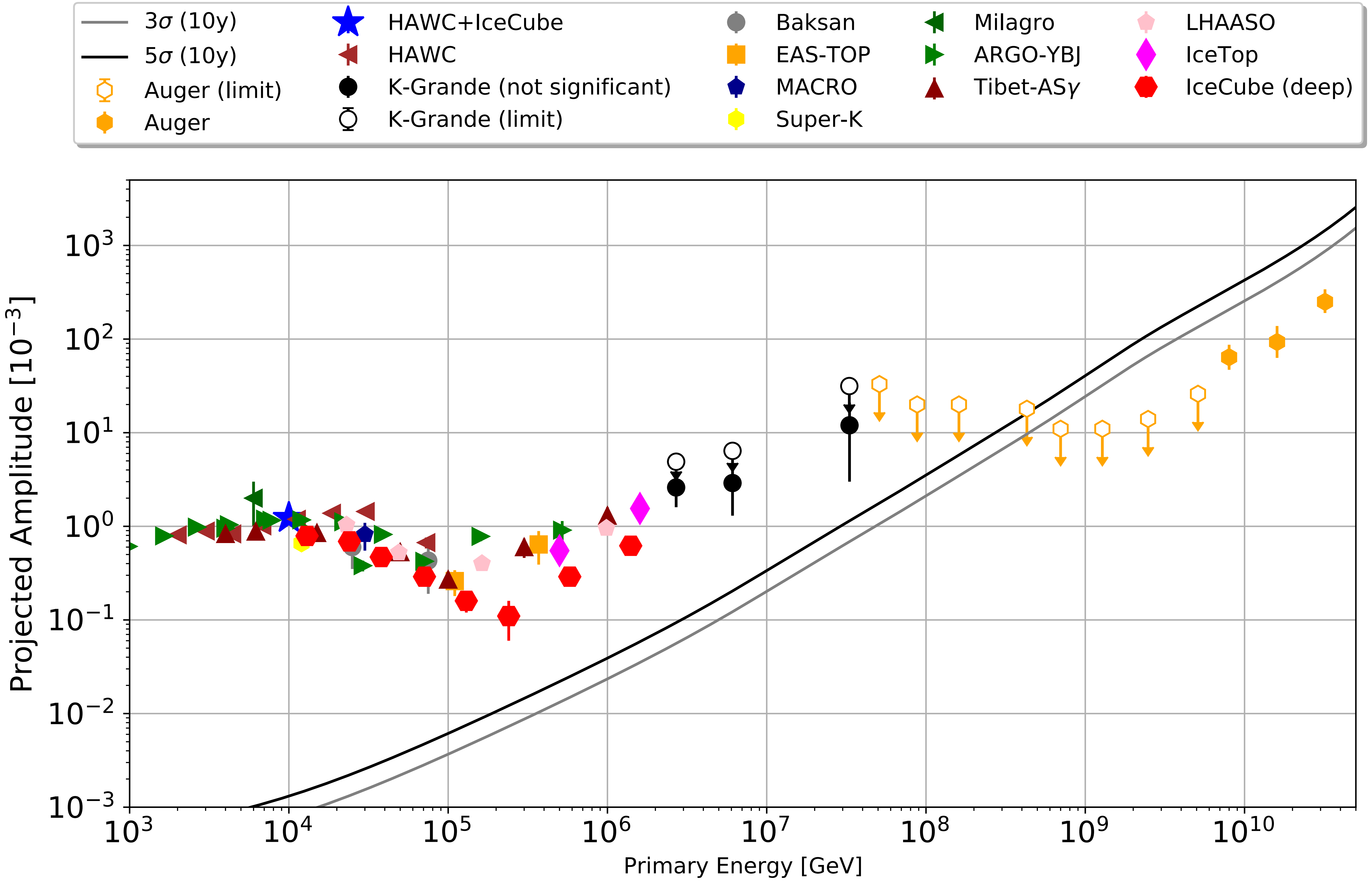

Figure 27: Sensitivity of cosmic-ray anisotropy measurements with IceCube-Gen2 with 10 years worth of data. The expected three and five sigma sensitivities to the equatorial plane component of the dipole anisotropy are shown. IceCube-Gen2 will be far the most sensitive detector for the PeV energy range, extending IceCube's energy range of anisotropies by more than an order of magnitude in energy. In particular, statistically non-significant measurements of the dipole amplitude by KASCADE-Grande [327], if true, can be confirmed at five sigma level. Note that KASCADE-Grande and Auger [328] results are shown with measurements (full symbols) and 90% CL upper limits (empty symbols) [327–341].